AD-A053 842 TENNESSEE UNIV KNOXVILLE ULTRASONICS LAB F/G 20/1
ULTRASONIC WAVE REFLECTION AT LIQUID-SOLID INTERFACES.(U)
FEB 78 M A BREAZEALE N00014-76-C-0177
UNCLASSIFIED NL

| OF |
AD A053842

END
DATE FILMED
6 -78
DDC

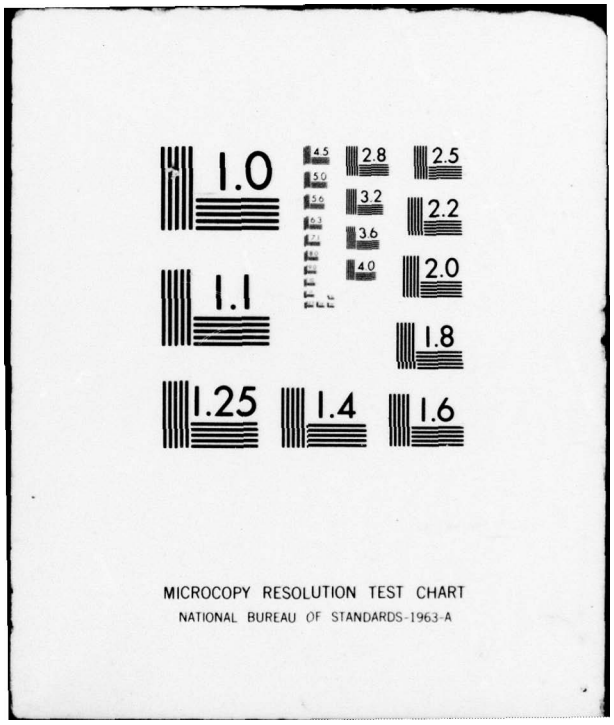
1.0
1.1
1.25
1.4
1.6
1.8
2.0
2.2
2.5
2.8
3.2
3.6
4.0
4.5
5.0
5.6
MICROCOPY RESOLUTION TEST CHART
NATIONAL BUREAU OF STANDARDS-1963-A

(13)

OFFICE OF NAVAL RESEARCH
CONTRACT NO. N00014-76-C-0177
PROJECT NO. 384-306

TECHNICAL REPORT NO. 15

ULTRASONIC WAVE REFLECTION AT LIQUID-SOLID INTERFACES

M.A. BREAZEALE
PRINCIPAL INVESTIGATOR

ULTRASONICS LABORATORY
DEPARTMENT OF PHYSICS

THE UNIVERSITY OF TENNESSEE
Knoxville, Tennessee

FEBRUARY 1978

OFFICE OF NAVAL RESEARCH
CONTRACT NO. N00014-76-C-0177
PROJECT NO. 384-306

ULTRASONIC WAVE REFLECTION AT LIQUID-SOLID INTERFACES

by

M. A. Breazeale

TECHNICAL REPORT NO. 15

Ultrasonics Laboratory
Department of Physics
The University of Tennessee
Knoxville, Tennessee 37916

February 1978

Unclassified

SECURITY CLASSIFICATION OF THIS PAGE (When Data Entered)

REPORT DOCUMENTATION PAGE		READ INSTRUCTIONS BEFORE COMPLETING FORM
1. REPORT NUMBER 15	2. GOVT ACCESSION NO.	3. RECIPIENT'S CATALOG NUMBER
4. TITLE (and Subtitle) ULTRASONIC WAVE REFLECTION AT LIQUID-SOLID INTERFACES		5. TYPE OF REPORT & PERIOD COVERED Interim 6. PERFORMING ORG. REPORT NUMBER
7. AUTHOR(s) M. A. Breazeale		8. CONTRACT OR GRANT NUMBER(s) N00014-76-C-0177
9. PERFORMING ORGANIZATION NAME AND ADDRESS Dept. of Physics The University of Tennessee Knoxville, TN 37916		10. PROGRAM ELEMENT, PROJECT, TASK AREA & WORK UNIT NUMBERS
11. CONTROLLING OFFICE NAME AND ADDRESS Office of Naval Research, Code 468 Department of the Navy Arlington, VA 22217		12. REPORT DATE February 1978 13. NUMBER OF PAGES 72
14. MONITORING AGENCY NAME & ADDRESS(if different from Controlling Office)		15. SECURITY CLASS. (of this report) Unclassified 15a. DECLASSIFICATION/DOWNGRADING SCHEDULE

16. DISTRIBUTION STATEMENT (of this Report)

Approved for public release; distribution unlimited.

17. DISTRIBUTION STATEMENT (of the abstract entered in Block 20, if different from Report)

18. SUPPLEMENTARY NOTES

19. KEY WORDS (Continue on reverse side if necessary and identify by block number)

Ultrasonic wave reflection
Rayleigh angle
Liquid-solid interface
Surface wave phenomena

20. ABSTRACT (Continue on reverse side if necessary and identify by block number)

This technical report comprises ten publications on the reflection of ultrasonic waves at liquid-solid interfaces made by members of the Ultrasonics Group at The University of Tennessee between January 1975 and April 1978. Description is given of both experimental and theoretical advances in the understanding and utilization of reflection phenomena. Attention is concentrated primarily on the angles at which leaky surface waves are excited along

DD FORM 1 JAN 73 1473 EDITION OF 1 NOV 65 IS OBSOLETE

S/N 0102-LF-014-6601

SECURITY CLASSIFICATION OF THIS PAGE (When Data Entered)

20 (continued)

the interface. Rayleigh angle phenomena are described, as well as the backward shift resulting from a periodicity superimposed on the interface. Utilization of these phenomena in nondestructive evaluation and in underwater acoustics is mentioned.

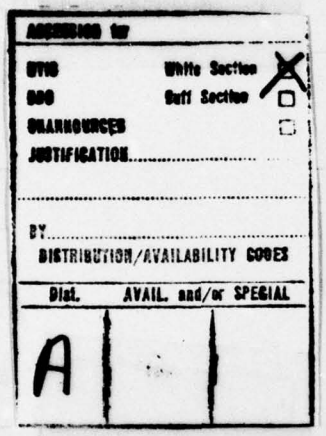

PREFACE

This technical report comprises publications on the reflection of ultrasonic waves at a liquid-solid interface made between January 1975 and the present. During this period a number of publications have been made on other subjects; however, we prefer to concentrate on the reflection problem in this technical report in order to present a unified picture of the development of this subject. A later technical report will cover other subjects.

The report begins with the English language version of a paper whose Russian-language counterpart was included in Technical Report No. 11. It may be worthwhile to point out that our Russian colleagues were impressed with the paper enough to make it the lead article in Akusticheskii Zhurnal for the year 1975.

In this paper we were able to get agreement between theory and experiment at the Rayleigh angle sufficient to permit us to plot them on the same graph. (Up until this time theory and experiment were agreeing only qualitatively so that such a comparison was not possible.) The agreement was made possible by advances both in experiment and in theory. The experimental advance was the use of a transducer which produced a truly Gaussian amplitude distribution in the incident beam (see Technical Report No. 8). The theoretical advance was the retention of higher-order terms in the power series expansion of the phase shift upon reflection than had been used previously by Brekhovskikh. This led to a complicated expression for the reflected beam, a power series expansion in Fresnel integrals, which had to be evaluated by computer.

A mathematical improvement resulted from interaction between the author and Werner G. Neubauer and Larry Flax of NRL. Rather than a series expansion, a closed-form solution in terms of error functions was introduced. This is contained in the second paper.

In the third paper we show that a considerable improvement of the agreement between theory and experiment results from the use of the theory of Bertoni and Tamir, with modification to account for the propagation distance of the incident beam. The data in this paper also are very carefully taken.

The fourth paper, given at the XV International Conference on Acoustics-Ultrasound in Prague, is a summary paper describing the application of the theory of Bertoni and Tamir to the results on stainless steel. In this paper we also indicate that a corrugated interface makes possible coupling to a surface wave which propagates in the negative-x direction along the interface. The fifth paper shows that this negatively directed surface wave causes the reflected beam to be displaced in the opposite direction from that observed at the Rayleigh angle.

The sixth paper shows not only that the displacement observed at liquid-solid interfaces can be observed at water-sediment interfaces, but also that the backward displacement phenomenon might exist because of the periodicity resulting from the granularity of the sediment. Furthermore, the water-sediment interface corresponds to a water-solid interface for which $V_L > V > V_S$, a situation which previously had not been observed to give a displacement of the reflected beam. However, such a displacement does exist for this class of liquid-solid reflectors,

as we show in the seventh paper. The displacement is observed near the critical angle for water-plexiglass, not the Rayleigh angle, however, for there is no Rayleigh angle.

The eighth paper is an application of the surface wave phenomena to the detection of subsurface flaws in metals. The surface waves generated at the Rayleigh angle are described in the theory of Bertoni and Tamir as "leaky waves" because the energy "leaks" from them back into the liquid to become the reflected beam. The ninth paper shows how these leaky waves can be used to detect subsurface flaws in solids. The final paper begins a study of the effect of the introduction of a layer on the solid.

M. A. Breazeale
February 1978

TABLE OF CONTENTS

Paper No. 1

Energy Redistribution of a Gaussian Ultrasonic Beam Reflected from Liquid-Solid Interface (M. A. Breazeale, Laszlo Adler, and James H. Smith), Akust. Zh., 21, 1-10 (1975) [Sov. Phys. Acoust. 21, 1-6 (1975)].

Energy redistribution of a Gaussian ultrasonic beam reflected from liquid–solid interface

M. A. Breazeale, Laszlo Adler, and James H. Smith
Department of Physics, University of Tennessee, Knoxville, Tennessee
(Submitted February 4, 1974)
Akust. Zh., 21, 1-10 (January-February 1975)

The problem of the reflection of an ultrasonic beam from a liquid–solid interface is considered. The concept of "beam displacement" is reexamined by studying the internal structure of the reflected beam. This study is carried out by means of a transducer which produces a Gaussian distribution of energy across the beam width. Experimental results show that the energy of the reflected beam is redistributed into two or more beams for angles near the angle of optimum generation of surface waves on the interface. Reasonable agreement is obtained between theory and experiment for water–aluminum and water–brass interfaces.

1. INTRODUCTION

Consider an ultrasonic beam incident on a liquid–solid interface. For a wide range of angles of incidence this problem can be mathematically described by solving the boundary-value problem under the assumption of energy conservation. At the critical angles, however, experimental verification of the calculated results is complicated by the fact that the reflected beam appears to be "displaced." This effect is especially pronounced at the angle for excitation of surface waves along the interface, as has been demonstrated by Schoch.[1] The "displacement" of the reflected beam is attributed to the fact that a beam does not behave as an infinitely extended plane wave, as is tacitly assumed in the simplified theory.

The situation is shown in Fig. 1. An ultrasonic beam is incident upon an interface at an angle θ_0 (approximately the angle at which surface waves are excited on the interface). The beam, assumed to be infinitely extended in a direction normal to the figure, is displaced a distance Δ upon reflection. In developing a theory to describe this effect, one includes the mutual phase relation of partial waves in the reflected beam by expanding the expression for the phase shift upon reflection $\Phi(p)$ into a power series of the form

$$\Phi(p)=\Phi+\Phi'(p-\alpha)+{}^1/_2\Phi''(p-\alpha)^2\ldots, \qquad (1)$$

where

$$\Phi=\Phi(\alpha),\quad \Phi'=\left(\frac{\partial\Phi}{\partial p}\right)_{p=\alpha},\quad \Phi''=\left(\frac{\partial^2\Phi}{\partial p^2}\right)_{p=\alpha},$$

$$p=k\sin\theta,\quad \alpha=k\sin\theta_0,\quad k=2\pi/\lambda,$$

λ = the ultrasonic wavelength in the liquid, θ_0 is the angle of incidence, and θ is the angle of incidence of a wavelet in the incident beam. By carrying out this analysis in the first approximation, one finds that the displacement is

$$\Delta=-\left(\frac{\partial\Phi}{\partial p}\right)_{p=\alpha}=-\Phi'. \qquad (2)$$

In this approximation, the beam profile of the reflected beam (i.e., the amplitude distribution of the reflected beam measured parallel to the interface) is the same as the beam profile of the incident beam. Such profiles are sketched on Fig. 1 as Fig. 1a and Figure 1b.

In making a comparison between theory and experiment, it has been found that there is nominal agreement between the measured "displacement" and that calculated from relation (1); however, the experiment is complicated by the presence of unexpected reflected beams. For this reason, it is necessary to carry out the analysis in the second approximation, to include the second-order terms in relation (1). In this higher approximation, the "beam displacement" loses its meaning. The profile of the reflected beam is not the same as that of the incident beam, i.e., there is an "energy redistribution" in the reflected beam. (Figure 1b would no longer be the same as Figure 1a.)

Brekhovskikh [2] has developed a detailed theory for the reflection of a bounded ultrasonic beam at a liquid–solid interface. From this theory he obtained an expression for the amplitude of the reflected beam and for the "displacement" of the reflected beam. Brekhovskikh also pointed out that the structure of the reflected beam is in general different from that of the incident beam, i.e., that there is an "energy redistribution." He obtained an expression for the amplitude distribution in the reflected beam as a function of the distance along the interface, and solved a special case under the assumption that the incident beam is accurately described by a step function.

In a comparison between theory and experiment, we have encountered the fact that a step-function distribution in the incident ultrasonic beam leads to diffraction effects which confuse the comparison. For this reason, we have developed a transducer which produces an amplitude distribution in the incident beam which is accurately described by a Gaussian function.[3] The Gaussian function amplitude distribution produces a single well-defined beam without diffraction lobes. The purpose of the present work is to show how closely the experimental results obtained with a Gaussian distribution of amplitudes in the incident ultrasonic beam agree with those calculated from the approximate extension of the Brekhovskikh theory.

2. ENERGY REDISTRIBUTION OF A REFLECTED GAUSSIAN BEAM: THEORY

In order to represent the beam as a superposition of plane waves, Brekhovskikh writes the field in the plane $z = l$ (at the interface) as a Fourier integral. By introducing the amplitude reflection coefficient $V(\theta_0)$, which is a function of the angle of incidence θ_0, the general form of the solution to the wave equation which describes the reflected beam is written as

$$\psi_{\text{refl}}(x)=\frac{1+i}{2}V(\theta_0)\exp\{i[\alpha x+\sqrt{(k^2-\alpha^2)}\,l]\}$$
$$\times\int_{-\infty}^{\infty}\left\{\exp\left(-i\frac{\pi}{2}u^2\right)\right\}F(x+\Phi'+\sqrt{\pi\Phi''}u)\,du, \qquad (3)$$

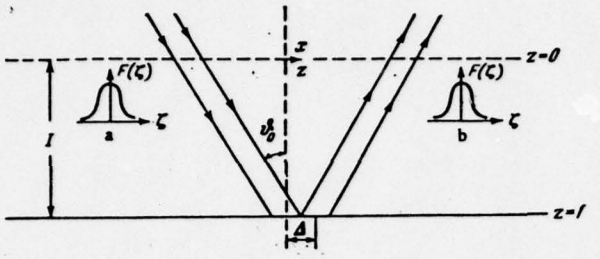

Fig. 1. First-order representation of the reflection of an ultrasonic wave at a liquid–solid interface. a) Incident beam cross section; b) reflected beam cross section.

where l is the normal distance between the transmitter and the liquid–solid interface, $u = (x+\Phi'-\zeta)/\sqrt{\pi\Phi''}$, ζ is the variable of integration in the original Fourier integral, and $F(x+\Phi'+\sqrt{\pi\Phi''}\,u)$ describes the incident beam functional dependence on the amplitude distribution along the interface. [In Eq. (3) the higher approximation, inclusion of second-order terms in Eq. (1), has been made.]

For the present purposes, $F(x+\Phi'+\sqrt{\pi\Phi''}\,u)$ is to be a Gaussian function. Such a function does not change appreciably over a distance of one wavelength along the propagation direction. This satisfies the requirement imposed by the manner in which Eq. (3) was derived. The Gaussian function describing the incident beam can be written

$$F(x+\Phi'+\sqrt{\pi\Phi''}\,u)=A\exp[-B(x+\Phi'+\sqrt{\pi\Phi''}\,u)^2], \tag{4}$$

where A and B are experimentally determined constants which depend on the characteristics of the transducer. The amplitude of the reflected beam then may be obtained by substituting Eq. 4 into Eq. 3:

$$\psi_{\text{refl}}(x)=\frac{1+i}{2}V(\theta_0)\exp\{i[\alpha x+\sqrt{k^2+\alpha^2}\,l]\}$$
$$\times A\int_{-\infty}^{\infty}\left\{\left[\exp\left(-i\frac{\pi}{2}u^2\right)\right]\exp[-B(x+\Phi'+\sqrt{\pi\Phi''}\,u)^2]\right\}du. \tag{5}$$

A solution to Eq. (5) can be obtained if the limits on the integrals are defined as follows:

$$u_1=-\frac{1}{\sqrt{\pi\Phi''}}(a+x+\Phi'); \tag{6}$$

and

$$u_2=+\frac{1}{\sqrt{\pi\Phi''}}(a-x-\Phi'), \tag{7}$$

where a is the half-width of the Gaussian beam at a point where the energy decreases to 1/e of its maximum value. Then, using $e^{-iy}=\cos y-i\sin y$ to express the first exponential under the integral, and expanding the second exponential into a power series, one obtains a series whose terms are integrable.[4] Terms up to fourth order are kept in the following expressions. The energy distribution for the reflected beam is then obtained by multiplying the integrated form of Eq. (5) by its complex conjugate:

$$E(x)=\psi(x)\psi^*(x)=\frac{V(\theta_0)^2}{2}A^2\{\exp[-2B(x+\Phi')^2]\}[(T_1+T_2+T_3+T_4+T_5+T_6+T_7)^2+(T_8+T_9+T_{10}+T_{11}+T_{12}+T_{13}+T_{14})^2]. \tag{8}$$

where

$$T_1=C(u_2)-C(u_1); \tag{9}$$

$$T_2=-2B^2\Phi''^2\left[u_2^2\sin\left(\frac{\pi}{2}u_2^2\right)+2\cos\left(\frac{\pi}{2}u_2^2\right)-\pi u_1^2\sin\left(\frac{\pi}{2}u_1^2\right)-2\cos\left(\frac{\pi}{2}u_1^2\right)\right] \tag{10}$$

$$T_3=-8\sqrt{\frac{\pi}{2}}B^2\Phi''^{3/2}(x+\Phi')\left[u_2\sin\left(\frac{\pi}{2}u_2^2\right)-S(u_2)-u_1\sin\left(\frac{\pi}{2}u_1^2\right)+S(u_1)\right]; \tag{11}$$

$$T_4=-4B^2\Phi''(x+\Phi')^2\left[\sin\left(\frac{\pi}{2}u_2\right)^2-\sin\left(\frac{\pi}{2}u_1\right)^2\right]; \tag{12}$$

$$T_5=-\Phi''^2B^2\left[2\pi u_2^2\sin\left(\frac{\pi}{2}u_2\right)^2+\frac{\pi}{2}u_2\cos\left(\frac{\pi}{2}u_2\right)^2-\frac{\pi}{\sqrt{2}}C(u_2)-2\pi u_1^2\sin\left(\frac{\pi}{2}u_1\right)^2-\frac{\pi}{2}u_1\cos\left(\frac{\pi}{2}u_1\right)^2+\frac{\pi}{\sqrt{2}}C(u_1)\right]; \tag{13}$$

$$T_6=-\sqrt{\Phi''^3}(x+\Phi')B^2\left[\frac{\pi}{3}u_2^3\sin\left(\frac{\pi}{2}u_2\right)^2+0.9\cos\left(\frac{\pi}{2}u_2\right)^2+\frac{\pi}{3}u_1^3\sin\left(\frac{\pi}{2}u_1\right)^2-0.9\cos\left(\frac{\pi}{2}u_1\right)^2\right]; \tag{14}$$

$$T_7=-\Phi''^2B^2(x+\Phi')^2\left[2.5u_2\sin\left(\frac{\pi}{2}u_2\right)^2-2\pi S(u_2)-2.5u_1\sin\left(\frac{\pi}{2}u_1\right)^2+2\pi S(u_1)\right]; \tag{15}$$

$$T_8=S(u_2)-S(u_1); \tag{16}$$

$$T_9=-2B^2\Phi''^2\left[-\pi u_2^2\cos\left(\frac{\pi}{2}u_2^2\right)+2\sin\left(\frac{\pi}{2}u_2^2\right)+\pi u_1^2\cos\left(\frac{\pi}{2}u_1^2\right)-2\sin\left(\frac{\pi}{2}u_1^2\right)\right], \tag{17}$$

$$T_{10}=-8B^2\sqrt{\frac{\pi}{2}}\Phi''^{3/2}(x+\Phi')\left[-u_2\cos\left(\frac{\pi}{2}u_2^2\right)+C(u_2)+u_1\cos\left(\frac{\pi}{2}u_1^2\right)-C(u_1)\right]; \tag{18}$$

$$T_{11}=-4B^2\Phi''(x+\Phi')^2\left[-\cos\left(\frac{\pi}{2}u_2^2\right)+\cos\left(\frac{\pi}{2}u_1^2\right)\right]; \tag{19}$$

$$T_{12}=-\Phi''^2B^2\left[-2\pi u_2^2\cos\left(\frac{\pi}{2}u_2\right)^2+\frac{\pi}{2}u_2\sin\left(\frac{\pi}{2}u_2\right)^2-\frac{\pi}{\sqrt{2}}S(u_2)-2\pi u_1^2\cos\left(\frac{\pi}{2}u_1\right)^2+\frac{\pi}{2}u_1\sin\left(\frac{\pi}{2}u_1\right)^2+\frac{\pi}{\sqrt{2}}S(u_1)\right]; \tag{20}$$

$$T_{12}=-\sqrt{\Phi''(x+\Phi')}B^2\left[1.1u_2^2\sin\left(\frac{\pi}{2}u_2\right)^2+0.9\cos\left(\frac{\pi}{2}u_2\right)^2\right.$$
$$\left.-1.1u_1^2\sin\left(\frac{\pi}{2}u_1\right)^2-0.9\cos\left(\frac{\pi}{2}u_1\right)^2\right]; \quad (21)$$

$$T_{11}=-\Phi''B^2(x+\Phi')\left[-2.5u_2\cos\left(\frac{\pi}{2}u_2\right)^2+2\pi C(u_2)\right.$$
$$\left.+2.5u_1\cos\left(\frac{\pi}{2}u_1\right)^2-2\pi C(u_1)\right]; \quad (22)$$

where the C(u) and S(u) are the cosine and sine Fresnel integrals, respectively. The other parameters have been determined experimentally, and Eq. (8) has been programmed for a computer calculation.

3. ENERGY REDISTRIBUTION OF A REFLECTED GAUSSIAN BEAM: EXPERIMENT

Apparatus

The experimental apparatus is shown in Fig. 2. The electronic system is a standard pulse arrangement, with the signal from the receiver transducer being displayed on an oscilloscope. Two aspects of the arrangement are unique, however: the goniometer and the transducers. In the experimental situation both the driver and the receiver transducer are mounted on the goniometer and this unit is placed in a tank of water.

Goniometer system. A schematic diagram of the goniometer is shown in Fig. 2. The system is designed so that the face of the specimen (or reflector) forms a vertical plane at the center of a circle formed by rotation of the two arms. A vernier scale on each arm permits the angular position of each arm to be read to two minutes of arc. Both arms have transducer holder stages mounted on riders that allow the transducers to be moved up to 50 cm in a radial direction. In addition, the transducer on the receiver arm can be moved perpendicular to the arm (or radius). This way accurate scanning of the reflected beam can be accomplished. The reflectors have dimensions of 10×5×2.5 cm and have machined surfaces.

Transducer. Details of the behavior of an ultrasonic wave reflected from an interface depend fundamentally on the energy distribution in the cross section of the incident ultrasonic beam [see Eq. (3)]. The mathematical interpretation of the results is facilitated if the energy distribution in the incident beam cross section can be described in a simple relation such as a Gaussian function. The experimental measurements are also more straightforward if one uses a Gaussian function distribution in the ultrasonic beam. This can be demonstrated by schlieren photography.

Figure 3a is a schlieren photograph of a 4 MHz ultrasonic beam from a narrow transducer incident at an angle of 35 deg upon a water–aluminum interface. This beam has a step function distribution of amplitudes near the transducer. The interpretation problem resulting from the diffraction lobes is obvious. Figure 3b shows an ultrasonic beam of approximately the same width and frequency with a Gaussian amplitude distribution across its width. This beam, produced by a new transducer,[3] is incident on the same interface at the same angle of incidence. In addition to the absence of diffraction lobes, there is less divergence in the Gaussian ultrasonic beam.

The Gaussian distribution was obtained by using a narrow electrode at the back of the quartz transducer and grounding the entire front plane. Fringing of the electrical field in the quartz transducer material closely approximates a Gaussian function if the ratio of the width W of the back electrode to the thickness T of the transducer material is $2 < W/T < 4$.

The ultrasonic beam profile emitted by these transducers could be obtained by using the goniometer system with the sample removed. All measurements with the goniometer system were made at a frequency of 2 MHz. A plot of the energy distribution obtained by using the new transducers both as transmitter and receiver is given in Fig. 4. The experimental points have been fitted by a Gaussian function of the form, $A\exp(-Bx^2)$, where A = 1

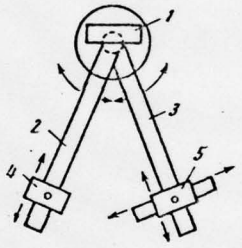

Fig. 2. Experimental apparatus (diagram of goniometer. 1) Specimen (reflector); 2, 3) rotating arms; 4) movable emitting transducer; 5) movable receiving transducer.

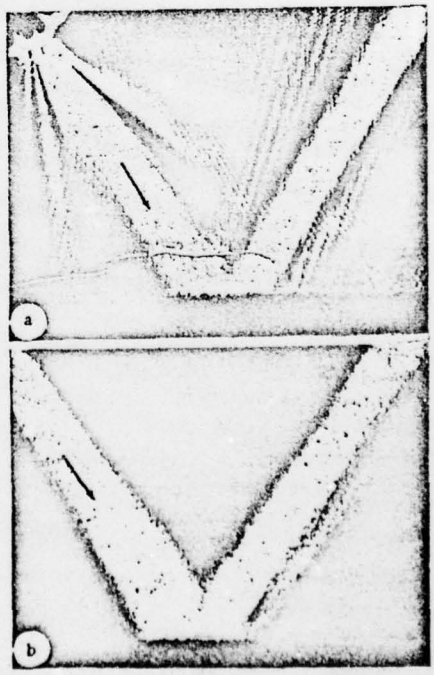

Fig. 3. Schlieren photographs of transducer outputs. a) Step-function output; b) Gaussian output.

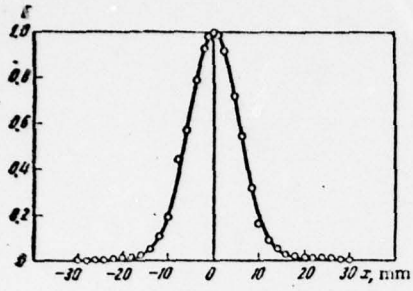

Fig. 4. Cross section of transducer output.

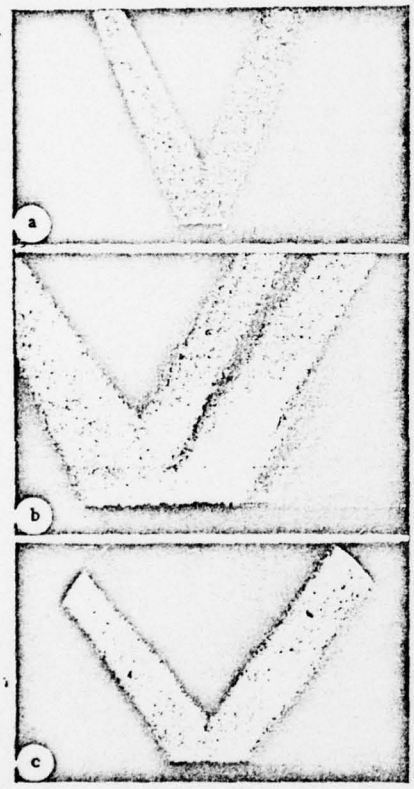

Fig. 5. Schlieren photographs of actual energy redistribution in reflected Gaussian ultrasonic beam. a) $\theta_1 < \theta_R$; b) $\theta_1 = \theta_R$, the angle for excitation of Rayleigh surface waves; c) $\theta_1 > \theta_R$.

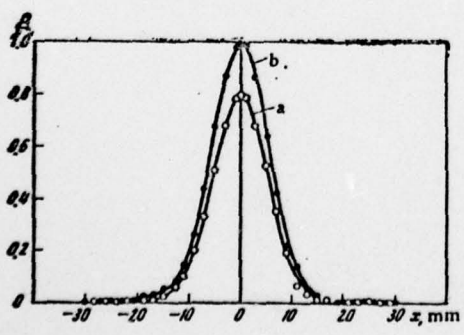

Fig. 6. Cross section of reflected Gaussian beams at $\theta_1 < \theta_R$(a) and $\theta_1 > \theta_R$(b).

and B = 0.016. The agreement between the calculated curve and the experimental points indicates that the ultrasonic beam produced by the new transducers is accurately described by a Gaussian function.

Experimental Procedure

To be able to compare experimental results on the energy distribution in the reflected beam with the theoretical predictions, it is necessary to determine both Φ' and Φ''. In addition to determining the slope of the measured and calculated phase shift Φ done previously,[5] one can determine Φ' directly by measuring the "displacement," and compare these results with those calculated from the theory of Brekhovskikh. The quantity Φ'' is then the slope of Φ' at the appropriate angle of incidence.

Measurement of Φ'. From relation (2), the quantity Φ' is the negative of the "displacement." This is measured as follows. The transmitter arm of the goniometer is set at the desired angle of incidence and the receiver arm is rotated until a maximum signal is obtained on the oscilloscope. The receiver transducer is then shifted laterally (perpendicular to the receiver arm) in both directions. An increase of received signal indicates the direction of the "displacement." A maximum in the received signal locates the position of the displaced beam. This displacement is then measured for different angles of incidence. A correction is made for the fact that the motion is perpendicular to a radius rather than parallel to the interface, as assumed in the theory.

Measurement of the energy redistribution. The energy redistribution is more meaningfully studied by measuring the energy distribution in the reflected beam both at the angle at which surface waves are excited on the interface (maximum displacement) and at angles at which displacement is imperceptible. The procedure was as follows.

By means of the goniometer, the incident beam was set at a previously chosen angle of incidence. The receiver arm was set at the same (reflection) angle. The receiver transducer was then displaced perpendicular to the receiver arm in increments of 2 mm in both directions. The receiver transducer output was monitored by means of the oscilloscope. Considerable care was necessary to determine the exact angle of incidence for maximum displacement.

4. RESULTS AND DISCUSSION

Careful schlieren photography has shown us that even with the transducers which produce a Gaussian distribution of energy in the incident beam, the beam is reflected as multiple beams when the angle of incidence is that at which surface waves are excited on the interface (maximum displacement). This is shown in Fig. 5b for a water–brass interface. Figs. 5a and 5c are schlieren photographs for angles of incidence respectively smaller and larger than this angle.

Data from scans of the reflected beams with the goniometer system for angles corresponding to Figs. 5a and 5c are shown in Fig. 6. A brass reflector was used. An incident angle of 10° is well below the longitudinal critical angle for brass; an angle of 54° is well above the angle

for excitation of surface waves. A straightforward calculation from the simplified theory gives an energy reflection coefficient of 80% at 10° and 100% at 54°. These values are consistent with the maximum values of the curves in Figure 6.

The displacement (of the reflected beam in a direction parallel to the interface) as a function of the angle of incidence was determined for a water–aluminum interface and a water–brass interface. The results are shown in Figs. 7 and 8. Experimental data are indicated by points. The curves are the results of computer calculations based on the theory of Brekhovskikh. On these curves the values of the critical angle for the longitudinal wave in the solid (θ_{Cl}) and for the shear wave in the solid (θ_{CS}), as well as the optimum angle for excitation of surface waves on the interface (θ_R) are indicated. The maximum displacement of the principal beam occurs at θ_R. Also, at θ_R there is an energy redistribution as shown in Fig. 5b.

The graphs in Figs. 7 and 8 are plots of the negative of the quantity Φ', as indicated in Eq. (2). That value of most importance to the following comparison between theory and experiment is the maximum value occurring at $\theta_R = 30.5°$ for aluminum and $\theta_R = 47.0°$ for brass. The values of these quantities evaluated from these data and used in the computer calculation of Eq. (8) were $(\Phi')_R = -14.5$ mm for aluminum and $(\Phi')_R = -16.5$ mm for brass.

The quantity Φ'' could also be determined from these curves, although this was a much less precise measurement. The values used in the computer calculation of Eq. (8) were $(\Phi'')_R = -5$ mm^2 for aluminum and $(\Phi'')_R \doteq -7$ mm^2 for brass.

Energy Redistribution in the Presence of Surface Waves

Measured values of the energy as a function of position of the receiver transducer for ultrasonic waves reflected from a water–aluminum interface at the angle $\theta_R = 30.5°$ are shown in Fig. 9a. The solid line is calculated from Eq. (8) with values of the various parameters as follows: $\Phi' = -14.8$ mm, $\Phi'' = -5$ mm^2, $a = 8$ mm, A = 1, B = 0.016.

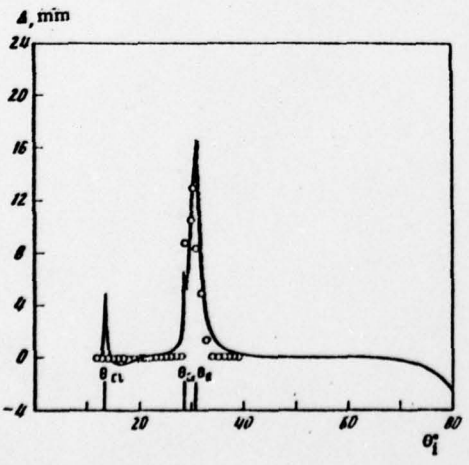

Fig. 7. Comparison between "displacement" and $-\Phi'$ (first derivative of phase shift upon reflection) as a function of incident angle for water–aluminum interface.

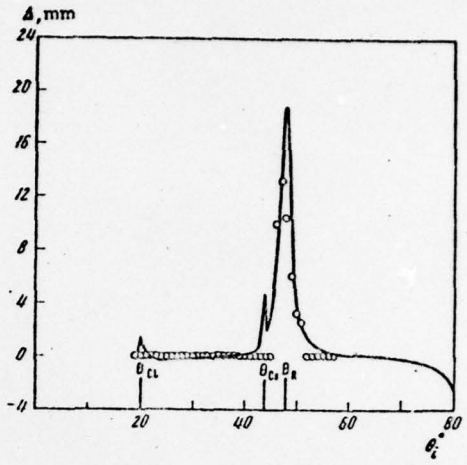

Fig. 8. Comparison between displacement and $-\Phi'$ for water–brass interface.

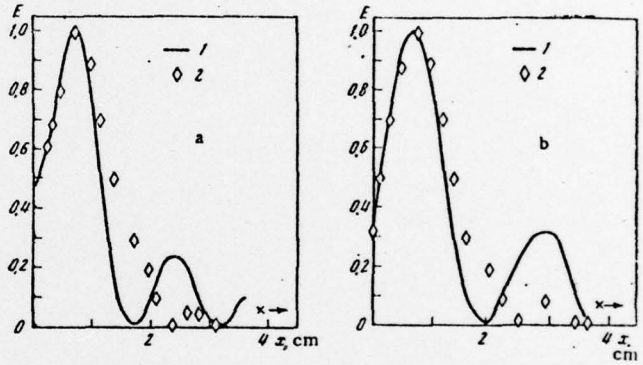

Fig. 9. Energy redistribution in a Gaussian ultrasonic beam reflected from: a) a water–aluminum interface; b) a water–brass interface; $\theta_i = \theta_R$ in both cases.

Energy redistribution in an ultrasonic Gaussian beam from a water–brass interface is shown in Fig. 9b. The angle of incidence was the optimum angle for surface wave generation $\theta_R = 47.0°$. The theoretical curve was calculated from Eq. (8) with the following experimentally determined parameters: $\Phi' = -16.5$ mm, $\Phi' = -7$ mm^2, $a = 8$ mm, A = 1, and B = 0.016.

Both the experimental and the theoretical curves in Figs. 9a and 9b indicate that an incident Gaussian beam, upon reflection at the angle of optimum generation of surface waves, is redistributed into multiple beams (two of which were detectable over the distance of traverse of the receiver transducer). The schlieren photograph Figure 5b indicates that there are actually more than two reflected beams.

5. SUMMARY

It has been suggested in this paper that an ultrasonic beam reflected from a liquid–solid interface at the angle at which surface waves are generated has a different energy distribution from the incident beam. Therefore, the concept of the "beam displacement" expresses only a

gross effect. Applying the mathematical analysis which was introduced by Brekhovskikh, an analytic expression was derived for the reflected amplitude for the case of an incident Gaussian beam. The theory was experimentally tested for water–aluminum and for water–brass interfaces. The transmitter and the receiver transducers were specially designed apodized transducers with a Gaussian output. Both the theoretical and the experimental results indicate that the incident Gaussian beam is redistributed by the reflection process into multiple beams. The position and the relative heights of these beams are functions of the transducer characteristics. They depend also on the liquid–solid interface through the first and second derivative of the phase shift upon reflection. There is fair agreement between theory and experiment concerning the position and height of the secondary beam, while good agreement is obtained for the position of the principal beam.

To understand the "displacement" phenomenon, one can consider the finite extension of the beam as a superposition of partial plane waves whose mutual phase relations are sensitive functions of their angle of reflection. The individual plane wave components are therefore superimposed with mutual phase relations which differ from those of the incident beam. The change of the mutual phase relations of the plane wave components is interpreted as the physical origin of the "beam displacement," or, in fact, the energy redistribution.

[1]A. Schoch, Acustica 2, 18-19 (1952).
[2]L. M. Brekhovskikh, Waves in Layered Media, Academic Press, New York (1960).
[3]F. D. Martin and M. A. Breazeale, J. Acoust. Soc. Am. 49, 1668-1669 (1971).
[4]I. S. Gradshteyn and I. M. Ryzhik, Table of Integrals, Series, and Products. Academic Press, New York (1965).
[5]A. L. Van Buren and M. A. Breazeale, J. Acoust. Soc. Am. 44, 1014-1020 (1968).

Paper No. 2

Reflection of a Gaussian Ultrasonic Beam from a Liquid-Solid Interface (M. A. Breazeale, Laszlo Adler, and Larry Flax), J. Acoust. Soc. Am. 56, 866-872 (1974)

Reflection of a Gaussian ultrasonic beam from a liquid–solid interface*

M. A. Breazeale and Laszlo Adler

Department of Physics, The University of Tennessee, Knoxville, Tennessee 37916

Larry Flax

Naval Research Laboratory, Washington, D.C., 20375

(Received 11 December 1973; revised 8 February 1974)

A Gaussian distribution of amplitudes in an ultrasonic beam reflected from liquid–solid interfaces is used in the reexamination of the concept of "beam displacement" which occurs at the angle of excitation of surface waves on the interface. Experimental results show that the energy of the reflected beam is redistributed into two or more beams at (or near) this angle. The theory of Brekhovskikh has been extended to include both a Gaussian input beam and the second derivative of the phase shift upon reflection. Reasonable agreement is obtained between theory and experiment for water–aluminum and water–brass interfaces. For water–beryllium and water–stainless steel the agreement is fair.

Subject Classification: 35.24, 35.26; 20.30; 45.10.

INTRODUCTION

Consider an ultrasonic beam incident on a liquid–solid interface. For a wide range of angles of incidence this problem can be mathematically described by solving the boundary value problem under the assumption of energy conservation. At the critical angles, however, experimental verification of the calculated results is complicated by the fact that the reflected beam appears to be "displaced." This effect is especially pronounced at the angle for excitation of surface waves along the interface, as has been demonstrated by Schoch.[1] The "displacement" of the reflected beam was attributed to the fact that a beam does not behave as an infinitely extended plane wave.

The situation is shown in Fig. 1. An ultrasonic beam is incident upon an interface at an angle θ_0 (approximately the angle at which surface waves are excited on the interface). The beam, assumed to be infinitely extended in a direction normal to the figure, is displaced a distance Δ upon reflection. In developing a theory to describe this effect, one defines the reflection coefficient as a complex quantity $Re^{i\Phi(p)}$ and includes the mutual phase relation of partial waves in the reflected beam by expanding the expression for the phase shift upon reflection $\phi(p)$ into a power series of the form[2]

$$\phi(p) = \phi + \phi'(p-\alpha) + \tfrac{1}{2}\phi''(p-\alpha)^2 + \cdots , \qquad (1)$$

where $\phi = \phi(\alpha)$, $\phi' = (\partial\phi/\partial p)_{p=\alpha}$, $\phi'' = (\partial^2\phi/\partial p^2)_{p=\alpha}$, and $p = k\sin\theta$, $\alpha = k\sin\theta_0$, $k = 2\pi/\lambda$, λ = the ultrasonic wavelength in the liquid, θ_0 is the angle of incidence, and θ is the angle of incidence of a wavelet in the incident beam. By carrying out this analysis in the first approximation, one finds that the displacement is[2]

$$\Delta = -(\partial\phi/\partial p)_{p=\alpha} = -\phi' . \qquad (2)$$

In this approximation, the beam profile of the reflected beam (i.e., the energy distribution of the reflected beam measured parallel to the interface) is the same as the beam profile of the incident beam. Such profiles are sketched on Fig. 1 as Fig. 1(a) and Fig. 1(b).

In making a comparison between theory and experiment, it has been found[1–3] that there is nominal agreement between the measured "displacement" and that calculated from Eq. 1; however, the experiment is complicated by the presence of unexpected reflected beams. For this reason, it is necessary to carry out the analysis in the second approximation to include the second-order terms in Eq. 1. In this higher approximation, the "beam displacement" loses its meaning. The profile of the reflected beam is not the same as that of the incident beam; i.e., there is an "energy redistribution" in the reflected beam. [Figure 1(b) would no longer be the same as Fig. 1(a).]

Brekhovskikh[2] has developed a detailed theory for the reflection of a bounded ultrasonic beam at a liquid–solid interface. From this theory he obtained an expression for the amplitude of the reflected beam. Brekhovskikh also pointed out that the structure of the reflected beam is in general different from that of the incident beam, i.e., that there is an "energy redistribution." He obtained an expression for the amplitude distribution in the reflected beam as a function of the distance along the interface, and solved a special case under the assumption that the incident beam is accurately described by a rectangular function.

In a comparison between theory and experiment, we have encountered the fact that a rectangular function distribution in the incident ultrasonic beam leads to diffraction effects which confuse the comparison. For this reason, we have developed a transducer which produces an amplitude distribution in the incident beam which is accurately described by a Gaussian function.[4] The Gaussian function amplitude distribution produces a single well-defined beam without diffraction lobes. The purpose of the present work is to show how closely the experimental results obtained with a Gaussian distri-

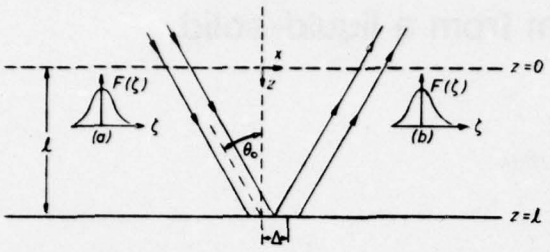

FIG. 1. Reflection of an ultrasonic wave at a liquid–solid interface. (a) Incident beam cross section. (b) First-order representation of reflected beam cross section.

bution of amplitudes in the incident beam agree with those calculated from the appropriate extension of the Brekhovskikh theory.

I. REFLECTION OF A GAUSSIAN BEAM-THEORETICAL CALCULATION OF ENERGY REDISTRIBUTION

In order to represent the beam as a superposition of plane waves, Brekhovskikh writes the field in the plane $z = l$ (at the interface) as a Fourier integral. By introducing the amplitude reflection coefficient $V(\theta_0)$, which is a function of the angle of incidence θ_0, the general form of the solution to the wave equation which describes the reflected beam is written as

$$\psi_{\mathrm{refl}}(x) = \frac{1+i}{2} V(\theta_0) \exp\{i[\alpha x + l\sqrt{(k^2-\alpha^2)}]\} \times \int_{-\infty}^{\infty} \left\{\exp\left(-i\,\frac{\pi}{2}u^2\right)\right\} F[x+\phi' + \sqrt{\pi\phi''}\,u]\,du\,, \tag{3}$$

where l is the distance between the transmitter and the liquid–solid interface, $u = (x+\phi'-\xi)/\sqrt{\pi\phi''}$, ξ is the

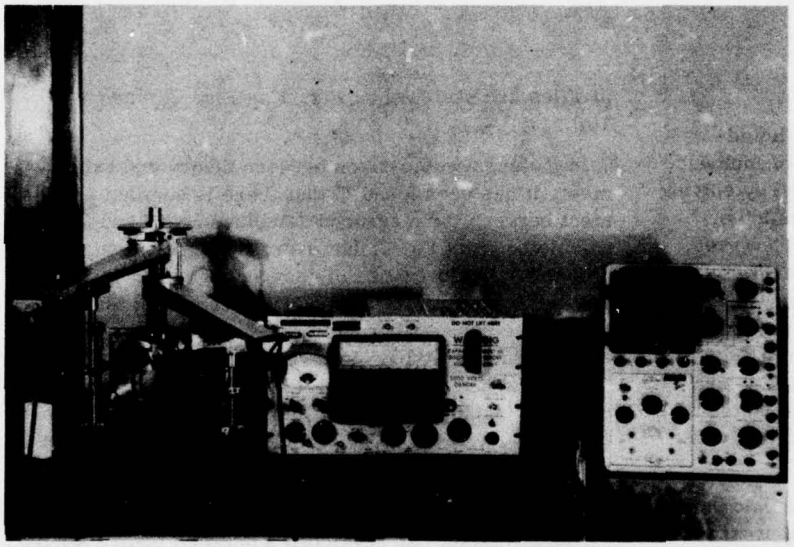

(a)

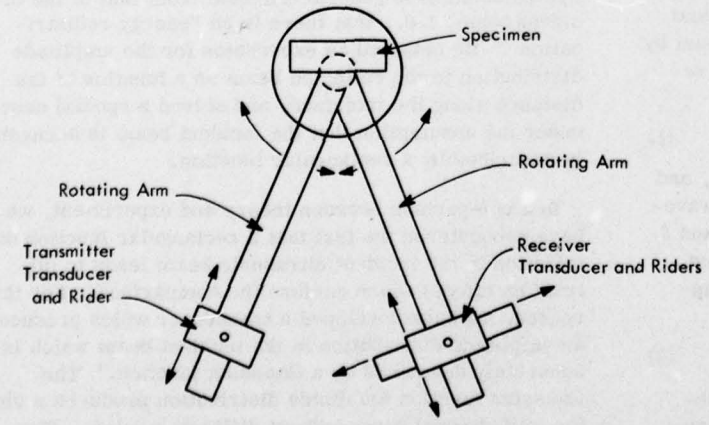

(b)

FIG. 2. Experimental arrangement. (a) Apparatus. (b) Diagram of goniometer.

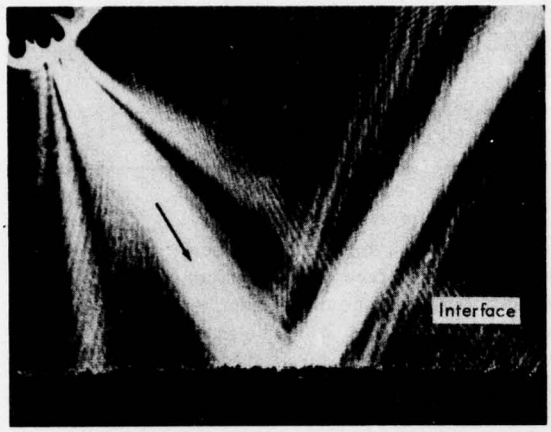

(a) Regular Transducer

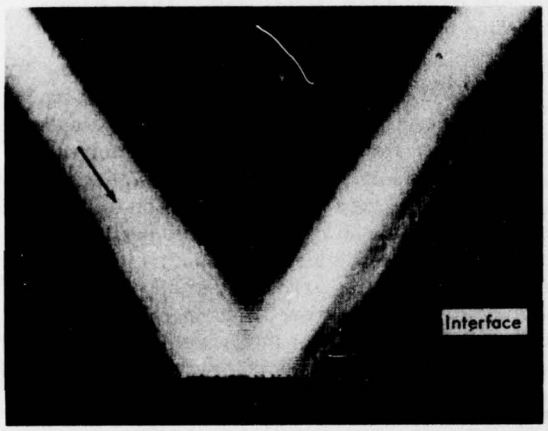

(b) Apodized Transducer

FIG. 3. Schlieren photographs of transducer outputs. (a) Rectangular function amplitude distribution. (b) Gaussian amplitude distribution.

variable of integration in the original Fourier integral, and $F(x+\phi'+\sqrt{\pi\phi''}\,u)$ describes the incident beam functional dependence on the amplitude distribution along the interface. (In Eq. 3 the higher approximation, inclusion of second-order terms in Eq. 1, has been made.)

For the present purposes, $F(x+\phi'+\sqrt{\pi\phi''}\,u)$ is to be a Gaussian function. Such a function does not change appreciably over a distance of one wavelength along the propagation direction. This satisfies the requirement imposed by the manner in which Eq. 3 was derived.[5] The Gaussian function describing the incident beam can be written

$$F(x+\phi'+\sqrt{\pi\phi''}\,u)=A\exp\left[-B(x+\phi'+\sqrt{\pi\phi''}\,u)^2\right], \quad (4)$$

where A and B are experimentally determined constants which depend on the characteristics of the transducer. The amplitude of the reflected beam then may be obtained by substituting Eq. 4 into Eq. 3:

$$\psi_{\mathrm{refl}}(x)=\frac{1+i}{2}\,V(\theta_0)\left\{\exp i\left[\alpha x+l\sqrt{(k^2-\alpha^2)}\right]\right\}$$
$$\times A\int_{-\infty}^{\infty}\left\{\left[\exp\left(-i\,\frac{\pi}{2}\,u^2\right)\right]\right.$$
$$\left.\times\exp\left[-B(x+\phi'+\sqrt{\pi\phi''}\,u)^2\right]\right\}du\,. \quad (5)$$

A solution of Eq. 5 can be obtained in the form of error functions by completing the square and writing the two exponential functions as a single exponential function whose argument is squared. The result is

$$\psi_{\mathrm{refl}}=\frac{A(1+i)\,V(\theta_0)}{\sqrt{4B\phi''+2i}}\left\{\exp i\left[\alpha x+l\sqrt{k^2-\alpha^2}\right]\right\}$$
$$\times\left\{\exp\left[\frac{-iB(x+\phi')^2}{2B\phi''+i}\right]\right\}, \quad (6)$$

where we have used the definition of the error function $2/\sqrt{\pi}\int_0^{\infty}\exp(-v^2)\,dv=1$. The energy distribution in the reflected beam is

$$\psi^*_{\mathrm{refl}}\,\psi_{\mathrm{refl}}=\frac{A^2V^2(\theta_0)}{\sqrt{4B^2\phi''^2+1}}\exp\left[\frac{-2B(x+\phi')^2}{4B^2\phi''^2+1}\right]. \quad (7)$$

This is basically a Gaussian function whose peak has been displaced a distance $-\phi'$ from the position $x=0$, but the width has been changed by the retention of ϕ''.

For the purposes of improving agreement between theory and experiment, one can also define limits on the integral[2] as follows:

$$u_1=-(\pi\phi'')^{-1/2}(a+x+\phi')$$

and

$$u_2=(\pi\phi'')^{-1/2}(a-x-\phi')\,,$$

where a is a measure of the width of the Gaussian beam over which the integration is taken. In this case, the reflected beam is described by

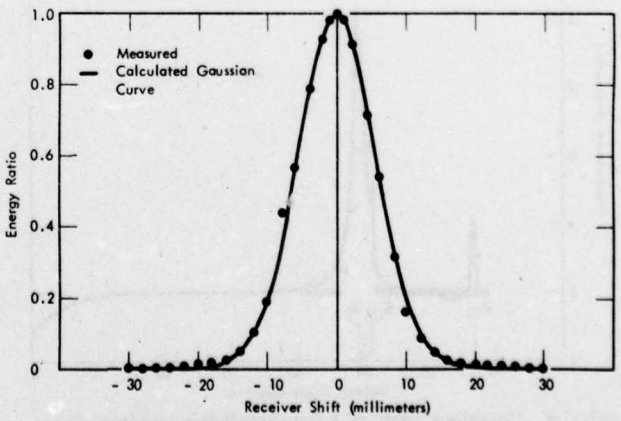

FIG. 4. Energy distribution in the ultrasonic beam emitted by the apodized transducers.

$$\psi_{\text{refl}} = \frac{(1+i)AV(\theta_0)}{4\sqrt{B\phi''+i/2}} \exp i\left[\alpha x + l\sqrt{k^2-\alpha^2} - \frac{2B^2\phi''(x+\phi')^2}{4B^2\phi''^2+1}\right] \exp\left[\frac{-B(x+\phi')^2}{4B^2\phi''^2+1}\right] \left\{\operatorname{erf}\left[u_2\sqrt{B\pi\phi''+i\frac{\pi}{2}} + \frac{B(x+\phi')\sqrt{\phi''}}{\sqrt{B\phi''+i/2}}\right]\right.$$
$$\left. - \operatorname{erf}\left[u_1\sqrt{B\pi\phi''+i\frac{\pi}{2}} + \frac{B(x+\phi')\sqrt{\phi''}}{\sqrt{B\phi''+i/2}}\right]\right\}. \quad (8)$$

This function can be evaluated by computer and the product $\psi^*\psi$ formed to evaluate the energy distribution as a function of position x. Such a function is no longer a simple Gaussian function.

II. REFLECTION OF A GAUSSIAN BEAM–EXPERIMENTAL MEASUREMENT OF ENERGY REDISTRIBUTION

A. Apparatus

The experimental apparatus is shown in Fig. 2. The electronic system is a standard pulse arrangement, with the signal from the receiver transducer being displayed on an oscilloscope. Two aspects of the arrangement are unique, however: the goniometer and the transducers. In the experimental situation both the driver and the receiver transducer are mounted on the goniometer and this unit is placed in a tank of water.

1. Goniometer system

A schematic diagram of the goniometer is shown in Fig. 2(b). The system is designed so that the face of the specimen (or reflector) forms a vertical plane at the center of a circle formed by rotation of the two arms. A vernier scale on each arm permits the angular position of each arm to be read to two minutes of arc. Both arms have transducer-holder stages mounted on riders that allow the transducers to be moved up to 50 cm in a radial direction. In addition, the transducer on the receiver arm can be moved perpendicular to the arm (or radius). This way accurate scanning of the reflected beam can be accomplished.

2. Transducer

Details of the behavior of an ultrasonic wave reflected from an interface depend fundamentally on the energy distribution in the cross section of the incident ultrasonic beam (see Eq. 3). The mathematical interpretation of the results is facilitated if the energy distribution in the incident beam cross section can be described in a simple relation, such as a Gaussian function. The experimental measurements are also more straightforward if one uses a Gaussian function distribution in the incident ultrasonic beam. This can be demonstrated by schlieren photography.

Figure 3(a) is a continuous-wave schlieren photograph of a 4-MHz ultrasonic beam from a narrow transducer incident at an angle of 35° upon a water–aluminum interface. This beam has a rectangular function distribution of amplitudes near the transducer. The interpretation problem resulting from the diffraction lobes is obvious. Figure 3(b) shows an ultrasonic beam of approximately the same width and frequency with a Gaussian amplitude distribution across its width. This beam, produced by a new transducer,[4] is incident on the same interface at the same angle of incidence. In addition to the absence of diffraction lobes, there is less divergence in the Gaussian ultrasonic beam.

The Gaussian distribution was obtained by using a narrow electrode at the back of the quartz transducer and grounding the entire front plane. Fringing of the electrical field in the quartz transducer material closely approximates a Gaussian function if the ratio of the width W of the back electrode to the thickness T of the

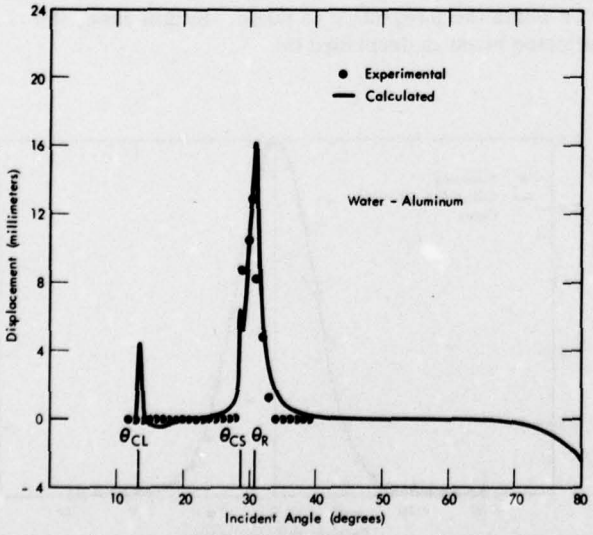

FIG. 5. "Displacement" of a Gaussian beam incident upon a water–aluminum interface, as a function of the angle of incidence.

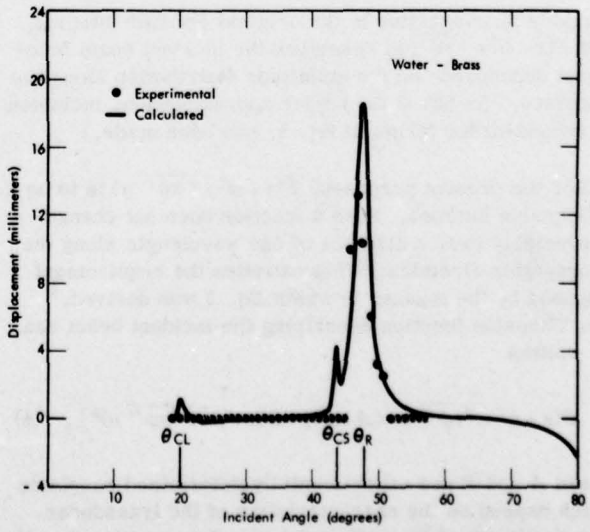

FIG. 6. "Displacement" of a Gaussian beam incident upon a water–brass interface as a function of the angle of incidence.

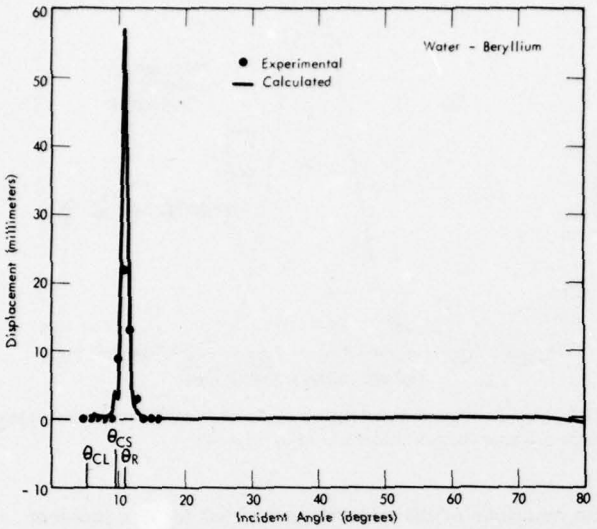

FIG. 7. "Displacement" of a Gaussian beam incident upon a water–beryllium interface as a function of the angle of incidence.

transducer material is $2 < W/T < 4$.

The ultrasonic beam profile emitted by these transducers could be obtained by using the goniometer system with the sample removed. All measurements with the goniometer system were made at a frequency of 2 MHz. A plot of the energy distribution obtained by using the new transducers both as transmitter and receiver is given in Fig. 4. (The transmitter is approximately five times as wide as the receiver.) The experimental points have been fit by a Gaussian function of the form Ae^{-Bx^2}, where $A = 1$ and $B = 0.016$ cm^{-2}. The agreement between the calculated curve and the experimental points indicates that the ultrasonic beam produced by the new transducers is accurately described by a Gaussian function. Since secondary diffraction maxima are no longer present, one could accurately describe these devices as "apodized tranducers."

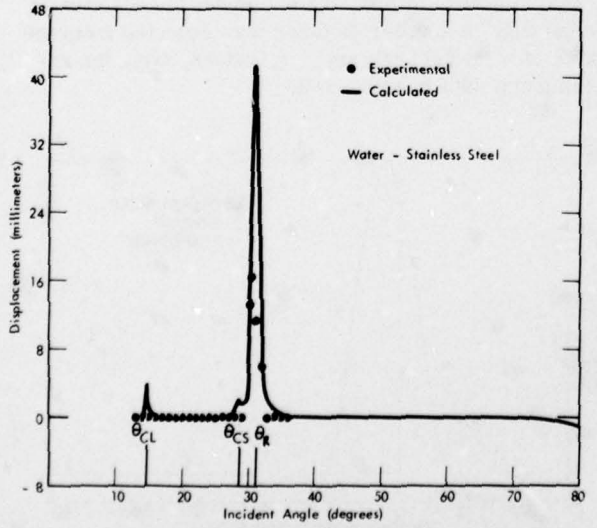

FIG. 8. "Displacement" of a Gaussian beam incident upon a water–stainless steel interface as a function of the angle of incidence.

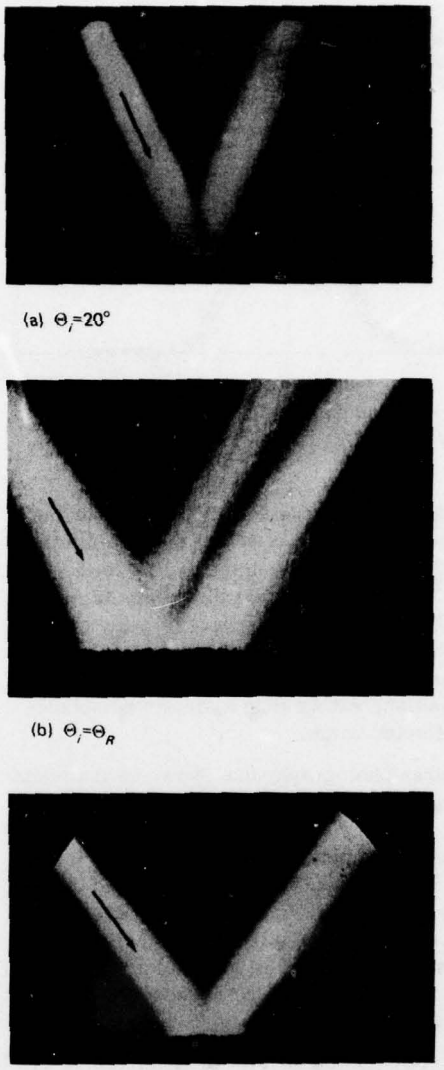

FIG. 9. Schlieren photograph of Gaussian ultrasonic beam reflected from a water–brass interface. (a) $\theta_0 < \theta_R$. (b) $\theta_0 = \theta_R$ energy redistribution is evident. (c) $\theta_0 > \theta_R$.

III. RESULTS

For various angles of incidence, one can follow the position of the maximum in the reflected beam. Within the approximations of the Schoch theory, a plot of the projection of the distance moved by the receiving transducer onto the plane of the face of the reflection would be the "displacement." Plots of this quantity for aluminum, brass, beryllium, and stainless steel are given in Figs. 5–8. Superimposed on the experimental data are plots of $-\phi'$, as indicated[6] in Eq. 2. The critical angle

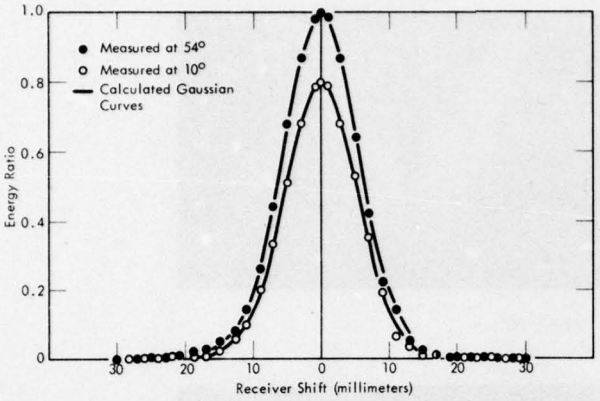

FIG. 10. Energy distribution in the ultrasonic beam reflected from a brass interface for $\theta_0 < \theta_R$ and $\theta_0 > \theta_R$.

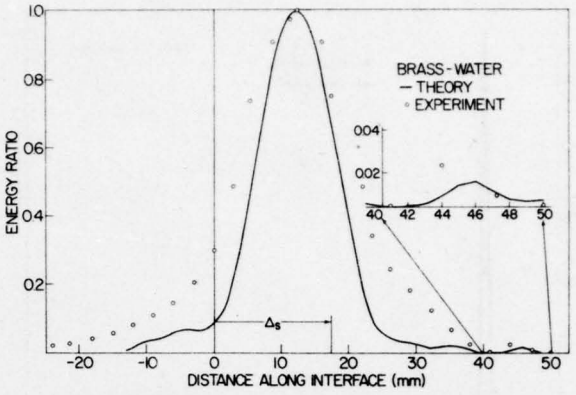

FIG. 12. Energy redistribution in an ultrasonic beam reflected from a water–brass interface at $\theta_0 = \theta_R = 47°$.

for the longitudinal wave in the solid (θ_{cl}), and for the shear wave in the solid (θ_{cs}), as well as the optimum angle for excitation of surface waves on the interface (θ_R) are indicated. It is characteristic that the values of $-\phi'$ at the angle for excitation of surface waves θ_R are consistently greater than the measured "displacement." This results from the fact that, at θ_R, there is in fact an energy redistribution, rather than a simple "displacement" of the reflected beam.

Careful schlieren photography has shown us that even with the apodized transducers, which produce a Gaussian distribution of energy in the incident beam, the beam is reflected as multiple beams when the angle of incidence is that at which surface waves are excited on the interface. This is shown in Fig. 9(b) for a water–brass interface, in which the null strip described by Neubauer[7] is visible. Figure 9(a) and 9(c) are schlieren photographs for angles of incidence respectively smaller and larger than this angle.

Scans of the reflected beams with the goniometer system for angles respectively smaller and larger than the angle for surface wave excitation gave undisplaced Gaussian distributions. The results for a brass reflector shown in Fig. 10 are typical. The curves are Gaussian functions of the same form as that for the incident beam shown in Fig. 4. An incident angle of 10° is well below the longitudinal critical angle for brass; an angle at 54° is well above the angle for excitation of surface waves. A straightforward calculation from the simplified theory gives an energy reflection coefficient of 80% at 10° and 100% at 54°. These values are consistent with the maximum values of the curves in Fig. 10. The other reflectors produced similar results.

Scans of the reflected beam with the incident beam striking the surface at the angle θ_R allowed a measure of the energy redistribution. These results can be compared directly with the theoretical predictions from either Eq. 7 or 8, if one separates out the effect of the "specular" beam described by Neubauer.[7]

Figures 11–14 give the experimental data points obtained by squaring the magnitudes measured across the reflected beam, correcting for the fact that the receiver moves perpendicular to the radius rather than parallel to the interface. Special attention was paid to making the receiver angle exactly equal to the angle of incidence. Because of this, the maximum is consistently "displaced" a smaller distance than expected from the value of ϕ' at the angle α_R, or, indeed, from the experimental data in Figs. 5–8.

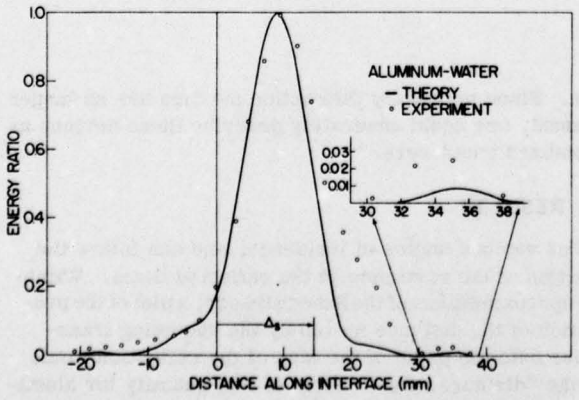

FIG. 11. Energy redistribution in an ultrasonic beam reflected from a water–aluminum interface at $\theta_0 = \theta_R = 30.5°$. Distance is measured from the center of the incident beam.

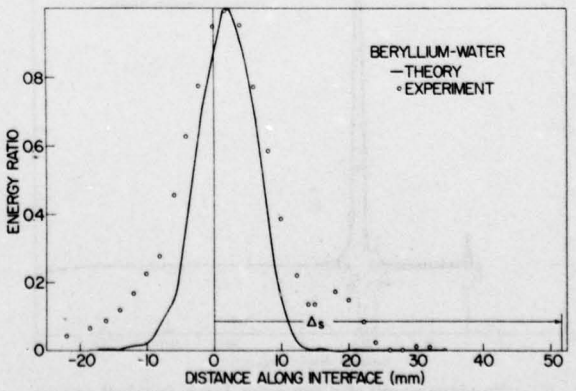

FIG. 13. Energy redistribution in an ultrasonic beam reflected from a water–beryllium interface at $\theta_0 = \theta_R = 12°$.

Superimposed on the experimental data in Figs. 11–14 are theoretical curves calculated from Eq. 8. For reference, values of the "displacement" Δ_S predicted by the Schoch theory are indicated. The fact that the peaks in the experimental data are consistently wider than the theoretical curves is probably associated with the fact that the receiving transducer does not have the ideal infinitesimal width. Values of the parameters ϕ', ϕ'', a, and B used in the calculation for each material are listed in Table I. The values of ϕ' were determined by the positions of the maxima in the experimental data. The value of ϕ'' is not readily measured; thus, a value was selected which produced best agreement between theory and experiment. The value of B was determined by projecting the Gaussian function shown in Fig. 4 onto the interface. The value of a came from the following considerations.

The photograph of Fig. 9(b), as well as the experimental data of Figs. 11–14, show secondary beams in addition to the main beams. Such secondary beams are not predicted by the theory—even including the term in ϕ''—unless the Gaussian function is truncated. A finite value of a is a measure of the position at which this truncation occurs. The value $a = 10$ gave the secondary peak at 34 mm in Fig. 11 for the aluminum data and improved agreement near -5 mm. This value was maintained for the other curves to determine the extent to which the secondary peaks would be predicted by theory for these materials as well.

TABLE I. Parameters used in calculating the theoretical curves.

	ϕ'	ϕ''	a	B
Aluminum	−9	−33	10	0.012
Brass	−12.4	−43	10	0.0076
Beryllium	−2	−13	10	0.016
Stainless steel	−7	−18	10	0.012

IV. SUMMARY AND CONCLUSIONS

The behavior of an ultrasonic wave at a liquid–solid interface is reasonably well described by a solution of the straightforward boundary value problem at most angles of incidence. At the angle of incidence for which the surface waves are excited, this description is inadequate. Schoch's introduction of the idea of a "displacement," while an improvement, also proves to be inadequate. At this angle one observes that the reflected beam has a different energy distribution from the incident beam.[8] Therefore, the concept of "beam displacement" expresses only a gross effect.

The existence of a transducer which produces a truly Gaussian distribution of amplitude has made it possible to make a direct comparison between experimental results from four different interfaces and a theory based on the approach of Brekhovskikh. Both the experimental and the theoretical results indicate that the incident Gaussian beam is redistributed in the reflection process into multiple beams. The positions and relative intensities of these beams are functions of the transducer characteristics. They depend on the characteristics of the liquid–solid interface through the first and second derivative of the phase shift upon reflection. The secondary beams also seem to be associated with truncation of the incident beam. There is reasonable agreement between theory and experiment for the aluminum and the brass interfaces, while the agreement for the beryllium and the stainless steel interfaces is less good. In all cases, the experimental value of the "displacement" is different from that predicted by Schoch.[1] This difference is quite great—a factor of 26—for beryllium.

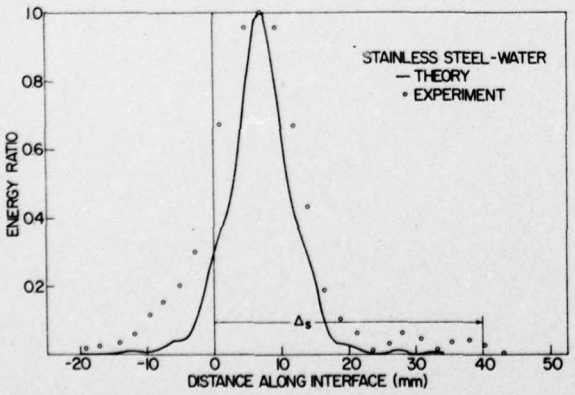

FIG. 14. Energy redistribution in an ultrasonic beam reflected from a water–stainless steel interface at $\theta_0 = \theta_R = 39.8°$.

ACKNOWLEDGMENT

It is a pleasure to acknowledge the helpful discussions and critical comments of Werner G. Neubauer during the period one of the authors (M. A. Breazeale) was Visiting Scientist at the Naval Research Laboratory. It is a pleasure also to acknowledge the contributions of James H. Smith to the experimental aspects of this problem.

*Research supported in part by the U. S. Office of Naval Research.

[1] A. Schoch, Ergeb. Exakten Naturwiss. 23, 127 (1950); Acustica 2, 18–19 (1952).
[2] L. M. Brekhovskikh, *Waves in Layered Media* (Academic, New York, 1960).
[3] O. J. Diachok and W. G. Mayer, IEEE Trans. Sonics Ultrason. 16, 219 (1969).
[4] F. D. Martin and M. A. Breazeale, J. Acoust. Soc. Am. 49, 1668–1669 (1971).
[5] Ref. 2, p. 101.
[6] The values of $-\phi'$ could be obtained by numerically taking derivatives of curves of ϕ such as those given by A. L. Van-Buren and M. A. Breazeale, J. Acoust. Soc. Am. 44, 1014–1020 (1968).
[7] W. G. Neubauer, J. Appl. Phys. 44, 48 (1973).
[8] M. A. Breazeale, L. Adler, and J. H. Smith, Akust. Zh. 20, No. 4 (1974).

Paper No. 3

Interaction of Ultrasonic Waves Incident at the Rayleigh Angle onto a Liquid-Solid Interface (M. A. Breazeale, Laszlo Adler, and Gerald W. Scott), J. Appl. Phys. 48, 530-537 (1977).

Interaction of ultrasonic waves incident at the Rayleigh angle onto a liquid-solid interface

M. A. Breazeale, Laszlo Adler, and Gerald W. Scott

Department of Physics, The University of Tennessee, Knoxville, Tennessee 37916
(Received 2 June 1976; in final form 25 October 1976)

The behavior of a Gaussian ultrasonic beam incident on a liquid-solid interface at the Rayleigh angle, the angle at which surface waves are excited on the interface, has been studied in some detail. The reflected beam is displaced in the manner predicted by Schoch; however, the "Schoch displacement" in general is too large. Good agreement is obtained between experimental results and the theory of Bertoni and Tamir, which assumes that the incident beam couples resonantly into a leaky surface wave at the Rayleigh angle and that the energy reradiated from this leaky surface wave interferes with specularly reflected energy. The propagation distance of the ultrasonic beam is explicitly included in describing the ultrasonic wave reflection at the Rayleigh angle.

PACS numbers: 68.25.+j, 43.35.+d, 68.30.+z

I. INTRODUCTION

A wave incident on a plane interface can experience total reflection under certain conditions. At the smallest angle at which total reflection occurs, one part of the reflected (or refracted) beam propagates tangentially along the surface. Interaction between this tangential component and other (reflected or refracted) components leads to a lateral displacement of the reflected beam. This interaction takes place because the wave has penetrated into the second medium—even under conditions of total reflection.

Even though these observations are consistent with electromagnetic theory, and even though Newton[1] in 1704 suspected that a light wave, upon total internal reflection at a glass-air interface, penetrates into the air, a direct demonstration of the effect did not appear until Goos and Hänchen[2] modified Newton's original experiment by bringing a silver layer into contact with a portion of the glass surface at which total reflection took place. Lateral displacement of the totally reflected beam was demonstrated by direct comparison with a portion of the same beam reflected from the silvered area in which negligible penetration occurred. The effect is greatest at the critical angle, and becomes less pronounced for larger angles of total reflection. An extensive survey of this subject is given by Lotsch,[3] who also mentions the acoustical analogue.

An ultrasonic wave incident upon a liquid-solid interface exhibits two critical angles—one for the longitudinal wave in the solid and one for the shear waves. For angles much larger than the critical angle for shear waves, total reflection also is observed. Near the shear wave critical angle, the reflected beam is displaced in a manner analogous to the optical beam. But it turns out that a different mechanism is responsible for most observed displacements of ultrasonic waves.

By using schlieren photography, Schoch[4] was able to demonstrate a displacement of the reflected beam by photographing the ultrasonic beams in the liquid. As shown in Fig. 1, the reflected beam is displaced a distance Δ laterally along the interface; however, the angle of maximum displacement is somewhat greater than the critical angle for shear waves. Schoch also developed a theory which predicted the lateral displacement of the ultrasonic wave after reflection. The "Schoch displacement" is attributed to the fact that the physically realizable ultrasonic beam does not behave as an infinitely extended plane wave as is usually assumed in solution of boundary-value problems. Schoch included the mutual phase relationship of partial waves in the reflected beam by expanding the expression for the phase shift upon reflection into a power series. The first derivative of the phase shift is identified as the "Schoch displacement".

Brekhovskikh[5] extended Schoch's theory, and by including the second derivative of the phase shift he derived an expression for the amplitude distribution of the reflected beam. This theory subsequently was modified to account for a Gaussian amplitude distribution in the incident beam, and an apodized transducer which produced a Gaussian amplitude distribution[6] in the incident beam was used in a comparison between theory

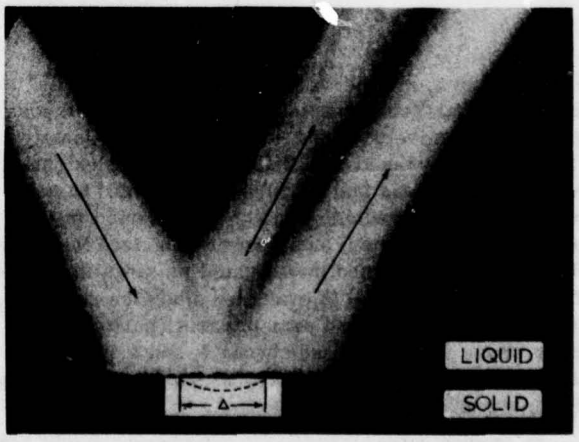

FIG. 1. Schlieren photograph of an ultrasonic beam incident on a liquid-solid (aluminum) interface at the Rayleigh angle. The reflected beam, as indicated, is split into two components: a specular beam and a beam displaced a distance laterally down the interface. Secondary beams are visible at greater distances.

and experiment.[7] A closed-form analytical solution improved the theory and simplified the calculation.[8] Nominal agreement between theory and experiment was obtained for water-aluminum and water-brass interfaces, and poor agreement was obtained for water-beryllium and water—stainless-steel interfaces. In spite of nominal agreement between theory and experiment, these theories were not totally satisfactory since the physical mechanism responsible for the displacement did not enter explicitly. Furthermore, they accounted for the displaced beam only. A number of theorists[5,9–11] and experimenters[12–14] have correctly associated the displaced beam with the excitation of surface waves on the interface, have pointed out that Lord Rayleigh studied surface waves on a free solid interface, and have labelled the angle at which the displacement is a maximum θ_R to distinguish it from the critical angle for shear waves in the solid.

Experimental studies of the reflection of ultrasonic waves from such solids as beryllium and Al_2O_3 revealed a second reflected beam which is not displaced, but is specularly reflected. This beam also is visible in Fig. 1. It is separated from the displaced beam by a "null strip" since the two beams are out of phase.[13]

Bertoni and Tamir[15] introduced a new theory to explain the acoustical Rayleigh-angle problem. This theory is based on earlier work[16] to describe the Goos-Hänchen effect in optics. Their postulated mechanisms include a specular wave and a reradiating surface wave, which they call a "leaky wave" because it leaks energy back into the liquid as the displaced beam. They present a solution for the reflected field which is strictly valid only if both source and point of observation are at the interface. In the present work we point out that it is necessary to include the ultrasonic wave propagation distance (from the emitting transducer to the interface to the receiving transducer) in order to account for the effect of diffraction. Although it is not necessary to include the propagation distance in the analogous optical problem, Horowitz and Tamir[17] recognized that it could be included. Since the dependence of this distance is omitted from the theory of Bertoni and Tamir,[15] we show how it enters. A detailed comparison is made of the theoretically predicted energy distribution with experimental results obtained with an ultrasonic goniometer using apodized transducers.

II. THEORY

An incident bounded beam is represented[15–17] by a Fourier transform pair as

$$v_{\rm inc}(x,z)=(1/2\pi)\int_{-\infty}^{\infty} V(k_x)\exp[i(k_x x+k_z z)]\,dk_x \tag{1}$$

and

$$V(k_x)=\int_{-\infty}^{\infty} v_{\rm inc}(x,0)\exp(-ik_x x)\,dx, \tag{2}$$

where k_x and k_z are the x and z components of the wave number $k=2\pi/\lambda$. $v_{\rm inc}(x,0)$ is the amplitude distribution of the incident beam at the liquid-solid interface. A solution for the reflected wave can also be written in the form of a Fourier integral as

$$v_{\rm refl}(x,z)=(1/2\pi)\int_{-\infty}^{\infty} V(k_x)R(k_x)\exp[i(k_x x-k_z z)]\,dk_x. \tag{3}$$

Here $R(k_x)$ is the reflection coefficient given as

$$R(k_x)=\frac{(2k_x^2-k_s^2)^2-4k_x^2[(k_x^2-k_d^2)(k_x^2-k_s^2)]^{1/2}-(ik_s^4/\rho)[k_x^2-k_d^2)/(k^2-k_x^2)]^{1/2}}{(2k_x^2-k_s^2)^2-4k_x^2[k_x^2-k_d^2)(k_x^2-k_s^2)]^{1/2}+(ik_s^4/\rho)[k_x^2-k_d^2)/(k^2-k_x^2)]^{1/2}}\,, \tag{4}$$

where k_d and k_s are the wave numbers corresponding to the longitudinal (compressional) and shear (transverse) waves, respectively, in the solid and ρ is the density ratio of solid to liquid. $R(k_x)$ displays a complex character which implies that k_x can be generalized to a complex variable and $R(k_x)$ can be represented in the complex plane. Bertoni and Tamir recognized the complex character of k_x and investigated its singular points. The integral in Eq. (3) is evaluated along the real axis, so singular points on and near the axis, particularly those whose real parts lie between k_s and k, will strongly affect its value. The pole near the real axis in this interval is located at

$$k_p=k\sin\theta_p+i\alpha\,, \tag{5}$$

where θ_p is near the Rayleigh angle. This pole represents a resonance of the system in the form of a propagating wave: $\exp(ik_p x)=\exp(ik\sin\theta_p x-\alpha x)$. This wave is similar to Rayleigh waves, except that the presence of the imaginary part α in Eq. (5) causes the wave to attenuate as it progresses along the x direction. Energy is continuously "leaking" away from the solid region to the liquid region. This leaky wave, then, is a modified form of the Rayleigh wave.

From the experimental results we wish to report, one cannot reliably evaluate α because of diffraction effects. We therefore follow Bertoni and Tamir[15] and introduce the relationship between α and the Schoch displacement Δ_s:

$$\Delta_s=\frac{2\alpha}{(k\sin\theta_i-k\sin\theta_p)^2+\alpha^2}\,, \tag{6}$$

where θ_i is the angle of incidence. As will be shown, Δ_s can be calculated from measurable physical quantities. If $\theta_i=\theta_p$, then

$$\alpha=2/\Delta_s. \tag{7}$$

Bertoni and Tamir[15] introduced a simpler function for $R(k_x)$—in order to carry out an analytical integration for Eq. (3)—in the form

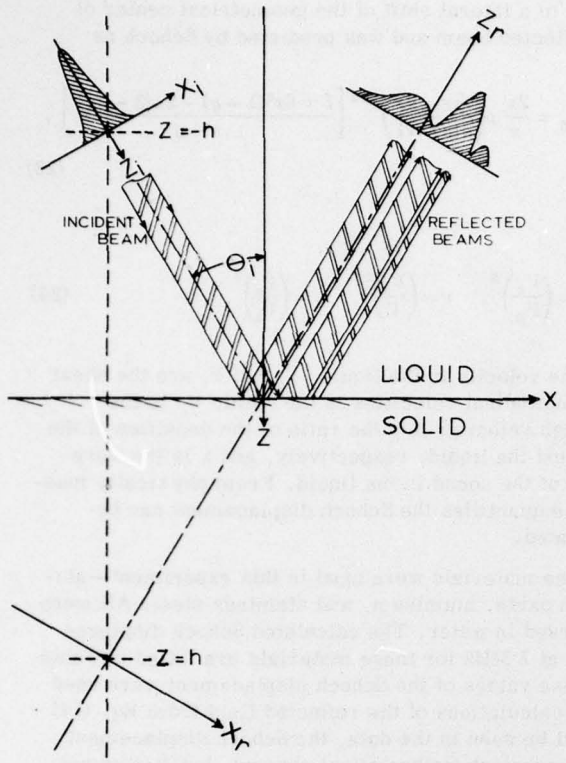

FIG. 2. Coordinate systems. Typical intensity distributions are superimposed for incident and reflected beams.

$$R(k_x) = \frac{k_x - k_p^*}{k_x - k_p}\ , \tag{8}$$

where k_p^* is the complex conjugate of k_p. Equation (8) results from a Laurent expansion around the pole k_p, and therefore is a good approximation only in the region near the pole, the region of interest in our experiment.

$R(k_x)$ then is written in the form

$$R(k_x) = R_0(k_x) + R_1(k_x), \tag{9}$$

where

$$R_0(k_x) = \frac{k_i - k_0}{k_i - k_p}\ , \tag{10}$$

$$R_1(k_x) = \frac{k_p - k_0}{k_p - k_i}\ \frac{k_x - k_i}{k_x - k_p}\ , \tag{11}$$

where k_i is a specific value of k_x corresponding to a particular angle of incidence, and k_0 is identical to k_p^* if the losses are negligible. In our comparison with experiment we assume losses are negligible. R_0 corresponds to the geometric reflection and R_1 accounts for the leaky-wave contribution. The reflected field can be calculated if the analytic form of the incident beam is given. For this experiment a specially designed[6] Gaussian transducer was used, and the incident beam is described as a Gaussian function:

$$V_{\text{inc}}(x,0) = \frac{\exp[-(x/w_0)^2 + ik_i x]}{\pi^{1/2} w_0 \cos\theta_i}\ , \tag{12}$$

where w_0 is the half-width of the area on the interface illuminated by the incident beam. Substituting Eq. (12) into Eq. (2) as an initial condition yields

$$V(k_x) = \frac{\exp[-(k_x - k_i)^2(\frac{1}{2}w_0)^2]}{\cos\theta_i}\ , \tag{13}$$

which, along with Eq. (9), is inserted into Eq. (3) to find the reflected field. The resulting reflected field is written in two terms as

$$V_{\text{refl}}(x,z) = V_0(x,z) + V_1(x,z), \tag{14}$$

where

$$V_0(x,z) = \frac{1}{2\pi}\left(\frac{k_i - k_0}{k_i - k_p}\right)\int_{-\infty}^{\infty} \frac{\exp[-(k_x - k_i)^2(\frac{1}{2}w_0)^2]}{\cos\theta_i} \times \exp[i(k_x x - k_z z)\, dk_x \tag{15}$$

and

$$V_1(x,z) = \frac{1}{2\pi}\left(\frac{k_p - k_0}{k_p - k_i}\right)\int_{-\infty}^{\infty} \left(\frac{k_x - k_i}{k_x - k_p}\right)\frac{\exp[-(k_x - k_i)^2(\frac{1}{2}w_0)^2]}{\cos\theta_i} \times \exp[i(k_x x - k_z z)]\, dk_x . \tag{16}$$

The field V_0 represents a specular or geometrical acoustic reflection, the type which occurs with varying amplitude at all angles. Its integrand is unaffected by the poles at k_p. The field V_1 represents the leaky-wave contribution, whose integrand is strongly affected by the pole at k_p.

Bertoni and Tamir[15] evaluated the integrals in Eqs. (15) and (16) for $z = 0$, i.e., at the interface. For $z \neq 0$, which describes our experimental situation, the integrals can be evaluated only if the relationship between k_z and k_x can be found. For the electromagnetic case, Tamir and Bertoni,[16] following the approach of Horowitz and Tamir,[17] approximated k_z by the first three terms of a Fresnel expansion

$$k_z = k\cos\theta - (k_x - k\sin\theta)\tan\theta - \left(\frac{(k_x - k\sin\theta)^2}{2k\cos^3\theta}\right). \tag{17}$$

(The physical assumption in arriving at this expression is that only those plane wavelets are considered whose propagation direction is essentially the same as the direction of the central beam.)

TABLE I. Properties of solids used in calculation of Schoch displacement.

Material	ρ	V_l ($\times 10^5$ cm/sec)	V_S ($\times 10^5$ cm/sec)	V_R ($\times 10^5$ cm/sec)	Δ_S (mm)
Aluminum	2.71	6.40	3.106	2.848	15.87
Stainless steel	7.85	5.80	3.130	2.827	43.10
Aluminum oxide	4.0	10.70	6.360	5.690	88.13

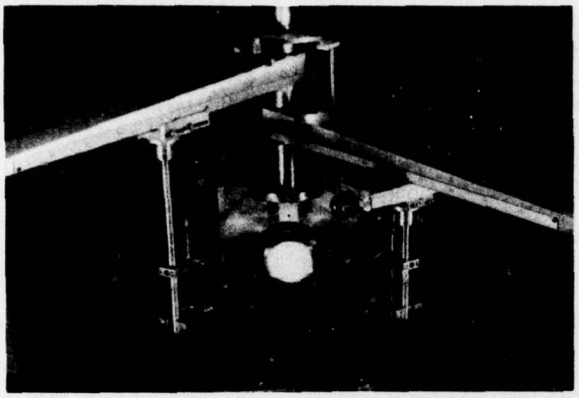

FIG. 3. Goniometer used in making intensity measurements.

By substituting Eq. (17) into Eqs. (15) and (16) one can solve the integral exactly (see Appendix of Ref. 17). The relationships between the fixed and reflected coordinate systems shown in Fig. 2 are

$$x_r = x\cos\theta - (h-z)\sin\theta, \tag{18}$$

$$z_r = x\sin\theta + (h-z)\cos\theta.$$

These relationships and the results of Tamir and Bertoni[16] are used to evaluate the expressions for V_0 and V_1 in the reflected coordinate system:

$$V_0(x_r z_r) = R_0 \frac{\exp[-(x_r/w_r)^2 + ik_1 x_r]}{\pi^{1/2} w_r \cos\theta_i}, \tag{19}$$

$$V_1(x_r z_r) = 2V_0(x_r, z_r)\left(1 - \frac{\pi^{1/2} w_r}{\Delta_s}\exp(\gamma^2)\,\mathrm{erfc}(\gamma)\right), \tag{20}$$

where

$$\gamma = \frac{w_r}{\Delta_s} - \frac{x_r}{w_r} + i\frac{2\pi}{\lambda}(\sin\theta_i - \sin\theta_R)w_r \tag{21}$$

and

$$w_r = w\left(1 - \frac{2i}{w^2 k}(z_r - x_r\tan\theta_i)\right)^{1/2}. \tag{22}$$

Here erfc is the complementary error function, w is the half-width of the incident beam, and Δ_s is the Schoch displacement which is characteristic of the interface. Since these expressions are to be compared with experiments performed at the Rayleigh angle (i.e., for $\theta_i = \theta_R$), we have used Eq. (7) to relate α and Δ_s.

The total reflected field at any point is given by the (vector) sum of two complex numbers V_0 and V_1. The field amplitude is equal to the modulus of the sum; the relative phase is computed from the quotient of the real and imaginary parts of $V_0 + V_1$. Both field amplitude and relative phase were calculated by use of FORTRAN. Energy is proportional to the square of the amplitude.

One of the important parameters which influences the distribution of the reflected amplitude is the so-called Schoch displacement, Δ_S [see Eqs. (20) and (21)]. Δ_S refers to a lateral shift of the geometrical center of the reflected beam and was predicted by Schoch as

$$\Delta_S = \frac{2\lambda}{\pi}\rho\left(\frac{r(r-s)}{s(s-1)}\right)^{1/2}\left[\frac{1+6s^2(1-q)-2s(3-2q)}{s-q}\right], \tag{23}$$

where

$$s = \left(\frac{V_s}{V_R}\right)^2, \quad r = \left(\frac{V_s}{V}\right)^2, \quad q = \left(\frac{V_s}{V_l}\right)^2, \tag{24}$$

V is the velocity in the liquid, V_s and V_l are the shear and longitudinal velocities in the solid, V_R is the Rayleigh velocity, ρ is the ratio of the densities of the solid and the liquid, respectively, and λ is the wavelength of the sound in the liquid. From physically measurable quantities the Schoch displacement can be calculated.

Three materials were used in this experiment—aluminum oxide, aluminum, and stainless steel. All were immersed in water. The calculated Schoch displacements at 2 MHz for these materials are listed in Table I. These values of the Schoch displacement were used in the calculations of the reflected field from Eq. (14). As will be seen in the data, the Schoch displacement is a convenient mathematical concept, but it does not accurately represent the lateral shift of the reflected beam.

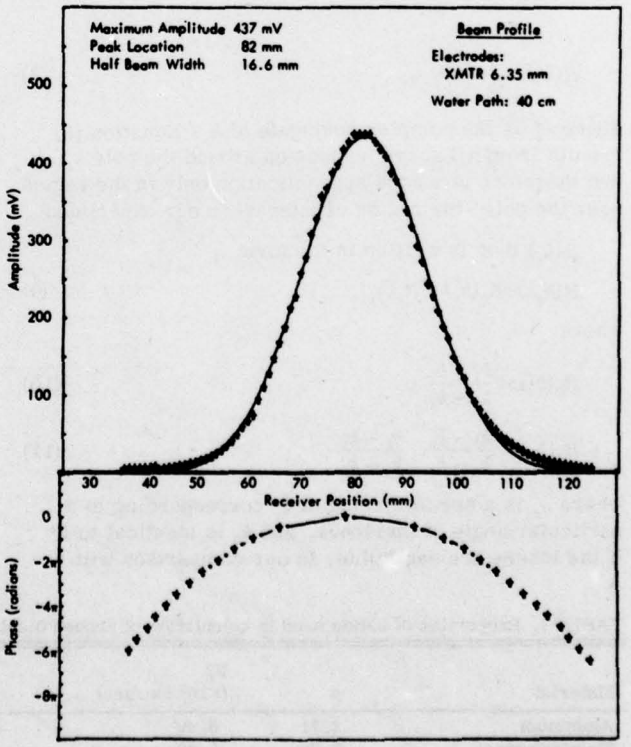

FIG. 4. Amplitude and phase profile of incident beam.

III. EXPERIMENTAL APPARATUS

A. Goniometer

The experimental apparatus consists of a two-crystal system. Pulsed ultrasonic waves are produced by a standard gated amplifier and are displayed on an oscilloscope. The transducers are mounted on a goniometer in such a manner that the ultrasonic beam, reflected from the metal interface of interest, is scanned by the movable receiver transducer. Figure 3 shows the goniometer removed from its water tank. For operation it is immersed in water up to a point about halfway between the top of the specimen holder and the base of the column on which the arms mount. The left arm carries the transmitter and the right arm carries the receiver (the slide moves the receiver perpendicular to the arm). The transducer carriages can be moved radially along the arms and clamped at radii between 5 and 50 cm.

The specimen holder accommodates rectangular blocks (2×4 in.) up to 1 in. thick and right-circular cylinders (3 in. in diameter) up to a few inches long. Either specimen type is restrained so that its front (reflecting) face coincides with the rotation axis of the arms. Figure 1 also shows a cylindrical aluminum oxide specimen in place. The aluminum oxide cylinder is 2.5 in. in diameter, so an aluminum ring is used to adapt it to the holder.

B. Transducers

For the present investigation, the transducers were 1-in.-diam x-cut quartz crystals plated with conducting material (gold or silver) on one side. The plated side was used at the front, or water, side. The rear electrode was a metal strip aligned to be symmetric about a diameter of the crystal, parallel to the goniometer axis. This electrode arrangement produced an ultrasonic beam with a Gaussian profile.[6] A 6.35-mm electrode was used in the transmitter to produce a narrow beam with good signal amplitudes at the receiver. The receiver had a 3.68-mm electrode which consistently produced narrow beam profiles. Figure 4 is the amplitude and phase profile made with these transducers at 2 MHz. The amplitude profile is fitted with a Gaussian curve of the form $A\exp[-(x-\mu)^2/b^2]$. This Gaussian amplitude variation across the wavefront makes possible a detailed comparison between theory and experiment, since it is the case that was solved analytically.

C. Amplitude measurement

An Arenberg unit was used in its pulsed-amplifier mode. It functions as a gate, turning the input from the external variable frequency oscillator on and off and feeding it into the amplifier section. The output is a tone burst, i.e., a burst of 2 MHz rf about 16 μsec long. Amplitudes were measured by reading the voltage developed across the receiver crystals from an oscilloscope.

D. Phase measurement

Several potential applications motivated efforts to measure phase—(1) goniometer alignment, (2) tracing wavefront contours in transducer-beam profiles, and (3) tracing wavefront contours in Rayleigh-angle reflections. A technique devised for detecting a constant phase led to improvements which allowed approximate, but repeatable, measurements of relative phase. Moving the oscilloscope trigger from the Arenberg trigger output to the transmitter cable causes the transmitter pulse to trigger the oscilloscope sweep and allows relative phase measurements.

The Arenberg trigger output is coincident with its gate, but these signals are both timed by a rate generator in the Arenberg which is not synchronized with the external rf input (from the VFO). Therefore, the gate and trigger pulse do not occur at the same point (or phase) on the rf waveform each time the gate opens. If the oscilloscope sweep is triggered by the Arenberg gate, the envelope of the pulse remains stationary on the CRT trace, but the rf waveform jitters back and forth inside the envelope. When the oscilloscope sweep is triggered directly by the transmitter pulse, it synchronizes with the rf waveform, and the waveform remains stationary on the CRT while its envelope jitters.

In this latter condition, the displayed signal from the receiver is locked in phase with the transmitter driving signal. All of the pulses are coherent with one another because they originate from the same cw source, and the oscilloscope trigger circuits fix the phase point on the rf waveform at which the sweep starts. The only remaining phase changes result from changes in the propagation delay of the acoustic signal along its water path, and these are observable on the CRT as movement of the entire waveform across the screen.

The slide motion of the receiver confines it to a plane in the propagation path of the acoustic wavefronts. The wavefronts are typically curved, so there will be a point of tangency with the receiver plane as the front advances. The signal detected by the receiver at the point of tangency occurs earlier in time than signals detected elsewhere in the receiver plane, and it appears farthest left on the CRT trace. This point was designated the "maximum phase excursion", and was defined as zero

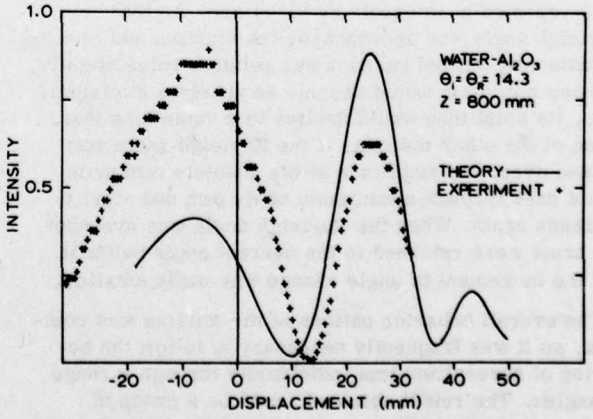

FIG. 5. Reflected intensity distribution for a water—aluminum oxide interface.

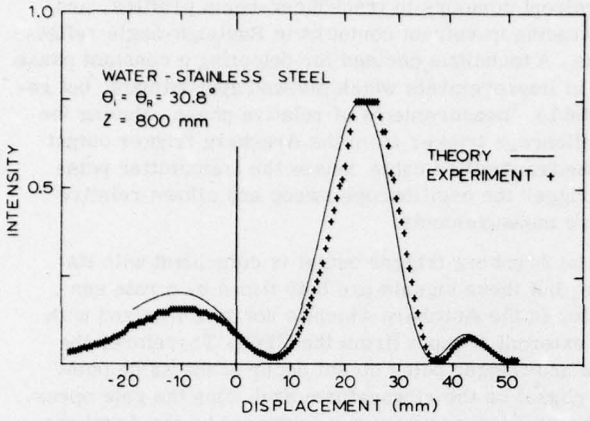

FIG. 6. Reflected intensity distribution for a water—stainless steel interface at $z_r = 800$ mm.

relative phase for all experimental measurements. Changes in relative phase were recorded in 90° increments according to the distance the waveform moved to the right on the CRT. All relative phases were recorded as negative with respect to the maximum phase excursion.

IV. EXPERIMENTAL PROCEDURE

Reports of other experimenters established a range of values where the Rayleigh angle for a material was expected to lie. Starting at angles 1—2° below the expected range, the transmitter and receiver arms were set at equal angles. Then the receiver was scanned through the full range of the cross slide, and the locations and values of all local maxima and minima in the amplitude were noted. The slide was set to a position corresponding approximately to the center of the incident beam. The oscilloscope was set to indicate zero relative phase at this position, and relative phase was observed as the slide was scanned away to the right and left. Locations of large or sudden changes in phase were noted.

The arms were repositioned and the scanning procedure repeated at intervals of 15′ of arc. As the Rayleigh angle was approached, the maxima and minima occasionally shifted position and relative value slightly, and one minimum would become an absolute minimum, i.e., its amplitude would decline to a value less than those of the other minima. If the Rayleigh angle was passed over, the amplitude at the absolute minimum would pass through a minimum of its own and start to increase again. When the Rayleigh angle was overshot, the arms were returned to the nearest angle below it, and the increment of angle change was made smaller.

The overall behavior pattern of the minima was complex, so it was frequently necessary to follow the behavior of several minima individually through a range of angles. The result obtained would be a group of angles, each of which corresponded to the lowest amplitude reached by one of the minima. Of these angles, that angle corresponding to the lowest amplitude among the mimimum values obtained was called the Rayleigh angle. In each case, the lowest minimum was accompanied by a rapid variation of the phase in its neighborhood, amounting to as much as 180° of shift. This phase variation provided some additional confidence in the identification.[13]

In early experiments the receiver and transmitter arms were set at equal angles. Ultimately, enough evidence was collected to demonstrate that the goniometer could not be aligned perfectly and that a genuine Rayleigh phenomenon could exist and be identified with the arms at slightly different indicated angles. As the critical angle for a particular minimum was approached, the arms could be manipulated independently and the desired angle found by watching the oscilloscope CRT presentation. This technique produced angle settings repeatable within ± 5′ of arc. The difference in arm angles at the final settings are typically 20′ of arc, or less. This figure is consistent with estimates of the alignment accuracy. Once the arm angles were set, amplitude and phase measurement followed procedures described in Secs. II and III. Amplitude measurements were made at position intervals of 0.5 mm.

V. RESULTS

The reflected intensity distribution for a water—aluminum oxide interface is shown in Fig. 5. The solid curve is calculated from Eq. (14). The crosses are experimental points. The total water path length z_r was 800 mm. The incident beam width was $2w = 6.35$ mm. The incident angle α_i was equal to the Rayleigh angle α_R which was 14.7°. The reflected field was scanned across 95 mm, from −15 to +50 mm. Zero is approximately the center of the incident beam. The theory predicts two minima. The second minimum was not observable experimentally because the aluminum oxide specimen was not wide enough, but the position of the two peaks and the first minimum agrees reasonably well with the calculation.

The stainless steel has smaller Schoch displacement and produced a different reflected intensity distribution

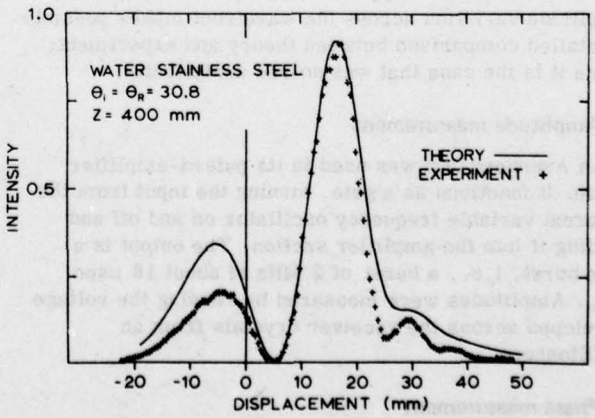

FIG. 7. Reflected intensity distribution for a water—stainless steel interface at $z_r = 400$ mm.

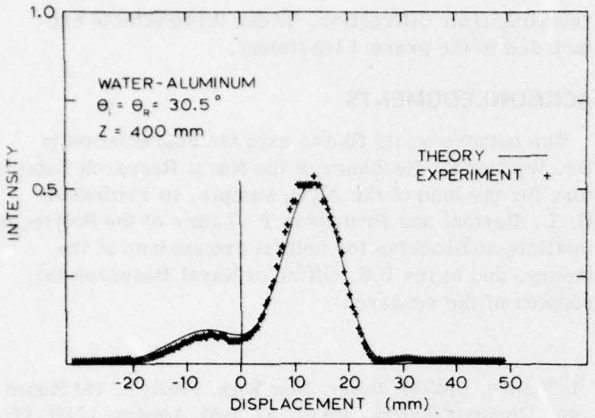

FIG. 8. Reflected intensity distribution for a water-aluminum interface.

as shown in Fig. 6. The incident beam width was 6.35 mm and the total path was 800 mm. The incident angle was the same as the Rayleigh angle for water–stainless steel which is 30.8°. A wider retangular specimen of stainless steel was used in this experiment. Now the second minimum is observed experimentally. There is also good agreement between theory and experiment.

The effect of the changing of the water path length z_r was investigated by reducing its value to 400 mm. The length of each arm of the goniometer was reduced by one-half; all other parameters remained the same. The result is shown in Fig. 7. It is clear that there is a strong distance dependence on the beam distribution which shows up in the difference between Figs. 6 and 7. The agreement between theory and experiment is nominally the same at the two distances.

The addition of z_r dependence to the theory has accounted for the diffraction effect. In Fig. 6 the secondary maximum between 40 and 50 mm results from diffraction. Somewhat less-pronounced maxima appear in Fig. 7, as well. Calculation shows that these secondary maxima vanish as z_r approaches zero. These secondary maxima also are visible in schlieren photographs such as Fig. 1.

Aluminum was the third material studied. Aluminum has the smallest Schoch displacement of all three materials, which is 16 mm for 2-MHz ultrasonic waves. The Rayleigh angle is 30.6° for a water-aluminum interface. Both theory and experiment indicate (see Fig 8) that the reflected beam has only one major peak. This is quite different from aluminum oxide and stainless steel. For aluminum the proper setting of the incident beam angle required careful alignment. Slight deviation from the Rayleigh angle produced significant changes in the intensity distribution. For example, a change of 6′ of arc produced the intensity distribution shown in Fig. 9. The position of the principal maximum has not changed much; however, a secondary maximum is now visible at 28 mm displacement, with another barely perceptible at 40 mm. Furthermore, the energy distribution has changed near the specular beam and to the left of zero displacement.

For the case shown in Fig. 9 we also measured the phase in the reflected beam and compared with theory. As can be seen, the measured phase is in nominal agreement with theory. The phase variation indicates that the center of the reflected beam is out of phase by as much as 8π with respect to the end points. This phase plot is actually a measure of the beam profile of the reradiated beam, indicating that the wavefront is far from being planar as is usually assumed in basic boundary-value problems.

Finally, as a test of the sensitivity of the theory to the incident angle, we kept the distance $z = 400$ mm and increased the incident angle by 0.5° increments. Two calculated curves for 0.5° and 1.0° greater than the Rayleigh angle are given in Fig. 10. As can be seen, the theory also is sensitive to incident angle in this range, as it should be.

VI. SUMMARY

The behavior of a Gaussian ultrasonic beam incident on a liquid-solid interface has been studied in some detail at the Rayleigh angle—the angle at which surface waves are excited on the interface. The reflected beam is displaced in the manner predicted by Schoch; however, the "Schoch displacement" in general is too large. Good agreement is obtained between the experimental results and the theory of Bertoni and Tamir which assumes that the incident beam couples resonantly into a leaky surface wave at the Rayleigh angle. The energy is reradiated from this leaky surface wave and interferes with specularly reflected energy. For water–

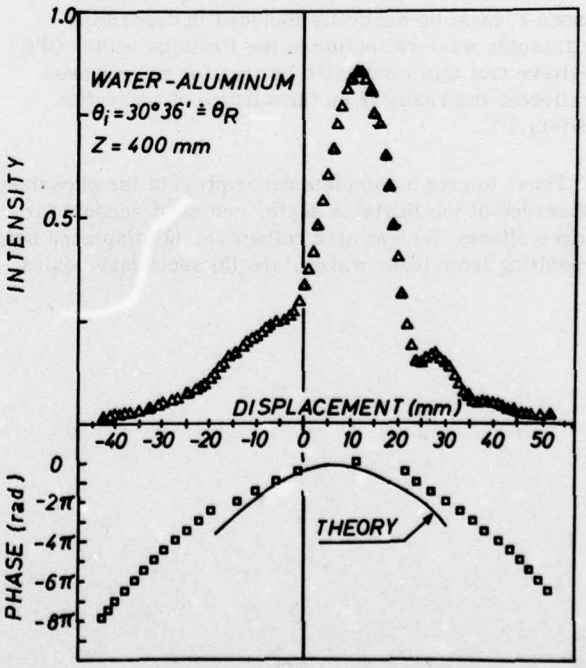

FIG. 9. Reflected intensity distribution and phase profile for a water-aluminum interface for an angle of incidence differing from θ_R by 6′ of arc.

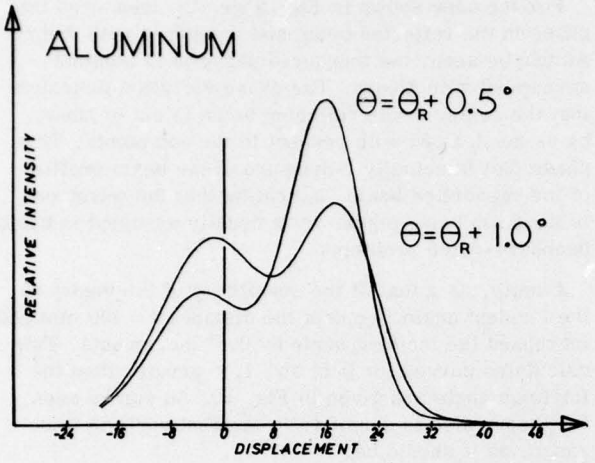

FIG. 10. Calculated intensity distribution for a water-aluminum interface for two angles near θ_R.

Al_2O_3, which has a very large Schoch displacement, the agreement between theory and experiment is fair. It is better for water—stainless steel, which has a smaller Schoch displacement. For water—aluminum, which has a relatively small Schoch displacement, the agreement can be quite good; however, sensitivity to incident angle makes necessary very careful alignment and measurement.

Although the approximation $z_r = 0$ is accurate enough in the analogous optical problem, the propagation distance z_r must be explicitly included in describing ultrasonic wave reflection at the Rayleigh angle. (We believe that this would also be true for microwaves reflected internally from the surface of a paraffin prism.)[18]

Thus, to give a complete description of the phenomena observed at the Rayleigh angle, one must account for three effects: (1) specular reflection, (2) displaced beam resulting from leaky waves, and (3) secondary beams resulting from diffraction. These three effects are included in the present treatment.

ACKNOWLEDGMENTS

The authors would like to express appreciation to Dr. Werner G. Neubauer of the Naval Research Laboratory for the loan of the Al_2O_3 sample, to Professor H. L. Bertoni and Professor T. Tamir of the Polytechnic Institute of Brooklyn for helpful discussions of the theory, and to the U.S. Office of Naval Research for support of the research.

[1]I. Newton, *Opticks* (Dover, New York, 1952), p. 194 [based on I. Newton, *Opticks*, 4th ed. (G. Bell, London, 1730), Observation I, Second Book].
[2]F. Goos and H. Hänchen, Ann. Phys. (Leipzig) 1, 333—346 (1947).
[3]H.K.V. Lotsch, Die Optik 32, 116—137 (1970); 32, 189—204 (1970); 32, 299—319 (1971); 32, 553—569 (1971).
[4]A. Schoch, Ergeb. Exakten Naturwiss. 23, 127—234 (1950); Acustica 2, 18—19 (1952).
[5]L.M. Brekhovskikh, *Waves in Layered Media* (Academic, New York, 1960).
[6]F.D. Martin and M.A. Breazeale, J. Acoust. Soc. Am. 49, 1668—1669. (1971).
[7]M.A. Breazeale, Laszlo Adler, and James H. Smith, Akust. Zh. 21, 1—10 (1975) [Sov. Phys. Acoust. 21, 1—6 (1975)].
[8]M.A. Breazeale, Laszlo Adler, and Larry Flax, J. Acoust. Soc. Am. 56, 866—872 (1974).
[9]H. Uberall, *Physical Acoustics*, edited by W.P. Mason and R.N. Thurston (Academic, New York, 1973), Vol. X, pp. 1—57.
[10]F.L. Becker and R.L. Richardson, J. Acoust. Soc. Am. 51, 1609—1617 (1972).
[11]G. Mott, J. Acoust. Soc. Am. 50, 819—829 (1971).
[12]W.G. Neubauer, *Physical Acoustics*, edited by W.P. Mason and R.N. Thurston (Academic, New York, 1973, Vol. X, pp. 61—125.
[13]W.G. Neubauer, J. Appl. Phys. 44, 48—55 (1973); W.G. Neubauer and L.R. Dragonette, J. Appl. Phys. 45, 618—622 (1974).
[14]O.I. Diachok and W.G. Mayer, J. Acoust. Soc. Am. 47 155—157 (1970).
[15]H.L. Bertoni and T. Tamir, Appl. Phys. 2, 157—172 (1973).
[16]T. Tamir and H.L. Bertoni, J. Opt. Soc. Am. 61, 1397—1413 (1971).
[17]B.R. Horowitz and T. Tamir, J. Opt. Soc. Am. 61, 586—594 (1971).
[18]J.J. Cowan and B. Anicin, J. Opt. Soc. Am. 64, 525 (1974).

Paper No. 4

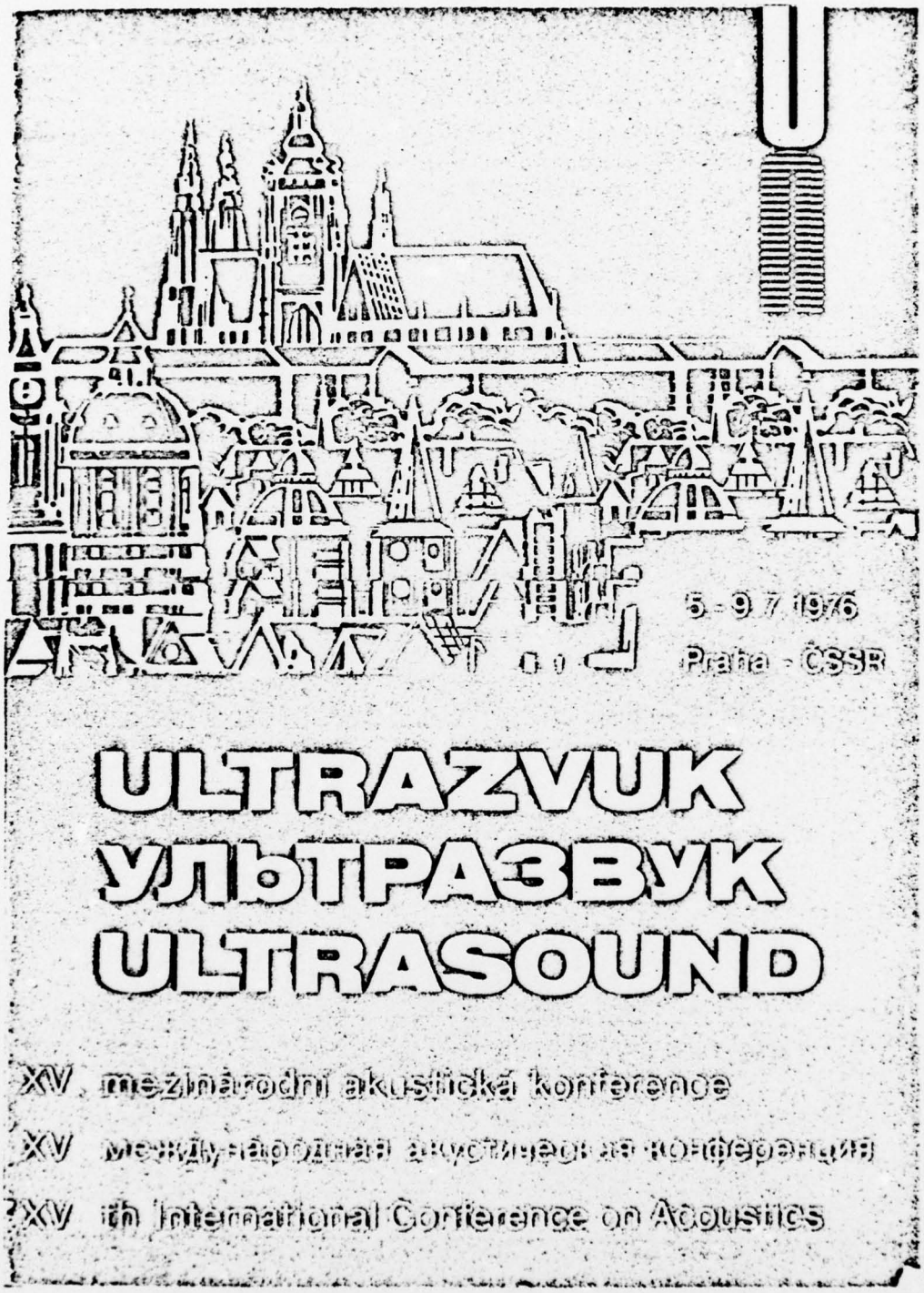

Ultrasonic Wave Reflection at a Plane Interface (M. A. Breazeale)
Proceedings of XVth International Conference on Acoustics, Prague, Czechoslovakia, July 7-9, 1976, pp. 114-118.

ULTRASONIC WAVE REFLECTION AT A PLANE INTERFACE

M. A. Breazeale
The University of Tennessee, Knoxville, Tennessee USA

The reflection of an ultrasonic wave at a plane interface has been studied in considerable detail in recent years. If the incident beam is infinitely extended, one can make a general definition of the energy reflection coefficient and solve the problem in closed form. In a special case, such as a water-stainless steel interface, the reflected energy as a function of the angle of incidence behaves as shown in Figure 1. Two critical angles are obtained. One for the longitudinal wave in the stainless steel, and one for the transverse wave in the stainless steel. At these angles the theory predicts that the energy is totally reflected. The reflection coefficient

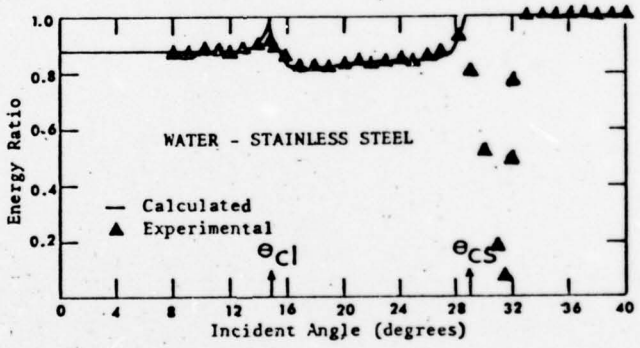

Figure 1. Energy Reflection Coefficient for Ultrasonic Waves Incident on a Plane Interface.

has unit magnitude. However, in attempting to verify the theory one typically obtains data such as those shown in

Figure 1. The experimental data follow the theoretical curve for incident angles below the critical angle for shear waves in the stainless steel, 29°, but above this angle there is considerable discrepancy between the theory and experiment. The theory predicts unity, but the experiment shows a deep minimum at 31°. The reason for this discrepancy lies in the fact that the actual ultrasonic beam is not infinitely wide. As Schoch[1] has shown, the reflected beam is "displaced" down the interface and does not strike the receiving transducer. Using the theory of Schoch, one can calculate the magnitude of this displacement. The variation of the displacement with angle of incidence is shown in Figure 2. The maximum occurs at 31°, in agreement with the data in Figure 1. The reason for this displacement is that the incident beam is phase

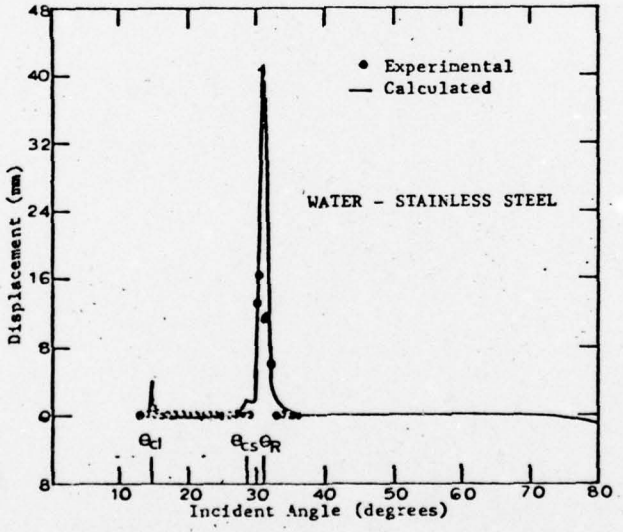

Figure 2. Schoch Displacement as a Function of the Angle of Incidence.

matched with a surface wave which propagates down the interface. The angle at which this occurs is often referred to as the Rayleigh angle θ_R since such surface waves were studied by Lord Rayleigh.

In Figure 2 it can be seen, however, that the calculated displacement is considerably greater than the value measured because, in fact, the energy is redistributed when it is reradiated by the surface wave.

Coupling with Surface Waves Propagating in the +X Direction

The situation can be described in terms of the coordinates shown in Figure 3. The incident beam has

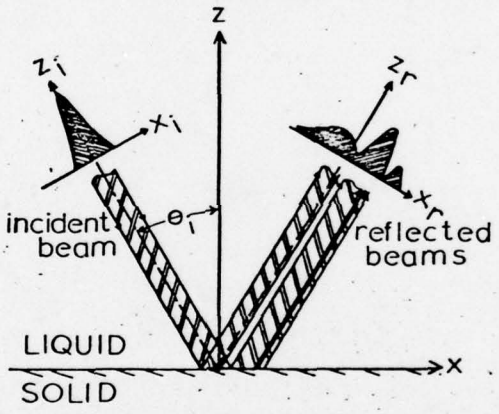

Figure 3. Coordinates Used in Solving the Reflection Problem.

coordinates X_i and Z_i; the reflected beam X_r and Z_r. In our experiments we used an incident beam which has a Gaussian profile[2] as shown. The reflected beam then has an intensity distribution that is not simply a Gaussian function displaced from the origin. It is more complicated, as indicated.

By using the theory of Bertoni and Tamir[3] one is able to redefine the reflection coefficient. Assuming a Gaussian

incident beam, one finds a different reflection coefficient for each of the partial plane waves in the Fourier transform representation of the reflected beam. In order to obtain the energy distribution in the reflected wave, one must make a point-by-point integration over the partial waves. The result is that with an incident Gaussian amplitude distribution

$$V_{inc}(x,0) = \frac{\exp[-(x/w_o)^2 + ik_i x]}{\sqrt{\pi}\, w_o \cos\theta_i} \qquad (1)$$

the reflected wave has an amplitude distribution made up of two parts: a specularly reflected component and a component reradiated by the surface wave,

$$V_{refl}(x,z) = V_0(x,z) + V_1(x,z) \ . \qquad (2)$$

The specular component has the form

$$V_0(x_r z_r) = R_o \frac{\exp[-(x_r/w_r)^2 + ik_i x_r]}{\sqrt{\pi}\, w_r \cos\theta_i} \ . \qquad (3)$$

The reradiated component has the form

$$V_1(x_r z_r) = 2V_0(x_r, z_r)\left[1 - \frac{\sqrt{\pi} w_r}{\Delta_s} \exp(\gamma^2)\operatorname{erfc}(\gamma)\right] \ , \qquad (4)$$

where

$$\gamma = \frac{w_r}{\Delta_s} - \frac{x_r}{w_r} + i\,\frac{2\pi}{\lambda}(\sin\theta_i - \sin\theta_R) w_r \qquad (5)$$

and

$$w_r = w\left[1 - \frac{2i}{k}(z_r - x_r \tan\theta_i)\right] \ . \qquad (6)$$

Here erfc is the complementary error function and Δ_s is the Schoch "displacement" which is characteristic of the interface. The total reflected field at any point is given by the (vector) sum of the two complex numbers V_0 and V_1. The energy is proportional to the product of this sum and its complex conjugate.

The use of this theory now makes possible a detailed comparison between theory and experiment such as that

shown in Figure 4. As can be seen, the calculated curve for a water-stainless steel interface agrees quite well with experiment. Data for other solid-liquid combinations we have tried are in similar agreement.

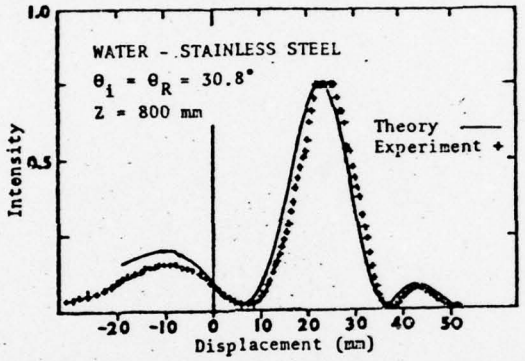

Figure 4. Energy Distribution in an Ultrasonic Beam Reflected at the Rayleigh Angle.

Coupling with Waves in the -X Direction

According to the theory of Bertoni and Tamir a surface wave which propagates in the negative X direction can be generated under special circumstances. A corrugated interface produces such a wave. We have been able to show unequivocally that such a phenomenon exists. The energy in the reflected beam is "displaced" in the negative X_r direction. This subject currently is under investigation. (Research supported by the Office of Naval Research.)

References

1. A. Schoch, Ergebnisse der exakten Naturwissenschaften 22, 160 (1950).
2. F. D. Martin and M. A. Breazeale, J. Acoust. Soc. Am. 49, 1668 (1971).
3. H. L. Bertoni and T. Tamir, Appl. Phys. 2, 157 (1973).

Paper No. 5

Backward Displacement of Waves Reflected from an Interface Having Superimposed Periodicity (M. A. Breazeale and Michael A. Torbett), Appl. Phys. Lett. *29*, 456-458 (1976)

Backward displacement of waves reflected from an interface having superimposed periodicity

M. A. Breazeale and Michael A. Torbett*

Department of Physics, The University of Tennessee, Knoxville, Tennessee 37916
(Received 21 June 1976)

An ultrasonic beam incident on a liquid-solid interface with superimposed grating is shown to be displaced in a backward direction at certain angles of incidence predicted by the theory of T. Tamir and H. L. Bertoni [J. Opt. Soc. Am. **61**, 1397–1413 (1971)]. The analogy between the ultrasonic phenomenon and the corresponding optical phenomenon is cited.

PACS numbers: 43.35.+d, 68.35.+q

An ultrasonic wave, incident on a liquid-solid interface at a certain angle of incidence, can couple into leaky surface waves, with the result that the reflected beam is displaced laterally down the interface.[1] Recently, we studied this phenomenon in some detail[2] and showed that the theory of Bertoni and Tamir[3] agrees well with experiment.[4] The theory of Bertoni and Tamir[3] in fact is an adaptation to the acoustical problem of a theory previously used to described the reflection of light at a dielectric interface.[5] In the optical theory, Tamir and Bertoni[5] also point out that if the interface has a periodic structure superimposed, it is possible to cause a leaky wave to propagate in the *backward direction*. In such a case they predict a *backward* beam displacement. In view of the close analogy between light reflection at a dielectric interface and ultrasonic wave reflection at a liquid-solid interface, we decided to verify the correctness of this prediction for ultrasonic waves, even though the corresponding optical experiment is yet to be reported.

The situation is diagrammed in Fig. 1. A beam of width $2w$ incident at an angle θ_i couples to a leaky wave propagating in the negative x direction indicated by the heavy arrow. The optimum angle for this to occur is given[5] as

$$\sin\theta_i = \frac{1}{K_{11q}}\left(\frac{2\pi}{d} - K_R\right) = V_{11q}\left(\frac{1}{fd} - \frac{1}{V_R}\right), \qquad (1)$$

where d is the period, f is the frequency, V_{11q} is the propagation velocity in the liquid, and V_R is the propagation velocity of the leaky wave. At this angle the incident

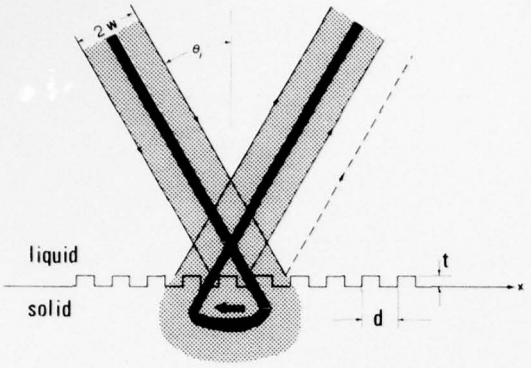

FIG. 1. Diagram of incident beam coupling to a backward-directed leaky wave to produce backward displacement of reflected beam.

beam is phase matched to a space harmonic of the leaky wave. This leads to a reflected beam laterally displaced in the negative x direction, as indicated.

The angle of incidence given by Eq. (1) is dependent upon frequency f, so that for certain frequencies the right-hand side can become greater than unity. This corresponds to an imaginary angle of incidence; i.e., the phenomenon does not occur for any real angle θ_i. We used this fact to produce the first unequivocal demonstration of this phenomenon as follows.

Schlieren photography was used to visualize ultrasonic beams in water reflected from a brass interface upon which were ruled parallel grooves of period $d=0.178$ mm and depth $t=0.025$ mm. Using $V_{liq}=1.49\times10^5$ cm/sec and $V_R=2.015\times10^5$ cm/sec, one predicts $\theta_i=41^\circ$ for 6-MHz ultrasonic waves. At 2 MHz, θ_i becomes imaginary, so the effect would not be observable at 2 MHz.

A 2-MHz apodized[6] quartz transducer was used to generate either 6- or 2-MHz ultrasonic beams. Figure 2 shows the result for 6 MHz. The reflected beam is displaced in the backward direction in the manner indicated in Fig. 1, because a leaky wave is excited in the grating interface. (The direction of this leaky wave suggests that a grating coupler intended as a thin-film optical beam coupler would be more efficient if it had a configuration different from that sketched in Fig. 13 of Ref. 5.)

Without making any adjustments except changing the frequency to 2 MHz, we obtained the photograph shown in Fig. 3. The negative displacement is no longer visible because the leaky wave is not excited at 2 MHz.

Measurement of the angle of incidence in Figs. 2 and 3 results in $\theta_i=22.5^\circ$, which is considerably smaller than predicted from Eq. (1). The reason for this difference probably results from the fact that the value $V_R=2.015\times10^5$ cm/sec is the velocity of a Rayleigh surface wave on brass, whereas the quantity appearing in Eq. (1) should be the velocity of the negatively directed leaky wave, whose magnitude at present is unknown. If one uses the measured angle of incidence in Eq. (1), one can calculate the velocity of this leaky wave as

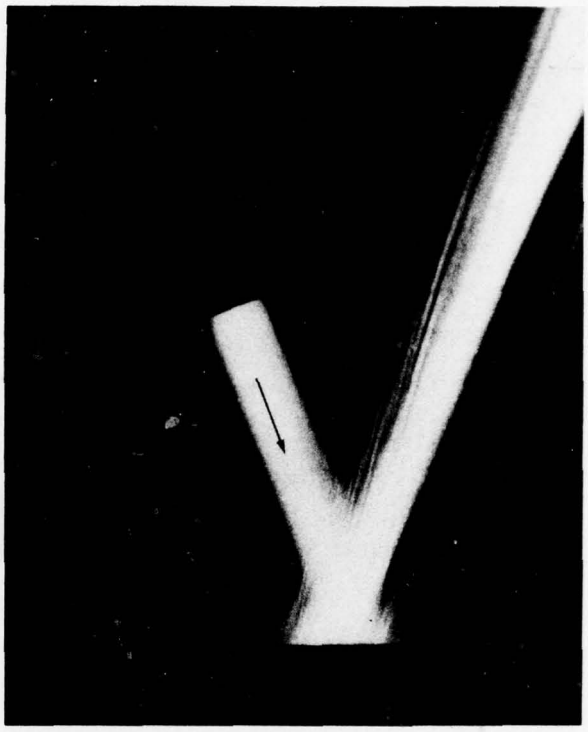

FIG. 2. Backwared displacement of 6-MHz ultrasonic beam at a water-brass grating interface.

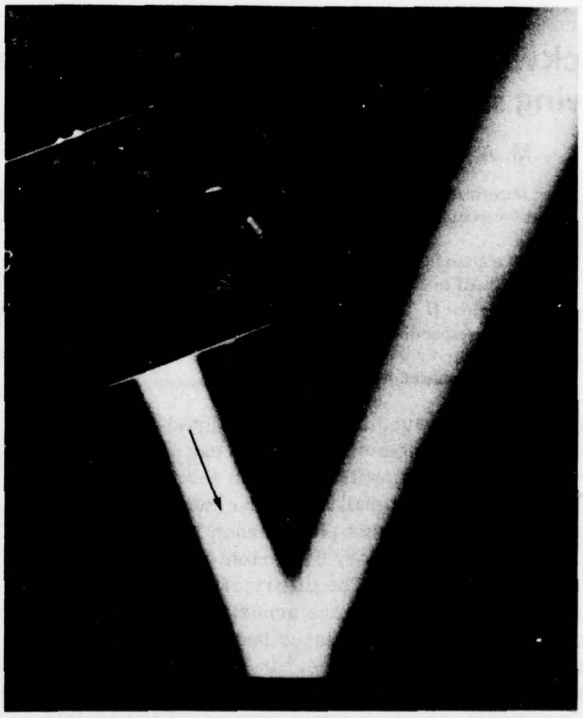

FIG. 3. Ultrasonic beam (2 MHz) incident on water-brass grating interface. Backward displacement is no longer observed.

1.47×10^5 cm/sec. This means that the velocity of these leaky waves differs considerably from the velocity of the Rayleigh surface wave on a plane interface. Further experiments will be required to determine whether there is any fundamental significance to the fact that this velocity is close to the velocity of ultrasonic waves in water.

In conclusion, it is possible to demonstrate in a direct manner that ultrasonic waves can couple into a backward-propagating leaky wave if the reflecting interface has a superimposed periodic structure. (This is an indirect verification of the validity of the prediction of Tamir and Bertoni[5] that light beams can undergo a backward beam shift.) This fundamental observation has implications in optical beam coupler technology as well as surface-acoustic-wave technology.

The authors are indebted to Professor H. L. Bertoni for Bringing this phenomenon to their attention. They are also indebted to the Office of Naval Research for research support.

*Present address: Ford Motor Company, Detroit, Mich.

[1]A. Schoch, Ergeb. Exakten Naturwiss. **23**, 127—234 (1950); Acustica **2**, 18—19 (1952).
[2]M. A. Breazeale, Laszlo Adler, and James H. Smith, Akust. Zh. **21**, 1—10 (1975) [Sov. Phys. Acoust. **21**, 1—6 (1975)]; M. A. Breazeale, Laszlo Adler, and Larry Flax, J. Acoust. Soc. Am. **56**, 866—872 (1974).
[3]H. L. Bertoni and T. Tamir, Appl. Phys. **2**, 157—172 (1973).
[4]M. A. Breazeale, Laszlo Adler, and Gerald W. Scott (unpublished).
[5]T. Tamir and H. L. Bertoni, J. Opt. Soc. Am. **61**, 1397—1413 (1971).
[6]F. D. Martin and M. A. Breazeale, J. Acoust. Soc. Am. **49**, 1668—1669 (1971).

Paper No. 6

Forward- and Backward-Displacement of Ultrasonic Waves Reflected from a Water-Sediment Interface (M. A. Breazeale and L. Bjørnø), to be published in Proceedings of Ultrasonics International, Brighton, England, June 28-30, 1977.

FORWARD- AND BACKWARD-DISPLACEMENT OF ULTRASONIC WAVES REFLECTED FROM A WATER-SEDIMENT INTERFACE

M. A. Breazeale* and L. Bjørnø

Fluid Mechanics Dept., Techn. Univ. of Denmark, 2800 Lyngby, Denmark

An ultrasonic wave incident on the interface between water and sediment has been studied by schlieren photography. Evidence is given that the incident beam may couple to backward-directed, as well as forward-directed leaky surface waves, with the result that the reflected beam may be displaced either in the forward- or the backward-direction depending upon frequency and grain size.

INTRODUCTION

An ultrasonic wave, incident onto a liquid-solid interface at a certain angle of incidence, can couple with leaky surface waves. This coupling causes the reflected beam to be displaced laterally down the interface [1]. Recently, this phenomenon has been studied in some detail [2-4] and it has been shown that the theory of Bertoni and Tamir [5] agrees well with experiments. The theory of Bertoni and Tamir is in fact an adaptation to the acoustical problem of a theory previously used to describe the reflection of light at a dielectric interface [6]. In the optical theory, Tamir and Bertoni also point out that if the interface has a periodic structure superimposed, it is possible to cause a leaky wave to propagate in the backward direction, giving rise to a backward beam displacement. Such a backward displacement of an ultrasonic wave reflected from a water-brass grating interface was demonstrated recently [7].

The theories involving coupling of ultrasonic waves to leaky surface waves, and their experimental verification, are considered only for liquid-solid interfaces which exhibit a shear wave critical angle. A shear wave critical angle is found if $V_L > V_S > V$, where V_L and V_S are respectively the velocities of the longitudinal and the shear wave in the solid, and V is the velocity of the (compressional) wave in the liquid. For such interfaces, the reflection coefficient as a function of the incident angle has the behavior shown in Figure 1, in which the critical angles for the longitudinal and the shear waves in the solid are labelled θ_{CL} and θ_{CS}. At the angle labelled θ_R, leaky surface waves can be excited [4], and they lead to a displacement of the reflected beam as shown in Figure 2. This schlieren photograph of a 1 MHz ultrasonic beam incident onto a water-glass interface shows two reflected beams, the displaced beam and the specularly reflected beam, with a null strip between.

*On leave of absence from Physics Dept., Univ. of Tenn., Knoxville, Tenn. 37916, U. S. A.

Heretofore, little attention has been given to experimental and theoretical studies of interfaces for which $V_L > V > V_S$. In this case one does not observe a critical angle for the shear wave in the solid, and hence θ_R does not exist. This is the velocity relationship characterizing a water-sediment interface, since, typically, V_L = 1742 m/sec, V = 1483 m/sec and V_S = 382 m/sec [8]. Even though theory has not been developed to describe reflection from this class of interfaces in detail, we report results of schlieren studies of the reflection of ultrasonic waves at a water-sediment interface and interpret our results by analogy with results observed at a water-solid interface.

THEORETICAL CONSIDERATIONS

If one assumes an infinite plane wave incident onto a water-solid interface, one can calculate the reflection coefficient from [9]:

$$R = \frac{Z_L \cos^2 2\theta_S + Z_S \sin^2 2\theta_S - Z}{Z_L \cos^2 2\theta_S + Z_S \sin^2 2\theta_S + Z} \tag{1}$$

where the normal impedances are defined by

$$Z = \frac{\rho_1 V}{\cos \theta_i} \qquad Z_L = \frac{\rho_2 V_L}{\cos \theta_L} \qquad Z_S = \frac{\rho_2 V_S}{\cos \theta_S} \tag{2}$$

and the subscripts i, L, and S refer, respectively, to the incident wave, the transmitted longitudinal wave, and the transmitted shear wave. For three different water-sediment interfaces these equations give the reflection coefficient as a function of the incident angle shown in Figure 3. In these curves we see that there is a critical angle for the longitudinal wave, θ_{CL}, at which each curve goes to unity. There is not a critical angle for the shear wave in the "solid" because $V > V_S$. These curves should be a good description of the reflection coefficient if the incident wave were plane; i. e. if the incident beam were infinitely wide.

In the experiments the incident beam has a finite width--as a matter of fact, the incident beam has a gaussian distribution across its finite width in order to get rid of diffraction side lobes. For this incident beam, Figure 3 should be a reasonable approximation to the reflection coefficient, but there may be detail in the actual experiment which cannot be anticipated from Figure 3.

Since there is a close analogy between light reflection at a dielectric interface and ultrasonic wave reflection at a liquid-solid interface, the prediction of a backward displacement of a light beam has in fact been verified for the ultrasonic analogue [7]. The optimum angle of incidence for an ultrasonic wave of beam width 2w to experience a backward beam shift by coupling to a leaky wave propagating in the negative x-direction, see Figure 4, is given by

$$\sin \theta_i = V\left[\frac{1}{f\ d} - \frac{1}{V_R}\right] \tag{3}$$

where d and f denote the period and the frequency, respectively, while V and V_R are the ultrasonic wave velocity in water and the

propagation velocity of the leaky wave, respectively. At this angle the incident beam is phase matched to a space harmonic of the leaky wave, which leads to a reflected beam which is laterally displaced in the negative x-direction. Since the angle of incidence given by Equation 3 is dependent upon both frequency and period, and since sin θ_i must have values between zero and unity for real θ_i, there is a relatively narrow range of grain sizes (which determine the period d) for which any specific frequency would be expected to couple to the leaky wave.

EXPERIMENTS AND DISCUSSION

By using schlieren photography we have observed that the reflection of an ultrasonic wave from a water-sediment interface nominally behaves in the manner shown in Figure 3 for $\theta_i < \theta_{CL}$. As the angle of incidence increases the reflection coefficient increases, and becomes fairly large for angles near to, and greater than, θ_{CL} the critical angle for the longitudinal wave in the sediment. Nominally, then, the reflection can be described in analogy with a water-solid model, as expected.

However, even with the qualitative nature of schlieren observations, one can see that between θ_{CL} and 90^o the reflection coefficient does not remain near unity as predicted by theory (see Fig.3). In fact, the schlieren pictures indicate that the reflection coefficient in this range of angles remains quite low - possibly one tenth that predicted by theory. There are at least two reasons for the difference between theory and experiment. First, the interface is not sharply defined in the experiment, so that there is a finite region over which the physical properties gradually change from those of the liquid to those of the sediment. Second, the sediment grains can act scattering centers for the incident ultrasonic wave. This scattering of the incident wave, in addition to reducing the reflection coefficient, also can lead to a small effect similar to the backward displacement described above. If one uses the mean grain size of 0.38 mm in Equation 3, and assumes that the leaky surface wave excited at the water-sediment interface is of the Stoneley type with $V_R = 0.9V$, then one can calculate that the angle for optimum coupling with the leaky wave would be $\theta_i = 59^o$ for 2 MHz. At an angle of incidence of approximately 57^o one sees the reflection phenomenon shown in Figure 5, in which the striations in the reflected beam presumably result from the interaction between the specularly reflected beam and the backward-displaced beam. These striations vanish for larger or smaller angles of incidence. Evidently the coupling to the backward-directed leaky wave is so weak that a clearly defined displacement as that given in reference 7 is not present with this particular water-sediment interface. However, the photograph given in reference 7 does show striations similar to those in Figure 5.

Finally, in the range of angles greater than the critical angle for the longitudinal waves θ_{CL}, one observes reflection such as shown in Figure 6, in which the reflected beam clearly is made up of two parts: the specularly reflected beam and a displaced beam, with a null strip between the two. Such phenomena have been studied in some detail for liquid-solid interfaces characterized by $V_L > V_S > V$ [4]. However, the water-sediment interface used here is characterized by $V_L > V > V_S$, for which presently available theory is not applicable. As for as we are aware, this photograph, taken at 1 MHz, is the first direct demonstration of the fact that a forward displaced beam can be observed slightly above the longitudinal critical angle. The incident angle here is 62^o, while the calculated critical angle is $\theta_{CL} = 58.3^o$. Coupling to the displaced beam in the manner shown here was observable

from approximately 50° to angles somewhat greater than 62°. This is interpreted to mean that the fact that the interface is granular, rather than plane, leads to a coupling with the leaky surface wave over a considerable range of angles depending upon the grain size distribution. With water-solid interfaces for which similar phenomena have been observed near the shear wave critical angle the excitation of the displaced beam is a very sensitive function of the incident angle. The phenomenon comes and goes within an angular span of only one degree of so [4].

CONCLUSION

We have studied the reflection of ultrasonic waves from a water-sediment interface, and have found that the reflection phenomena nominally can be described by analogy with the reflection of ultrasonic waves at a water-solid interface. In addition, we observe phenomena which probably are associated with the backward displacement of the reflected beam by the periodicity superimposed on the interface by the grains. A very clearly defined beam displaced in the forward direction is observed over a considerable range of incident angles slightly above the longitudinal wave critical angle. Presently available theory will need to be modified to account for this phenomenon.

We conclude that in situations involving reflection from sediments (such as those found in underwater acoustics experiments), or from other interfaces which may have a superimposed periodicity, interpretation of results must include the possibility that the incident beam may couple to either a forward-directed, or a backward-directed leaky wave. In sediments the density distribution at the interface is not as sharply defined as in solids. Nevertheless, we observe coupling to a leaky surface wave. The angle at which this coupling occurs is frequency-dependent for the backward-directed leaky wave [7] but is independent of the frequency for the forward-directed leaky wave [4]. These phenomena are to be expected even for those interfaces characterized by $V_L > V > V_S$. These considerations might be important with surface acoustic waves devices as well as underwater acoustics.

ACKNOWLEDGEMENT

The assistance of Laszlo Adler, Department of Physics, The University of Tennessee, USA, is gratefully acknowledged. Part of the research was supported by the US Office of Naval Research, and part by a travel grant from the Commission for Educational Exchange between Denmark and the USA.

REFERENCES

1 A. Schoch, Ergeb. Exakten Naturwiss. 23, 127-234 (1950); Acustica 2, 18-19 (1952).

1 M. A. Breazeale, L. Adler and J. H. Smith, Sov. Phys. Acoust. 21, 1-6 (1975).

3 M. A. Breazeale, L. Adler and L. Flax, J. Acoust. Soc. Amer. 56, 866-872, (1974).

4 M. A. Breazeale, Laszlo Adler and Gerald W. Scott, J. Appl. Phys. 48, 530-537 (1977).

5 H. L. Bertoni and T. Tamir, Appl. Phys. 2, 157-172 (1973).

6 T. Tamir and H. L. Bertoni, J. Opt. Soc. Amer. 61, 1397-1413 (1971).

7 M. A. Breazeale and Michael A. Torbett, Appl. Phys. Letters 28, 456-458 (1976).

8 L. Bjørnø, J. Acoust. Soc. Amer. 60, S96-97 (1976).

9 L. M. Brekhovskikh, Waves in Layered Media. (Academic, New York, 1960).

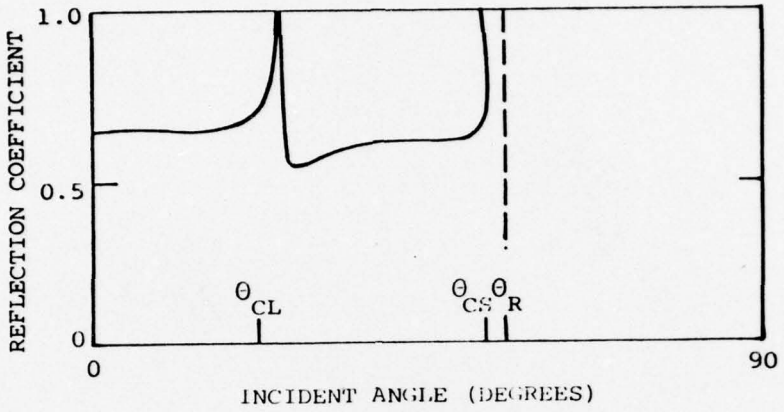

Fig. 1 Reflection coefficient for liquid-solid interfaces characterized by $V_L > V_S > V$.

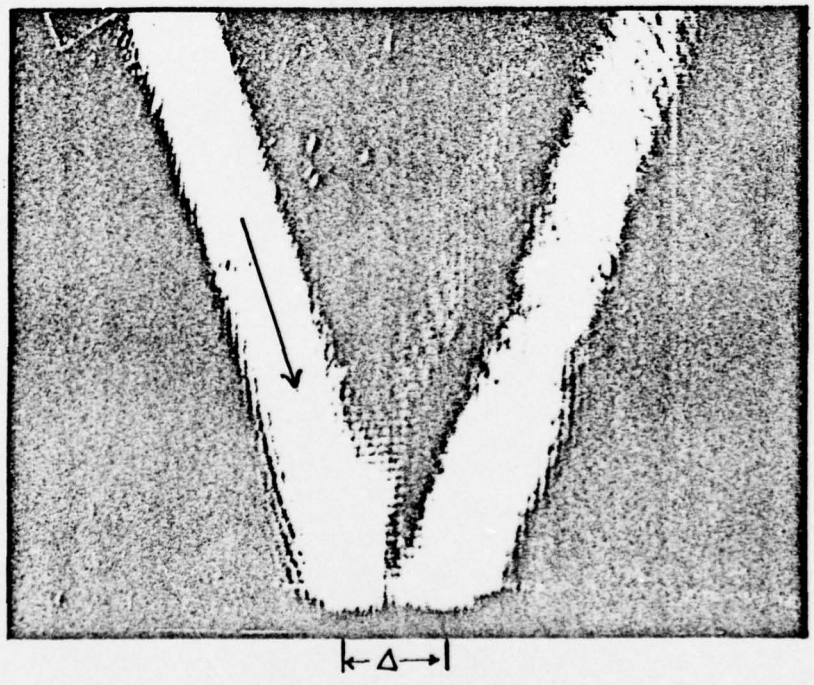

Fig. 2 Ultrasonic beam reflected from a water-glass interface for which $V_L > V_S > V$.

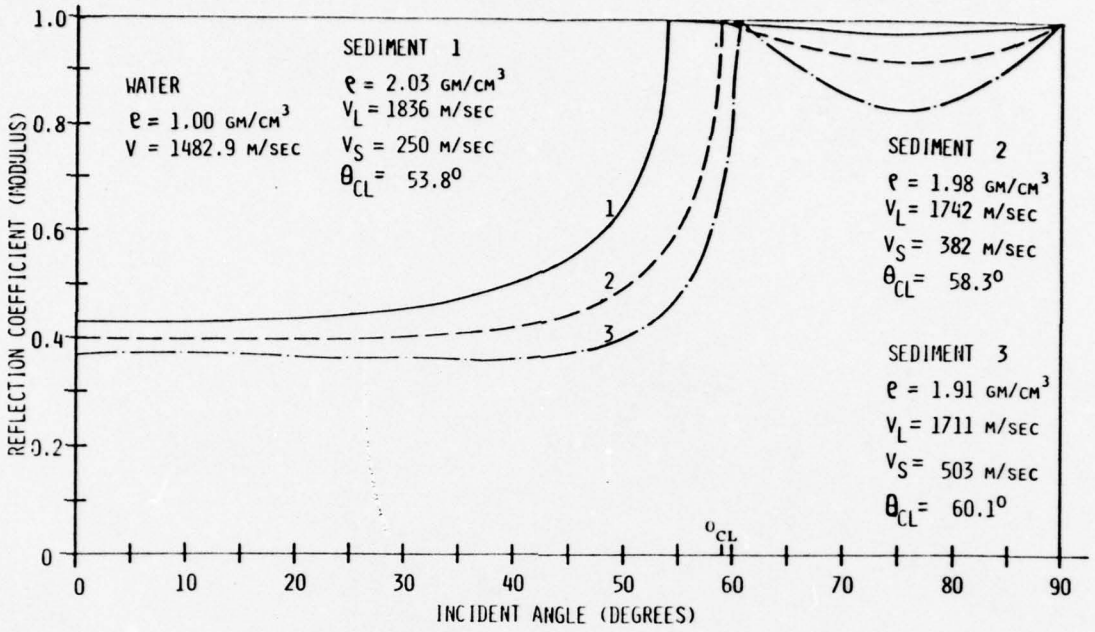

Fig. 3 Calculated reflection coefficient for three different water-sediment interfaces.

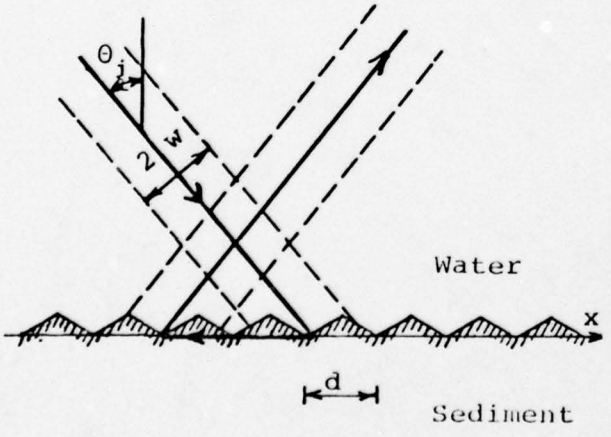

Fig. 4 Diagram of incident beam coupled to a backward-directed leaky surface wave.

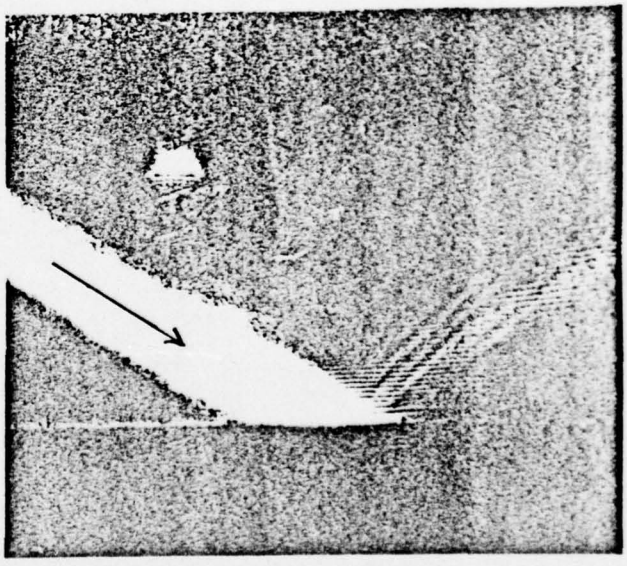

Fig. 5 Reflection of an ultrasonic beam from a water-sediment interface.

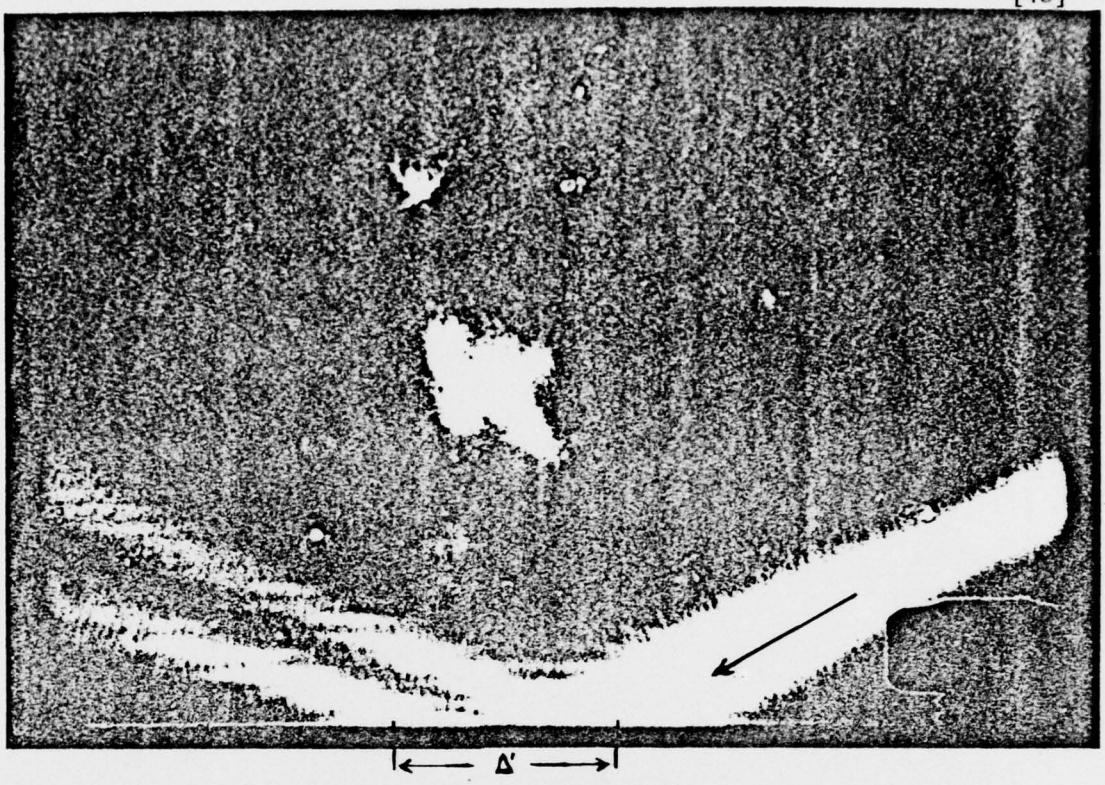

Fig. 6 Reflection of a 1 MHz ultrasonic beam from a water-sediment interface. Both specular and displaced beams are visible.

Paper No. 7

Reflection of a Gaussian Ultrasonic Beam from Water-Plexiglass Interface (Laszlo Adler).

Reflection of a Gaussian Ultrasonic Beam from Water-Plexiglass Interface

Laszlo Adler

In most of our previous studies for reflection of Gaussian ultrasonic beams from liquid-solid interfaces we were concentrating on the region at or near the Rayleigh angle. For solid materials where the shear velocity is smaller than the velocity of sound in the liquid no real value of the Rayleigh angle and of the leaky Rayleigh velocity exists. Such a material is plexiglass in water. Initial results for reflection of a Gaussian ultrasonic beam from water-plexiglass interface were taken by a continuous wave schlieren system and shown for several angles of incidence on Fig. 1. A double beam above the longitudinal critical angle (see Fig. 1C) is observed which resembles the pattern one observes at the Rayleigh angle for materials having real leaky Rayleigh velocity. The reflection coefficient calculated for an infinite plane wave from the plexiglass-water interface (Fig. 2) does not predict such behavior. The appearance of the double beam above the longitudinal angle was also observed for the sediment-water interface (see "Forward- and Backward-Displacement of Ultrasonic Waves Reflected from a Water-Sediment Interface," M. A. Breazeale and L. Bjørnø, Paper No. 6). The appearance of the double beam above the longitudinal critical angle is an indication that the finite beam couples to the interface and that the surface wave is leaking back to the liquid. No theoretical treatment of this problem is available at present. One needs to investigate the behavior of the

reflection coefficient for finite beams at the longitudinal critical angle in order to describe this phenomenon mathematically. It may be worthwhile to mention that this is much more a true analog to the optical Goos-Hänchen effect (observed at the critical angle for light waves from dielectrics). The reflection phenomenon at the Rayleigh angle is not really a true analog of the Goos-Hänchen effect.

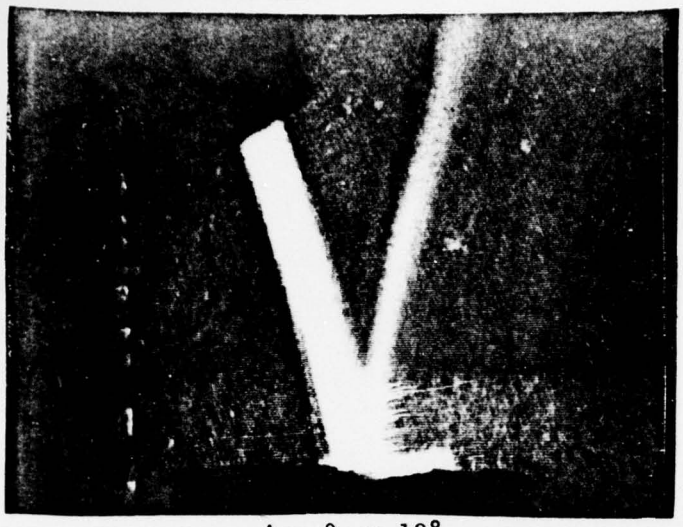

A. $\theta_i = 18°$

B. $\theta_i = \theta_{CL} = 34°$

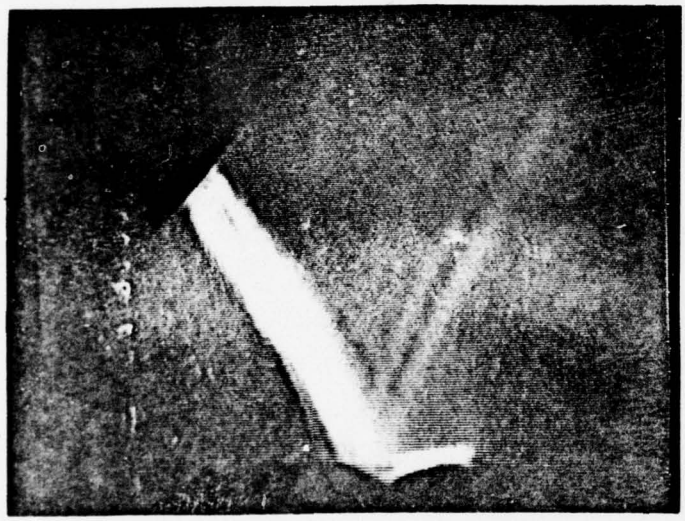

C. $\theta_i = 40°$

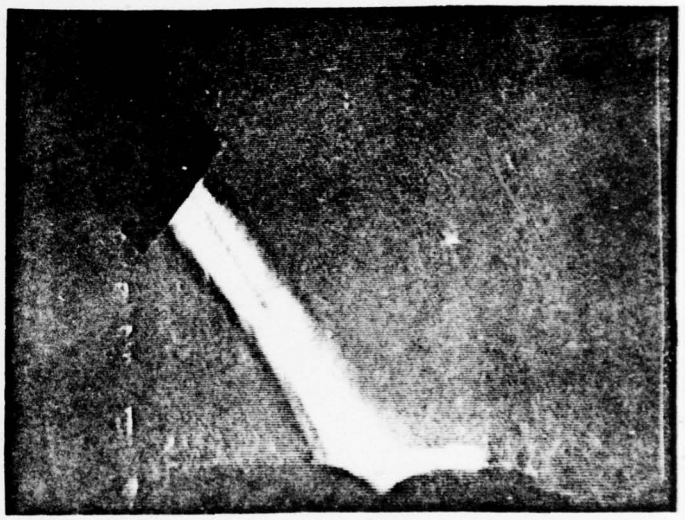

D. $\theta_i = 44°$

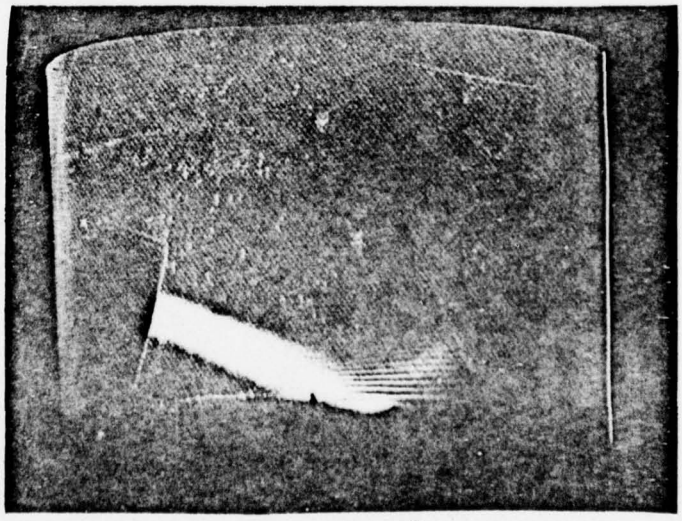

E. $\theta_i = 68°$

Figure 1

REFLECTION OF A GAUSSIAN ULTRASONIC BEAM FROM
A WATER-PLEXIGLASS INTERFACE

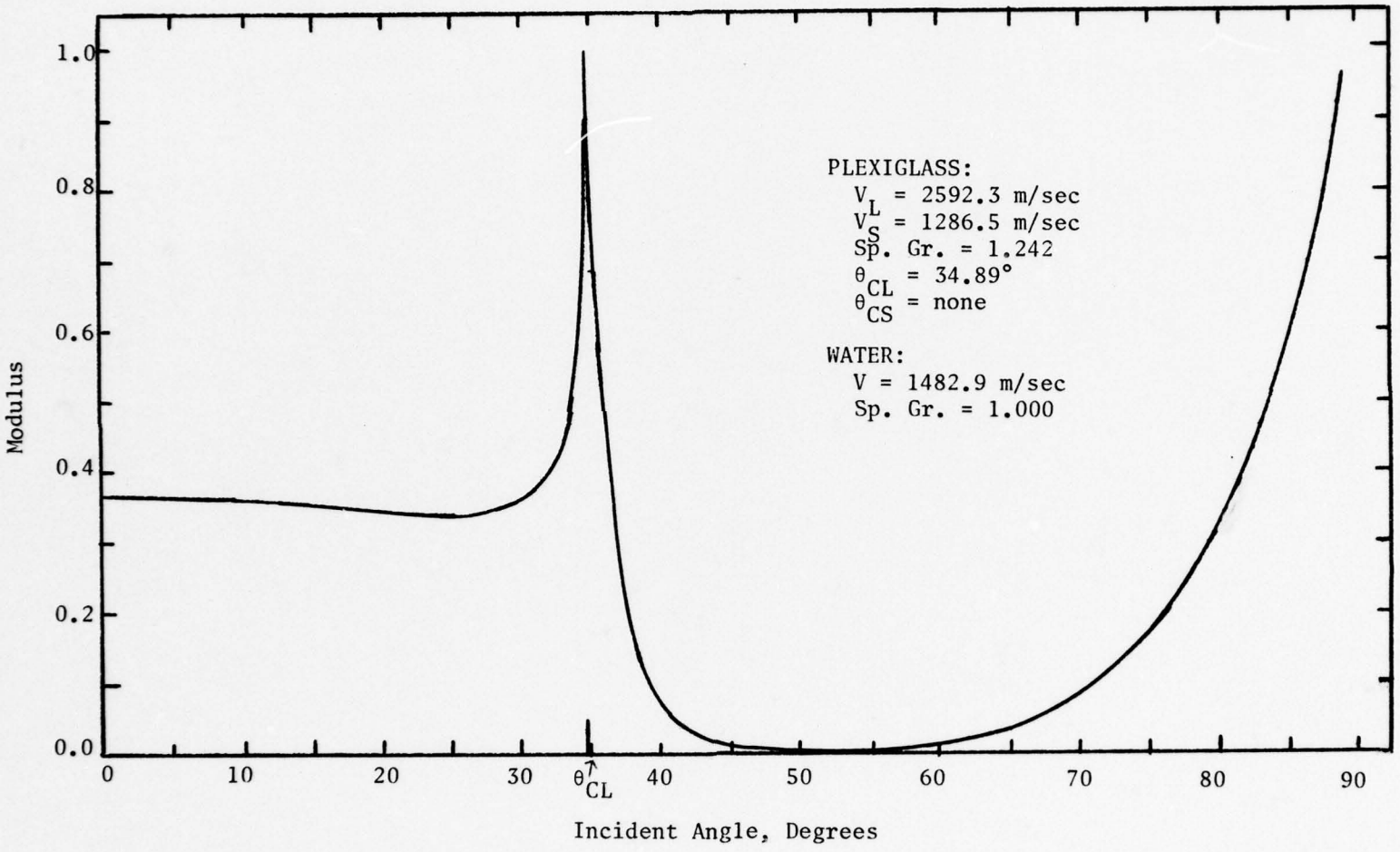

Figure 2. The Modulus of an Ultrasonic Wave Incident from Water onto Plexiglass as a Function of Incident Angle (Theoretical Plot).

Paper No. 8

The Structure of Ultrasonic Leaky Waves and Their Interaction with Subsurface Flaws (G. W. Scott and Laszlo Adler, Materials Evaluation 35, 54-58 (1977).

Submitted for publication in February 1976. Research sponsored by the Office of Naval Research under Contract No. N00014-76-C-0177.

The Structure of Ultrasonic Leaky Waves and Their Interaction with Subsurface Flaws

by G. W. Scott and Laszlo Adler

Abstract

Recent experiments and theoretical efforts indicate that the interaction of a bounded ultrasonic beam with a liquid-solid interface at the Rayleigh angle produces a specular reflection, which carries energy back into the liquid from the point of incidence, and a leaky Rayleigh wave, which propagates along the interface and continuously radiates into the liquid. Because the leaky wave penetrates only a few wavelengths below the solid surface, its potential for near-surface flaw detection has been investigated. An immersible acoustic goniometer system was used to measure the amplitude and phase distribution across the reflected beam from a water-metal interface for an incident Gaussian beam. This amplitude and phase distribution, which had been successfully compared to a theoretical model, was found to depend on the following test parameters: frequency, distance, beam width, and material properties. Specimens with and without artificial defects were investigated. The reflected (reradiated) field is altered when defects are present, as shown by these goniometer measurements and by schlieren photography.

INTRODUCTION

Surface (or Rayleigh) waves have been studied in detail and applied to many NDT problems.[1] They are most often launched and received by one or more contact transducers. The "leaky" wave, so-called by Bertoni and Tamir,[2] has a surface component with some properties similar to those of Rayleigh waves. However, it is the differences between the leaky wave system and ordinary Rayleigh waves which make leaky waves of potential value for NDT applications.

Theoretical[2,3] and experimental[3,4] investigations have established the structure and properties of the leaky wave system and provided methods for computing the phase and amplitude of the field. Simple field configurations, such as the Gaussian incident beam, can be solved by analytical approximation; more difficult problems may require complete machine computation of the solution.

The leaky wave system, generated by impingement from a liquid onto a liquid-solid interface, includes a specular, or directly reflected component, and a surface component which radiates (leaks) energy back into the liquid. The behavior of the surface component depends strongly on the acoustic properties of the interface materials, and the interference between the components in the liquid coupling medium produces the unique features of the system.

G. W. Scott, a development engineer with the NDT Group at Oak Ridge National Laboratory, received his BS and MS degrees in physics from M.I.T. and the University of Tennessee. He served with the U.S. Navy from 1957-1968 in various conventional and nuclear ship propulsion plant engineering assignments. His NDT experience since 1968 includes the development of methods, system designs, and QA programs for the inspection of nuclear weapons and U-235 enrichment facilities at Union Carbide Nuclear Division, Oak Ridge, TN. For inquiries concerning this work, contact the author at (615) 483-8611, X3-1922.

Dr. Laszlo Adler is Associate Professor in the Department of Physics at the University of Tennessee in Knoxville. He is also a consultant to the Nondestructive Testing Group at Oak Ridge National Laboratory. Dr. Adler is doing research in physical ultrasonics and its applications to NDT and to biomedical problems. He teaches a course on Principals of Nondestructive Testing to Physics and Engineering students at the University of Tennessee.

THEORY

Reflection at a Liquid-Solid Interface

Lord Rayleigh[5] first demonstrated theoretically that surface waves can be launched along a solid-gas or solid-vacuum interface by the impingement of waves from the solid at a characteristic angle, later named the "Rayleigh angle." Schoch[6] studied the impingement of a beam from the liquid onto a liquid-solid interface; he observed an apparent lateral displacement of the reflected beam at a characteristic angle which he also called the Rayleigh angle. Schoch also introduced the treatment of the bounded (i.e., finite-width) beam as a superposition of infinite (width) plane waves. His treatment formed the basis for the Bertoni-Tamir theory[2] in which the reflected field is represented by

$$v_{ref}(x,z)=\int_{-\infty}^{\infty} V(k_x)R(k_x)\exp[i(k_x x-k_z z)]dk_x. \quad (1)$$

The coordinate axes are shown in Figure 1; the k's are wave

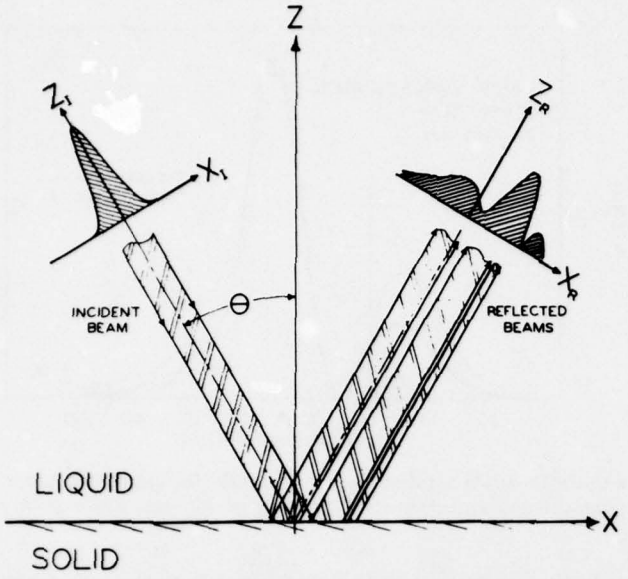

Figure 1—Coordinate system and schematic illustration of a Gaussian beam incident on a liquid-solid interface at the Rayleigh angle.

number components in the coordinate directions; $V(k_x)$ is the angular distribution of infinite plane waves, and $R(k_x)$ is the interface reflection coefficient.

In their development of an analytical approximation to the reflection integral (1), Bertoni and Tamir show that it divides into two parts and can be written as

2 $$v_{refl}(x,z) = v_0(x,z) + v_1(x,z).$$

$v_0(x,z)$ represents a specular reflection, which resembles the incident beam in its amplitude distribution but is shifted 180° in phase. $v_1(x,z)$ is the surface component, which is in phase with the incident beam over part of the interface and out of phase over the remainder; its amplitude distribution is, in general, significantly different from that of the incident beam and the specular component.

For a Gaussian incident beam, as used in the experiments described below, Bertoni and Tamir[2] obtained an analytical approximation valid at the interface. In order to compare theory with experiment, Breazeale, Adler, and Scott[3] corrected the approximation for points in the liquid halfspace. The expressions for the leaky wave field components are:

3 $$V_0(x_r,z_r) = \frac{1}{2\pi} \frac{\exp\{-(x_r/w_r)^2 + ik[x_r \sin\theta_p + (z_r - z_0)\cos\theta_p]\}}{\sqrt{\pi} w_r \cos\theta_p}$$

4 $$V_1(x_r,z_r) = -2V_1(x_r,z_r)\left[1 - \frac{\sqrt{\pi} w_r}{\Delta_s} \exp(\gamma^2)\,\mathrm{erfc}(\gamma)\right]$$

where

5 $$\gamma = \frac{w_r}{\Delta_s} - \frac{x_r}{w_r},$$

and

6 $$w^r = w\left[1 + \frac{2i(z_r - z_0)}{kw^2\cos\theta_p}\right]^{1/2}.$$

The beam halfwidth w is measured at z_0, θ_p is the liquid-solid equivalent of the Rayleigh angle, and Δ_s is the so-called "Schoch displacement." Δ_s was derived by Schoch in his original lateral displacement theory[6] and was shown[2] to be mathematically equivalent to a surface wave decay constant occurring in the Bertoni-Tamir approximation. It is a complex function of the acoustic velocities and densities of the interface media.

Modeling Subsurface Flaw Interactions

The surface component of the leaky wave system decays exponentially below the solid surface similarly to the Rayleigh wave. Therefore, it is sensitive to subsurface flaws in the same region of material, about one Rayleigh wavelength below the solid surface.[7]

The interaction with a flaw was modeled by writing the reflected field as

7 $$v_{refl}(x,z) = v_0(x,z) + a(x)v_1(x,z).$$

The defect tested was a side-drilled hole, represented as a cylinder of radius R, located at x_c. Then one can write

8 $$a(x) = \begin{cases} 1, & \text{for } x < x_c - R \\ 1 - \dfrac{(1+\alpha)}{2R}(x - x_c + R), & \text{for } x_c - R \le x \le x_c + R \\ \alpha, & \text{for } x > x_c + R \end{cases}$$

where α is the fraction of surface component amplitude remaining after interaction with the flaw.

EXPERIMENTAL APPARATUS AND PROCEDURES

Transducer Design and Operation

For the present experiments it was necessary to have a well-defined beam, free of side lobes. The effective width was not critical, although the theory[2] predicts some potential difficulties with very narrow beams. Gaussian amplitude variation across the wavefront was desired because this case had been solved analytically, providing a good opportunity for careful comparison of theory and experiment.

For the investigation, the transducers (2) were fitted with 1 in. diameter x-cut quartz crystals, plated with conducting material (gold or silver) on the liquid side. The rear electrode was a metal strip aligned to be symmetric about a diameter of the crystal, parallel to the goniometer axis. The transmitter was driven by a burst of 2 MHz RF, about 6 μsec long, which produced a pulse in the receiver about 20 μsec long.

Results showed that a 3.68 mm receiver electrode consistently produced the narrowest beam profiles, so that particular size was used in the receiver for all experiments.

A 6.35 mm electrode was used in the transmitter because its beam was narrower and diverging less rapidly at the distances selected for reflection measurements, and because it produced larger signal amplitudes at the receiver. Figure 2 is the amplitude and phase profile made with these electrodes.

The Acoustic Goniometer

Figure 3 shows the goniometer removed from its water tank. For operation it is immersed in water up to a point about halfway between the top of the specimen holder and the base of the column on which the arms mount. The left arm carries the transmitter and the right arm carries the receiver (the slide moves the receiver perpendicular to the arm). The transducer carriages can be moved radially along the arms and clamped at radii of about 5 to 50 cm.

The specimen holder accommodates rectangular blocks (2 by 4 in.) up to 1 in. thick and right circular cylinders (3 in. in diameter) up to a few inches long. Either specimen type is restrained so that its front (reflecting) face coincides with the rotation axis of the arms. Figure 3 shows a cylindrical aluminum oxide specimen in place.

Acoustical Measurements

Amplitudes were measured by reading the voltage devel-

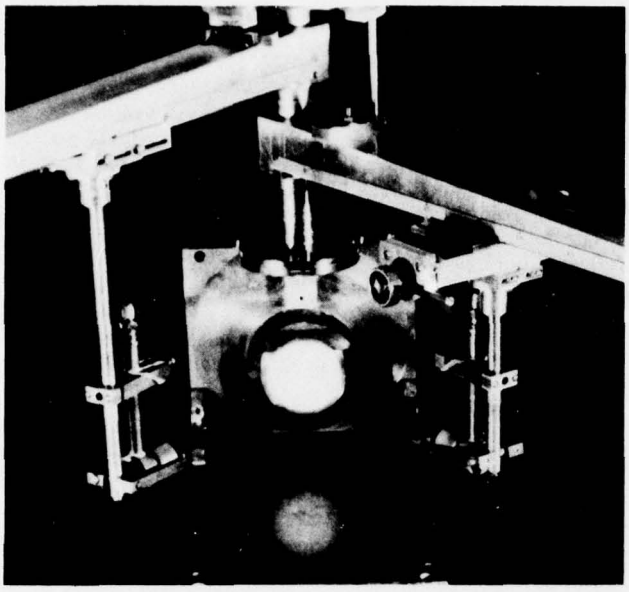

Figure 2—Acoustic goniometer.

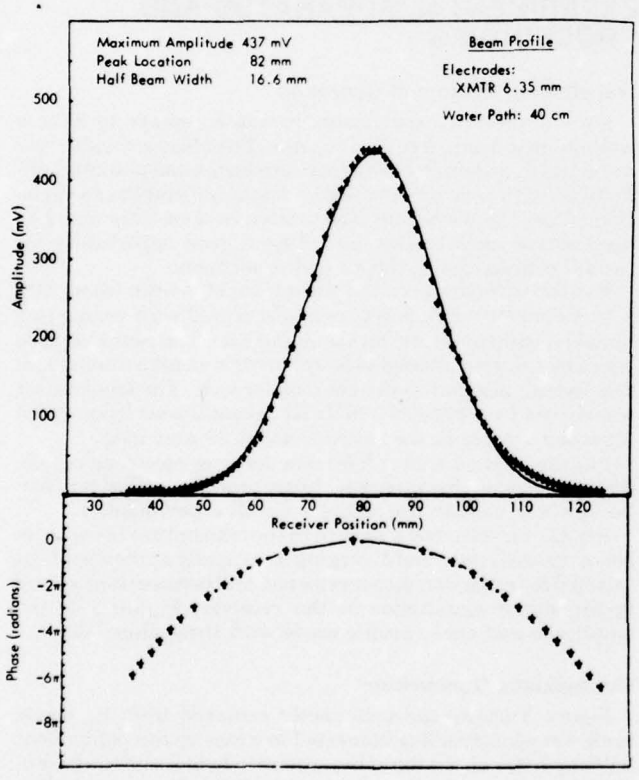

Figure 3—Amplitude and phase of the acoustic beam profile of a Gaussian transducer.

oped across the receiver crystals from an oscilloscope cathode ray tube.

Several potential applications motivated efforts to measure phase:[4] (1) goniometer alignment; (2) tracing wavefront contours in transducer-beam profiles; and (3) tracing wavefront contours in Rayleigh angle reflections. A technique devised for detecting a constant phase led to improvements which allowed approximate but repeatable measurements of relative phase. Triggering the oscilloscope from the transmitter pulse allows relative phase measurements.

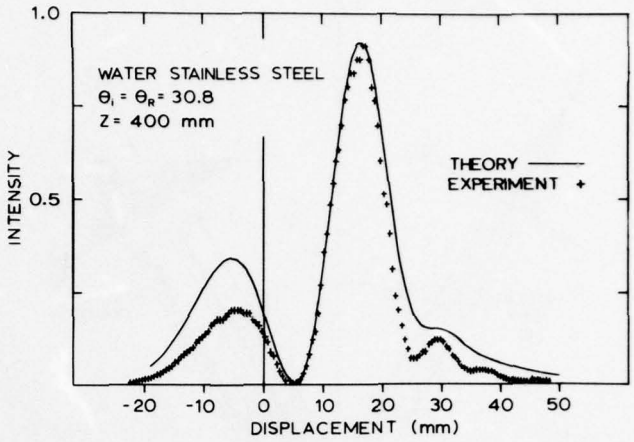

Figure 4—Intensity distribution of a reflected ultrasonic beam from a water-stainless steel interface at 400 mm water path.

In this condition, the displayed signal from the receiver is locked in phase with the transmitter driving signal. All of the pulses are coherent with one another because they originate from the same CW source, and the oscilloscope trigger circuits fix the phase point on the RF waveform at which the sweep starts. The only remaining phase changes result from changes in the propagation delay of the acoustic signal along its water path, and these are observable on the CRT as movement of the entire waveform across the screen.

Rayleigh Angle Identification

Reports of other experimenters established a range of values where the Rayleigh angle for a material was expected to lie. Starting at angles 1–2° below the expected range, the transmitter and receiver arms were set at equal angles. Then the receiver was scanned through the full range of the cross slide, and the locations and values of all local maxima and minima in the amplitude were noted. The slide was set to a position corresponding approximately to the center of the incident beam. The oscilloscope was set to indicate zero relative phase at this position, and relative phase was observed as the slide was scanned to the right and left. Locations of large or sudden changes in phase were noted.

As the Rayleigh angle was approached, the maxima and minima occasionally shifted position and relative value slightly, and one minimum would become an absolute minimum; i.e., its amplitude would decline to a value less than those of the other minima.

The overall behavior pattern of the minima was complex, so it was frequently necessary to follow the behavior of several minima individually through a range of angles. That angle corresponding to the lowest amplitude among the minimum values obtained was called the Rayleigh angle. In each case, the lowest minimum was accompanied by a rapid variation of the phase in its neighborhood, amounting to as much as 180° of shift. This phase variation provided some additional confidence in the identification.

Comparison of Reflection Theory and Experiment

Amplitude and phase measurements were made on solid stainless steel blocks with total water paths (transmitter-target-receiver) of 400 and 800 mm to observe the effect of distance. The smooth curves compared with the measured intensity data (computed by squaring the measured amplitudes) in Figures 4 and 5 are computed values of

$$|V_{refl}|^2 = |V_0 + V_1|^2. \quad (9)$$

The agreement between experiment and theory is excellent.

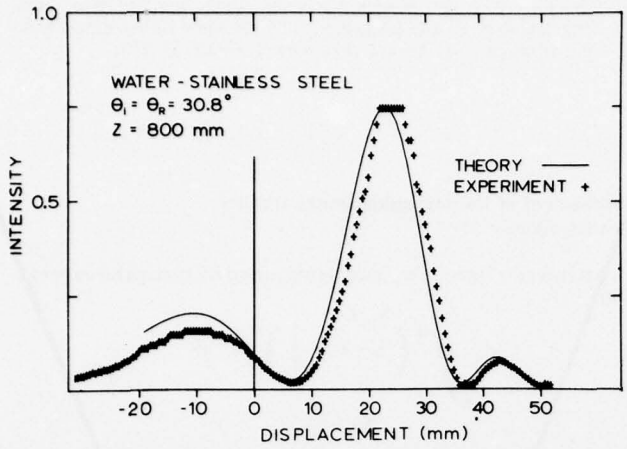

Figure 5—Intensity distribution of a reflected ultrasonic beam from a water-stainless steel interface at 800 mm water path.

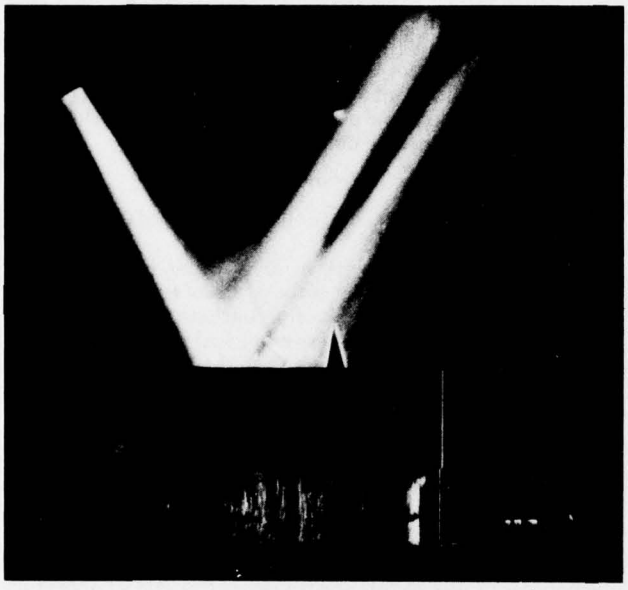

Figure 6—Schlieren photograph of the incident (left) and reflected field at the Rayleigh angle.

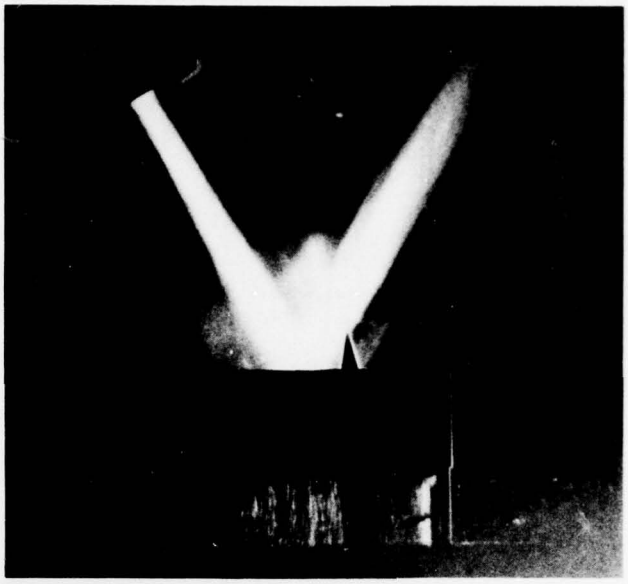

Figure 7—Schlieren photograph of the incident and reflected field at the Rayleigh angle. The leaky wave is highly attenuated by the near-surface defect.

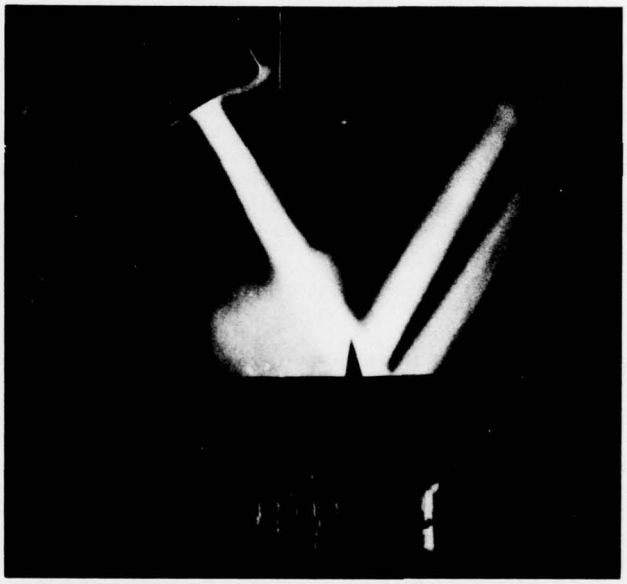

Figure 8—Schlieren photograph of the incident and reflected field at the Rayleigh angle.

The Effect of Near-Surface Flaws on Leaky Waves

A 6.35 mm (diameter) hole was side-drilled 0.75 mm (about one-half shear wavelength) beneath the 2×4 in. surface of a stainless steel block to form an artificial flaw. To illustrate the interaction between the leaky waves and the flaw a series of schlieren photographs was taken. In Figure 6 the incident beam hits the surface at a point far from the flaw (the pointer indicates the positions of the flaw). The two reflected beams correspond to the specular component and the reradiated leaky wave. The null point between these is due to interference. As the incident beam is moved toward the flaw, the leaky wave which penetrates into the steel is *interacting* with the flaw and is attenuated. In this case only the specularly reflected beam shows, as in Figure 7. When the incident beam is moved farther to the right, the leaky wave is not attenuated as much by the flaw and the two beams again will be visible, as shown in Figure 8. With this simple experiment we have demonstrated that near-surface flaws can be detected by leaky Rayleigh waves. The experiment was repeated with a flaw drilled about two shear wavelengths below the surface and no interaction of leaky waves with the flaw was observed.

To obtain more quantitative information about the variation of the reflected field when near-surface flaws are present, the goniometer experiment was repeated at 400 mm water path and the result is shown in Figure 9. The solid line is calculated from Equation 7.

CONCLUSIONS

The agreement between theory and experiment for stainless steel indicates that the leaky wave component contributes strongly to the total radiated field of ultrasonic waves from water-metal interfaces. The intensity distribution of the reflection depends on the ultrasonic test parameters such as water path length, beam width, and frequency as well as on

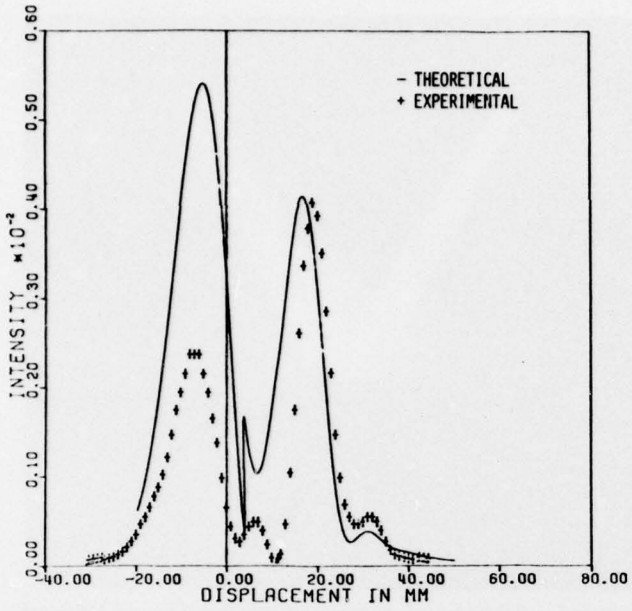

Figure 9—Intensity distribution of a reflected ultrasonic beam from a stainless steel block with 6.35 mm hole located 6.4 mm from incident beam center.

material properties. The leaky wave surface component which penetrates into the solid is affected by the presence of near-surface discontinuities. It is demonstrated by schlieren method and by goniometer measurement that the reflected field is strongly altered if a flaw is less than approximately two shear wavelengths below the surface. This effect suggests the possibility of using Rayleigh reflection methods to detect near-surface defects.

Application to NDT Situations

Knowledge of the amplitude distributions provides a basis for the design of near-surface flaw inspections. More detailed studies of this type would tell the designer the optimum locations of his transducers for maximum sensitivity and allow precise location of flaws with respect to the transducer positions. The studies displayed here show that neither the center of the specular reflection nor the classical "Schoch distance" provides the optimum location for the receiver.

This work also shows that significant changes in phase behavior occur when defects are present. The application of electronic phase measurement to defect detection would represent a significant step forward in the use of acoustic information for materials inspection.

References

1. Viktorov, I. A. *Rayleigh and Lamb Waves.* New York: Plenum Press, 1967.
2. Bertoni, H. L., and Tamir, T. *Appl. Phys.* 2 (1973): 157.
3. Breazeale, M. A.; Adler, L.; and Scott, G. W. "Interaction of Ultrasonic Waves Incident at the Rayleigh Angle Onto a Liquid-Solid Interface." *J. Appl. Phys.* 48 (1977): 530.
4. Scott, G. W. "Amplitude and Phase of Rayleigh-Angle Reflections of Gaussian Ultrasonic Beams Incident on Liquid-Solid Interfaces." AD-A016024, Aug. 1975 (NTIS).
5. Lord Rayleigh (J. W. Strutt). *Proc. London Math. Soc.* 17 (1885): 4–11.
6. Schoch, A. *Erg. der exakten Naturwissenschaften* 22 (1950): 160.
7. Hildebrand, B. P., and Becker, F. L. "Ultrasonic Holography at the Critical Angle." *J. Acoust. Soc. Amer.* 56 (1974): 459.

Paper No. 9

Application of Ultrasonic Leaky Waves in NDE (Laszlo Adler and Gerald W. Scott), 1976 Ultrasonics Symposium Proceedings, IEEE Cat. #76 CH1120-5SU, pp. 100-10.

APPLICATION OF ULTRASONIC LEAKY WAVES IN NDE*

Laszlo Adler and Gerald W. Scott
Department of Physics, University of Tennessee
Knoxville, Tennessee

ABSTRACT: Theoretical investigations by Bertoni and Tamir [J. Appl. Phys. 2, 157 (1973)] indicate that a bounded ultrasonic beam incident at the Rayleigh angle to a liquid-solid interface will produce a specularly reflected wave and a "leaky wave" which propagates along the interface and continuously radiates energy into the liquid. Since these leaky waves penetrate less than a few wavelengths into the solid, they should be attenuated and scattered by the presence of near-surface defects. An immersible goniometer system was used to measure the amplitude distribution across the reflected field from a water-stainless steel interface. Measurements indicate that the presence of near-surface defects will alter the distribution of the reflected field. Similarly, alteration of the theoretical calculation for the reflected amplitude is obtained when an attenuation mechanism is assumed for the leaky wave propagation.

INTRODUCTION

The application of surface or Rayleigh waves to NDE problems has been known and well investigated for some time.[1] Most often a contact transducer launches the waves and receives echoes returning from cracks or other defects. The technique described herein offers some alternatives to conventional surface wave techniques by generating the surface wave through fluid coupling and using two transducers in a pitch-catch arrangement. It has been recently established by theoretical[2] and experimental[3] investigations that when a well-defined (e.g., gaussian) ultrasonic beam falls onto a liquid-solid interface the reflected field has two components: (1) a specular reflection and (2) a surface or "leaky wave" which propagates along the interface and radiates (leaks) energy back into the liquid. The total field, which is the algebraic sum of the two components, can be measured and calculated in terms of the ultrasonic parameters and material properties of the interface. The information obtained lends itself to a quantitative technique which provides sensitivity to subsurface flaws.

THEORY

Schoch[4] was first to study the impingement of an ultrasonic wave from a liquid to a solid interface and observed an apparent lateral displacement of the beam at an angle which he referred to as a Rayleigh angle. Schoch also introduced the concept of treating a bounded beam as a superposition of infinite plane waves. The reflected wave is represented by

$$V_{refl} = \int_{-\infty}^{\infty} V(k_x)R(k_x)\exp[i(k_x x - k_z z)]dk_x \qquad (1)$$

where $R(k_x)$ is the reflection coefficient and $V(k_x)$ depends on the beam distribution of the incident beam.

Schoch approximates the reflection integral for a uniform incident beam and obtains a formula which gives lateral displacement of the reflected beam but preserves an amplitude profile similar to that of the incident beam. Experimental results of Breazeale, Adler, and Smith[3] showed, however, that the reflected beam has a different profile even when the incident beam is a gaussian as illustrated on Figure 1.

Bertoni and Tamir[2] developed a new approximation for the reflection integral (Eqn. 1) and derived a solution for the gaussian incident beam which is valid at the interface. Adler, Breazeale, and Scott[5] added corrections to the Bertoni-Tamir solution for distance from the interface. Their solution is written as

$$V_{refl}(x_r z_r) = V_0(x_r z_r) + V_1(x_r z_r) \qquad (2)$$

$$V_0(x_r z_r) = -\frac{1}{2w}\frac{\exp[-(x_r w_r)^2 + ik[x_r \sin\theta_p + (z_r - z_0)\cos\theta_p]]}{\sqrt{\pi}\, w_r \cos\theta_p} \qquad (3)$$

and

$$V_1(x_r z_r) = -2V_0(x_r z_r)\left[1 - \frac{\sqrt{\pi}\, w_r}{\Delta_S}\exp(\gamma^2)\operatorname{erfc}(\gamma)\right] \qquad (4)$$

where

$$\gamma = \frac{w_r}{\Delta_S}\cdot\frac{x_r}{w_r}, \qquad (5)$$

and

$$w_r = \left[1 + \frac{2i(z_r - z_0)}{kw^2\cos\theta_p}\right]. \qquad (6)$$

The beam halfwidth w is measured at z_0, θ_p is the liquid-solid equivalent of the Rayleigh angle, Δ_S is the so-called Schoch displacement, and it depends on the velocities and densities of the two media. The component $V_0(x_r z_r)$ is the specular reflection whose profile resembles the incident wave and $V_1(x_r z_r)$ is the "leaky wave" component which penetrates about one wavelength below the interface. If a subsurface void or flaw is present, the leaky wave will interact with it.

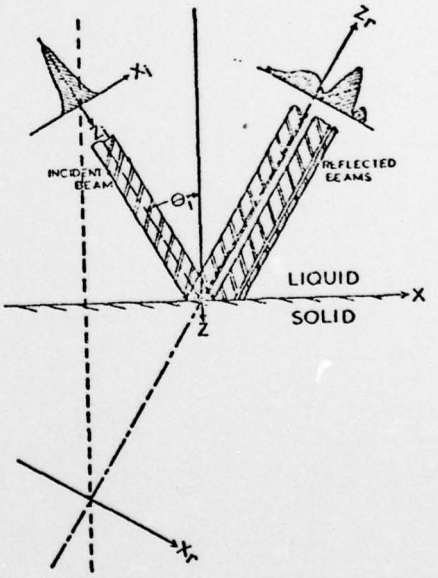

Fig. 1. Schematic Illustration of a Gaussian Ultrasonic Beam Incident on a Liquid-Solid Interface at the Rayleigh Angle. Typical Intensity Patterns of the Reflected Beams Are Also Shown.

MODELING SUBSURFACE FLAW INTERACTION

Let us assume a cylindrical void with radius R whose center is at x_c. The reflected field is modified as

1976 Ultrasonics Symposium Proceedings, IEEE Cat. #76 CH1120-5SU

$$V_{refl}(x,z) = V_0(x,z) + a(x)V_1(x,z) \qquad (7)$$

where

$$a(x) = \begin{cases} 1 \text{ for } x<x_c-R \\ 1 - \frac{(1+\alpha)}{2R}(x-x_c+R) \text{ for } x_c-R \le x \le x_c+R \\ \alpha \text{ for } x>x_c+R \end{cases} \qquad (8)$$

where α is the fraction of surface wave amplitude remaining after interaction with the void. Equations (2) and (7) have been experimentally verified.

REFLECTED FIELD MEASUREMENT

Figure 2 shows the goniometer system used to measure the reflected field. The transmitter is suspended from the left arm. The receiver is suspended

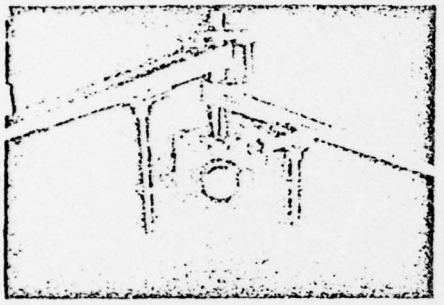

Fig. 2. Goniometer Used in Making Intensity Measurements.

from the cross-slide mounted on the right arm. The cross-slide carries the receiver along a path which is perpendicular to the goniometer arm. The transmitter was driven by a 2-MHz pulsed RF source. The receiver output was displayed on the delayed sweep of an oscilloscope for amplitude and relative phase measurements. In the experiment both transmitter and receiver were specially designed 2-MHz gaussian transducers. The amplitude and phase profile of the acoustic beam is shown on Figure 3 as observed 400 mm away in water. The amplitude distribution fits a gaussian function well. For reflection experiments both receiver and

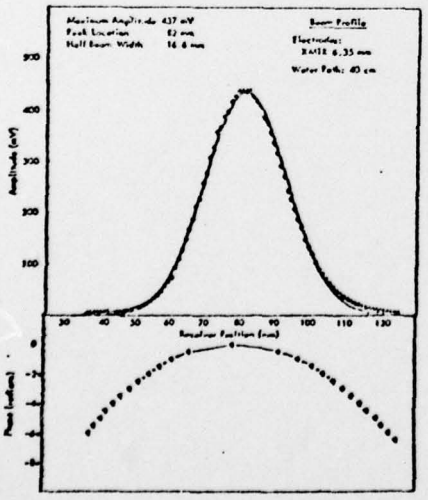

Fig. 3. Amplitude and Phase Profile of the Incident Beam.

transmitter arms are positioned to the Rayleigh angle with transducers equal distances from the reflector (specimen). The Rayleigh angle can be identified by observing the RF display on the oscilloscope of the reflected field amplitude. At that angle there is a so-called "null point" observed. This is the point where the specularly reflected wave interacts with the leaky wave with 180° phase shift between the two components as shown on Figure 4. The samples used were a stainless steel block with polished surfaces, one without any subsurface defects and one with a near-surface defect simulated by a cylindrical hole of 3 mm radius drilled a half wavelength below the surface.

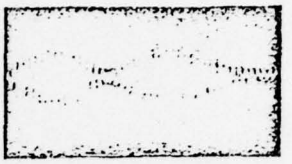

Fig. 4. Received Signal at the Rayleigh Angle. The two Components of the Reflected Field are Separated.

RESULTS

The measured intensity (computed by squaring measured amplitude) distribution of the reflected field from a stainless steel block together with the theoretical calculation is shown on Figure 5. The smooth

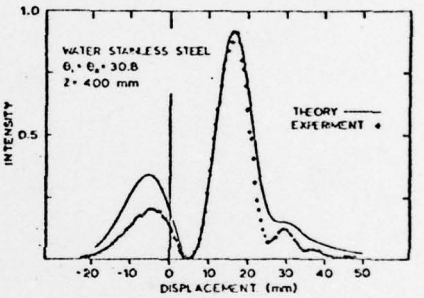

Fig. 5. Reflected Intensity Distribution from a Water-Stainless Steel Interface.

curves are plots of

$$|V_{refl}|^2 = |V_0 + V_1|^2 . \qquad (9)$$

The total distance between transmitter and receiver was 400 mm. The Rayleigh angle for the interface is 30.8°. The origin of the coordinates corresponds to the center of the incident beam. Both experimental and theoretical curves indicate that there is a small peak at the left, due to the specular reflection, and a larger peak (and some diffraction effects) at the right, due to the leaky wave component, with a well-defined "null point" where the two components are interfering.

When the experiment is repeated under the same conditions but with a near-surface void in the steel block, the intensity distribution is changed significantly, as shown on Figure 6. For the flaw, αV_1 was used in place of V_1 in Eqn. (9). The subsurface void is positioned 7 mm from the center of the incident beam. The additional peak appearing between the specular and leaky wave components is very significant. Its center appears to give the location of void x_c and its width the width of the void 2R. Furthermore, the leaky wave component is highly attenuated, as can be seen by comparing Figure 5 and Figure 6. The same effect can easily be demonstrated qualitatively by observing schlieren photography as on Figure 7. On Figure 7a the incident and reflected field is shown fr a stainless steel block. The position of the subsurface void (marked by the pointer) is far from the incident beam. The reflected field is not interacting with the flaw. Both specular component and the leaky wave

components are present with the "null point" between them. As the incident beam is moved toward the void at one point the leaky wave component of the reflected field is highly attenuated due to the interaction with the near-surface void as shown on Figure 7b.

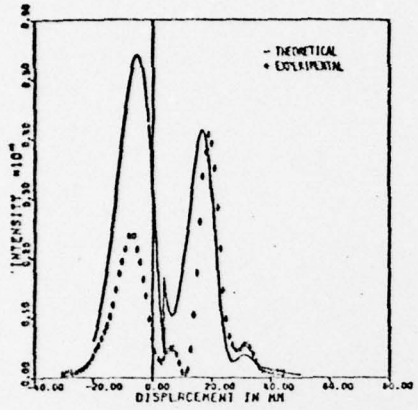

Fig. 6. Reflected Intensity Distribution for a Water-Stainless Steel Interface with a Subsurface Void.

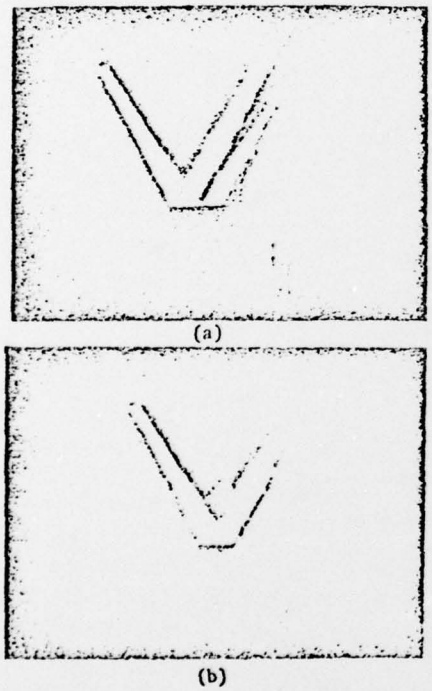

Fig. 7. Schlieren Photography of the Incident and Reflected Ultrasonic Fields. (a) The "Leaky Wave" is Not Interacting with the Void; (b) The "Leaky Wave" is Interacting with the Void. The position of the Void is Marked by the Pointer.

Conclusions

When a gaussian beam incident at the Rayleigh angle to a liquid-solid interface is reflected, the reflected field distribution has two interacting components: (1) specularly reflected waves and (2) surface "leaky waves" radiating back to the liquid. The reflected amplitude distribution can be described in closed analytic form in terms of ultrasonic test parameters and the physical properties of the liquid and solid. A near-surface void can be modeled as an attenuation mechanism and incorporated into the analytic expression. The calculation agrees reasonably well with the experiment. From the reflected field distribution one may obtain both position and size of a subsurface flaw. The interaction of the leaky wave with a void was also demonstrated by schlieren photography.

ACKNOWLEDGMENTS

The authors would like to express appreciation to Dr. M. A. Breazeale for his helpful suggestions and to the U.S. Office of Naval Research for support of the research.

REFERENCES

1. Victorov, I. A. Rayleigh and Lamb Waves, Plenum Press, New York, 1967.

2. Bertoni, H. L. and T. Tamir. Appl. Phys. 2, 157 (1973).

3. Breazeale, M. A., Laszlo Adler, and J. H. Smith. Akust. Zh. 21, 1-10 (1975) [Sov. Phys. Acoust. 21, 1-6 (1975)].

4. Schoch, A. Ergeb. exact. Naturwiss. 23, 127-234 (1950).

5. Adler, Laszlo, M. A. Breazeale, and G. W. Scott. J. Acoust. Soc. Amer. 57, S58 (1975).

Paper No. 10

Reflection of a Gaussian Ultrasonic Beam from Al_2O_3 Layer-Stainless Steel in Water at the Rayleigh Angle (László Adler and D. A. McCathern), accepted for publication in the Journal of Applied Physics.

REFLECTION OF A GAUSSIAN ULTRASONIC BEAM FROM Al_2O_3 LAYER-STAINLESS STEEL IN WATER AT THE RAYLEIGH ANGLE*

Laszlo Adler and D. A. McCathern
Department of Physics
The University of Tennessee
Knoxville, Tennessee 37916

ABSTRACT

The problem of ultrasonic wave reflection at a Rayleigh angle from Al_2O_3 layer-stainless steel in water was investigated. The so-called leaky Rayleigh velocity was measured by using an optical schlieren technique to identify the Rayleigh angle. The magnitude of the measured leaky Rayleigh velocity for the coated surface is smaller than the corresponding leaky Rayleigh velocity for either stainless steel or for Al_2O_3.

Recent experimental investigations by Neubauer[1] and Breazeale, Adler and Scott[2] based on the theory of Bertoni and Tamir[3] have established that a mode of elastic energy propagation can exist at a liquid-solid interface. Excitation of this so-called leaky Rayleigh wave takes place when an ultrasonic beam of Gaussian distribution is incident at or near the Rayleigh angle to the interface. The reflected ultrasonic beam contains a so-called null strip which is the result of the 180° phase difference between the specularly reflected beam and the reradiated leaky Rayleigh wave. Figure 1 is a schlieren photograph of the incident and reflected ultrasonic beam from a water-stainless steel interface below, at, and above the Rayleigh angle. The null strip appears when the incident beam is at the Rayleigh angle. It has been suggested[1] that this null strip could be used to identify and evaluate the Rayleigh velocity for the interface by using

$$C_R = \frac{C_W}{\sin\theta_R} \tag{1}$$

where C_R is the leaky wave velocity, θ_R is the measured Rayleigh angle, and C_W is the velocity of sound in water. The leaky Rayleigh velocity can be calculated exactly from theory[4] by solving for the roots of secular equation

$$4\left(\frac{C_T}{C}\right)^2\left[1-\left(\frac{C_T}{C}\right)^2\right]^{1/2}\left[\left(\frac{C_T}{C_L}\right)^2-\left(\frac{C_T}{C}\right)^2\right]^{1/2}+\left[1-2\left(\frac{C_T}{C}\right)^2\right]^2 = -\frac{\rho_W}{\rho}\left[\frac{(C_T/C_L)^2-(C_T/C)^2}{(C_T/C_W)^2-(C_T/C)^2}\right]^2 \tag{2}$$

where one solution for C is identified as C_R. C_T and C_L are the shear and longitudinal velocity of the solid and ρ_W and ρ are the density of water and the solid, respectively.

The objective of this paper is to report experimental observations of the reflection of an ultrasonic wave from a semiinfinite solid when a

thin layer of solid is added to its surface. This is an important problem for testing materials under coated surface, as well as for some surface wave device applications. The solid layer-solid in air is treated by Farnell and Adler.[5] According to their analysis, one has to distinguish between loading [C_T (substrate) > C_T (layer)] and stiffening [C_T (layer) > C_T (substrate)] of the layer on the substrate. In the case of loading the Rayleigh velocity is lowered; in the case of stiffening the Rayleigh velocity will increase. No theoretical treatment of the "leaky Rayleigh wave" propagation for the water-solid layer-solid exists at the present time. It is hoped that the experimental observations which are described in the next paragraph will stimulate some investigators.

Turning toward our experiment, the sample used is a stainless steel block with dimensions 2.5 cm x 5 cm x 10 cm and it is coated with a .24 mm thin aluminum oxide layer on the largest surface (shown on Figure 2). The thickness of the layer is less than the wavelength corresponding to the 2 MHz ultrasonic beam used in this experiment. The incident beam had a Gaussian distribution and a half width of 4 mm. Using a schlieren optic technique to observe both incident and reflected beam from the coated surface, the angle was adjusted until the null strip appeared, indicating the presence of a leaky Rayleigh wave. This angle was recorded to be 35°. The corresponding leaky Rayleigh velocity for the coated surface then is 2.61×10^5 cm/sec. The leaky Rayleigh velocities were measured from water-stainless steel and from water-Al_2O_3 surface in the same way. The results are given together with calculated values (from Eq. 2) in Table 1. The agreement between measured and calculated values for both cases are in good agreement. It appears that the Al_2O_3 layer on steel lowers the value of the Leaky Rayleigh velocity. The same

result was obtained on stainless steel when a zirconium oxide layer coating was used. These results are the opposite of what one would expect for the air-solid layer-solid case based on the theory of Farnell and Adler.

Table 1

Samples	Density (gm/cm^3)	Longitudinal Velocity $V_L \times 10^5$ (cm/sec)	Shear Velocity $V_S \times 10^5$ (cm/sec)	Leaky Rayleigh Wave, V_R Calculated (cm/sec)	Leaky Rayleigh Angle, θ_R	
					Measured	Calculated from V_R
Stainless Steel	8.09	5.61	3.18	2.93	30.5	30.54
Al_2O_3	4.0	10.46	6.01	5.53	15.5°	15.6°

*Research sponsored by the Office of Naval Research

References

1. W. G. Neubauer, J. Appl. Phys. 44, 48-55 (1973); W. G. Neubauer and L. R. Dragonette, J. Appl. Phys. 45, 618-622 (1974).
2. M. A. Breazeale, Laszlo Adler, and Gerald W. Scott, J. Appl. Phys. 48, 530-537 (1977).
3. H. L. Bertoni and T. Tamir, Appl. Phys. 2, 157-172 (1973).
4. H. Uberall, Physical Acoustics, edited by W. P. Mason and R. N. Thurston (Academic, New York, 1973), Vol. X, pp. 1-57.
5. G. W. Farnell and E. L. Adler, Physical Acoustics, edited by W. P. Mason and R. N. Thurston (Academic, New York, 1972), Vol. IX, pp. 35-127.

List of Figures

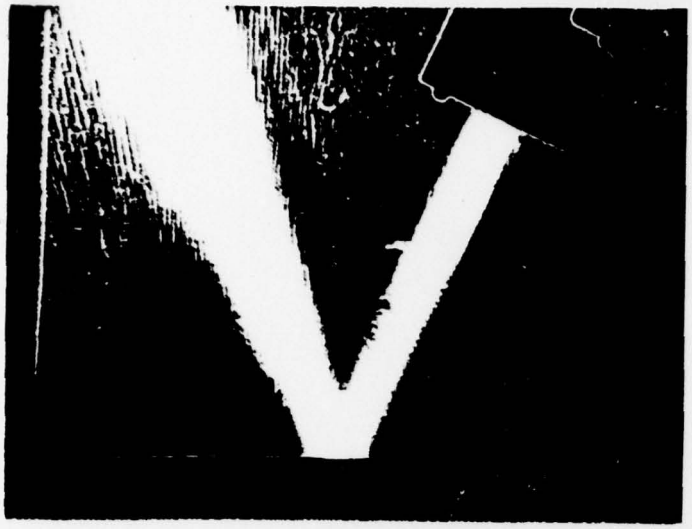

Fig. 1a

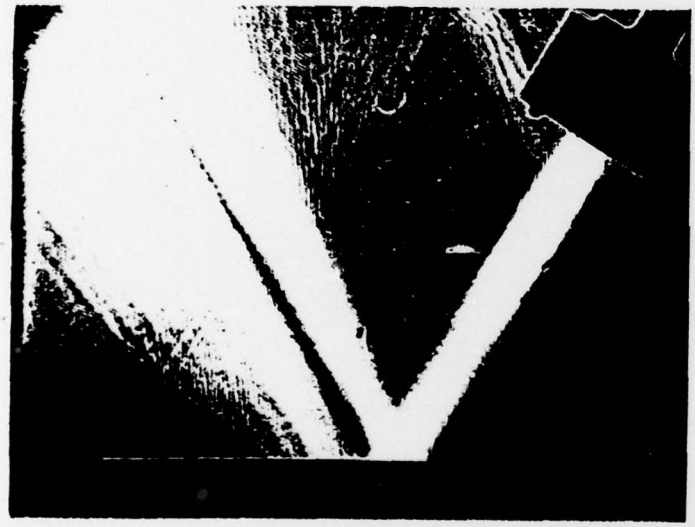

Fig. 1b

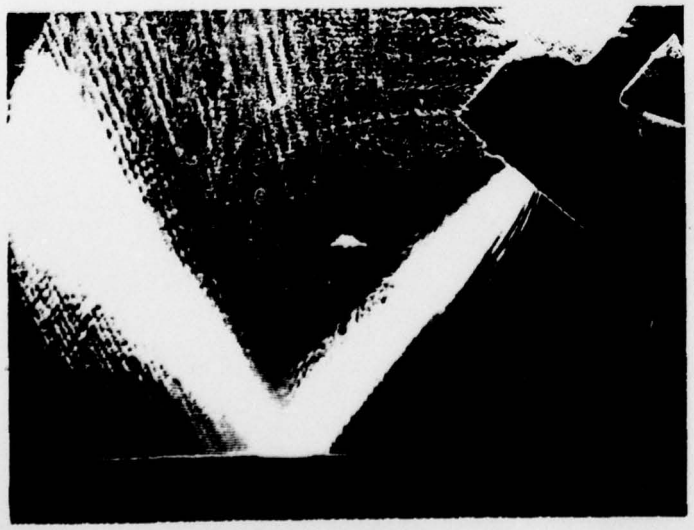

Fig. 1c

- Fig. 2